Deliverable T1.7.2
Consolidated Report on Site and Turbine Modelling

Rev	Date	Description	Prepared by	Approved by
1.0	04/11/2022	Initial version for comment	E. Mackay[1] J. Hardwick[1] D. Coles[2] P. Mercier[3] J. Thiébot[3] S. Guillou[3] G. Pinon[4]	
1.1	07/12/2022	Revised version for approval by PSG	E. Mackay[1] M. Sedrati[5] P. Thies[1]	P. Thies[1]
1.2	12/01/2023	Final version	E. Mackay[1] H. Mullings[6] T. Stallard[6] P.Ouro[6] M. CampsSantamasas[6]	P. Thies[1]

Affiliations: 1. University of Exeter. 2. University of Plymouth. 3. University of Caen Normandy. 4. University of Le Havre Normandy. 5. University of Southern Brittany. 6. University of Manchester

Abstract

Tidal energy projects require numerical modelling for the assessment of tidal site conditions and turbine/array performance. The TIGER project has offered a unique opportunity to concurrently implement a range of available models. This report provides an overview and comparison of the different numerical models developed by academic partners in the TIGER project. The models cover a variety of spatial and temporal scales. The largest scale models provide long-term climatic studies covering the entire English Channel region, at relatively low resolution, whilst the highest-resolution models provide detailed information about short-term and small-scale turbulent flow and its interaction with tidal turbines. The models are used for different purposes. At one end of the scale, the models have been used to inform the large-scale techno-economic assessment of tidal energy and its impact on the energy mix in the UK and France. At the other end of the scale, the numerical models provide information which feeds into detailed engineering design of tidal turbines at particular sites, and assessment of the energy yield. The models showcase the range of computational tools available to aid the development of the tidal energy industry. This report will be useful for investors, technology developers and project stakeholders to identify suitable models to support and develop ongoing and future tidal stream projects.

Table of contents

1 Introduction

This report describes the numerical modelling conducted by academic partners in the TIGER project, for estimation of tidal site conditions and tidal turbine/array performance and loading. The models considered cover a wide range of spatial and temporal scales, and are used for a correspondingly wide range of purposes.

An overview of the models used within TIGER is presented in Table 1.1, and a high-level schematic of the scales and indicative computational cost of each model is shown in Figure 1.1. The models are classified as turbine-scale, site scale, and regional scale. Turbine-scale models compute the interaction between the local flow conditions and a turbine. Depending on the model, this interaction may be one-way (i.e. flow influences turbine but not vice versa) or two-way (flow and turbine influence each other). Turbine-scale models cover short time scales, of the order of 10-30 minutes, over which the mean flow conditions can be considered approximately stationary. Site-scale models compute the interaction between the flow and detailed bathymetry over a site, corresponding to an area of a few kilometres or less. Depending on the model, the interaction between the flow and turbines may be included, where the turbine may be represented at various levels of detail, depending on the application. Some site-scale models are run for short periods of 30 minutes or less and compute fine-scale features of the flow, such as turbulence induced by bathymetric features. Other site-scale models aim to characterise spatial variability in mean flow characteristics, over longer time scales, spanning multiple tidal cycles. Regional-scale models may be used to identify areas for potential deployments, or to provide boundary data for higher-resolution site-scale or turbine-scale models. Some of the models used span multiple scales.

Figure 1.1 also shows indicative computational requirements for each model type. Computational requirements can vary significantly between particular applications of each model, the domain size, resolution, number of cases considered, etc. However, the indicative ranges show that computational requirements vary by several orders of magnitude. The higher fidelity models provide some information that is not available from the lower-fidelity models, but at higher computational cost.

Further information on each of the models is presented in the sections below. The intention is not to provide detailed descriptions of each model and results. Rather, this report is intended to provide an overview of the different types of model and their respective uses, presented in a consistent format, with references to publications where further details can be found. For each model we describe:

- The governing equations that the model solves
- Representation of tidal turbines within the model (where applicable)
- Intended uses of the model
- Model setup
    - Spatial and temporal resolution and extent
    - Model inputs and boundary conditions
- Example outputs from the model

The numerical models have been applied to assess turbine performance and site conditions across five sites:

1. Raz Blanchard,
2. Perpetuus Tidal Energy Centre (PTEC),
3. Ramsey Sound,
4. Paimpol-Bréhat,
5. Gulf of Morbihan.

For the Raz Blanchard site, multiple types and scales of model have been run. Comparisons of these models are presented in Annex A.

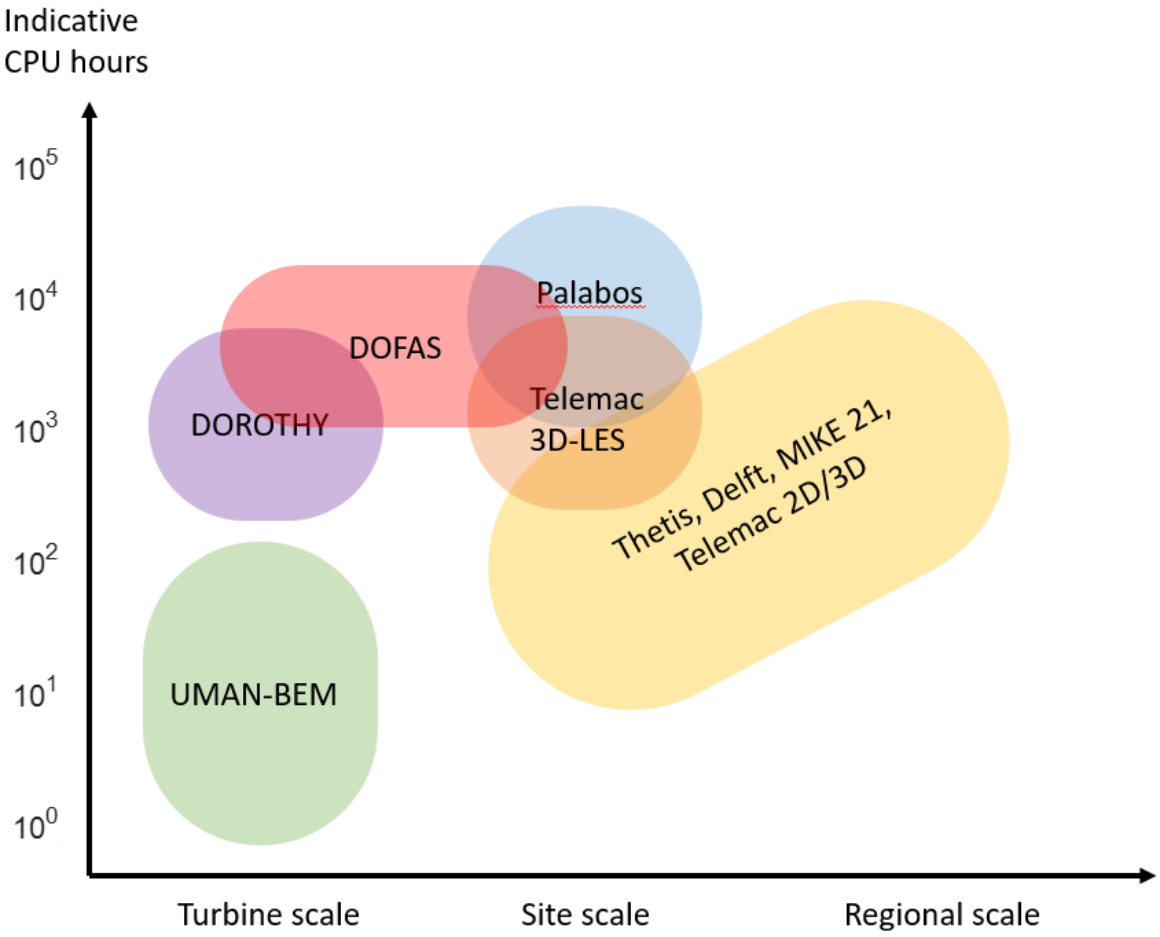

Figure 1.1. Indicative scales and computational requirements for numerical models used in TIGER

Table 1.1. Overview of numerical models used in TIGER

Model name	Governing equations for flow	Representative spatial extent and resolution	Representative temporal extent and resolution	Representation of tidal turbine(s)	Representation of turbulence	Representation of waves	Intended uses
Delft suite	2D shallow water equations & 3D RANS equations	Regional model covering O(1-100) km at resolutions between ~1km and 20m	Multi-year periods with outputs every 20 mins	None	Eddy-viscosity model	Spectral wave model with one- or two-way coupling to flow model	- Regional to site scale resource assessment - Investigation of wave-current interactions - Assessment of extreme conditions
Thetis	2D shallow water equations	Regional model covering O(1-100) km at resolutions between ~1km and 20m	Weeks to months with outputs at 10 min steps	Drag term	Eddy-viscosity model	None	- Regional and local resource assessment - Optimisation of array layouts - Impacts of arrays on the tidal flow
Palabos	Lattice-Boltzmann method (LBM) large eddy simulation (LES)	Site-scale model (~0.5km^2) at high resolution (~0.3m)	~30 mins with high frequency output (<1s)	None	LES	None	Characterisation of turbulent tidal flows generated by seabed roughness
Telemac 2D/3D	2D shallow water equations & 3D RANS equations	Regional model covering O(1-100) km at resolutions between ~10km and 10m	Approx. 1-year for 2D model, 1 month for 3D model	Drag term (2D) Actuator disc (3D)	Eddy-viscosity model	None	- Resource assessment - Impact of energy extraction on the resource - Array layout assessment
MIKE 21	2D shallow water equations	Local model covering O(10) km at resolutions between ~1km and 10m	1 month	None	Eddy-viscosity model	None	Resource assessment

Telemac LES	Large eddy simulation (LES)	Site scale model with resolution 10km – 1m	Approx. 1 week with outputs at 1Hz	None	LES	None	Resource assessment with focus on turbulence
DOROTHY	Vortex Particle Method	Turbine scale model with O(10^5) particles	Simulation durations of the order 100s	Lifting line model	LES	None	- Performance evaluation - Wake characterisation - Fluctuating loads along blades
DOFAS	LES	Array-scale model with resolution 5 m - 0.2m	From minutes to tidal phase length (3-5 hours)	Geometry-resolved Actuator-line Actuator-disc	LES	Level-set method	-Turbine array layout design -Bathymetry-induced turbulence characterisation -Wave-induced loading -Wake recovery characterisation -Inform lower fidelity models from high-fidelity data
UMAN-BEM	Blade element momentum theory	Device Scale Model, overall domain approx. 2Dx2D.	Multiple time steps over a tidal flow, for each 10min case.	Blade element momentum theory	LES/VK	Linear Theory	- Performance evaluation - Fluctuating loads along blades - Loading/Fatigue evaluation - Efficient load prediction, spatial variation of loads.

2 Delft3D FM-SWAN: University of Exeter

2.1 Overview of model and intended use

A fully coupled flow-wave model has been developed using Delft3D Flexible Mesh (DFlow FM) and SWAN. DFlow FM is the hydrodynamic flow solver which forms the core of the Delft3D Flexible Mesh suite of models. The Delft3D FM suite also integrates support for the SWAN 3rd generation spectral wave model, referred to as D-Wave within the Delft3D framework. This integration enables the models to be fully coupled within the software without the need to develop an independent coupling tool. The models have been developed to calculate flow and wave conditions across the region for use in multiple applications within TIGER by University of Exeter and other project partners. Within the TIGER project, the models have been used to generate a 32-year hindcast dataset of flow and wave conditions throughout the English Channel with a focus on two sites: the PTEC site off the Isle of Wight and the Alderney Race. The models were used for: resource quantification, extreme value modelling, input to techno-economic modelling, input to model the dynamic analysis of structures, and model comparisons. As well as being used in research studies at the University of Exeter data were provided to:

- ORE Catapult, to feed into the techno-economic assessment of the PTEC site.
- B&V consultants, on behalf of Orbital Marine Power, for both PTEC and Alderney Race.
- University of Manchester, to provide input to their modelling work.

In addition to this report the model data was used in the following TIGER tasks/deliverables.

- T3.1.2 Data Collection & Survey Best Practice Report
- T1.6.2 Definition of deployment projects for tidal farms

Several academic publications produced using the data from the model:

- Hardwick J, Ashton IGC, Mackay E, Smith HCM, Thies PR. (2020) Coupled flow-wave modelling for regional tidal site characterisation in the English Channel, *Developments in Renewable Energies Offshore*, 601-606, DOI:10.1201/9781003134572-68.
- Hardwick J, Mackay E, Ashton I, Smith H, Thies PR. (2021) Quantifying the effects of wave-current interactions on tidal energy resource at sites in the English Channel using coupled numerical simulations, *Energies*, volume Special Issue Tidal Turbines, DOI:10.3390/en14123625.
- Mackay E, Hardwick J. (2022) Joint extremes of waves and currents at tidal energy sites in the English Channel, *ASME 2022 41st International Conference on Ocean, Offshore & Arctic Engineering OMAE2022*, Hamburg, Germany, 6th - 9th Jun 2022.

The model has also provided input to presentations or posters at the following local and international events:

- RENEW 2020: 4th International Conference on Renewable Energies Offshore 12 - 15 October 2020, Lisbon, Portugal
- OMAE 2021: 40th International Conference on Ocean, Offshore & Arctic Engineering, Hamberg, Germany
- PRIMARE 2022: 9th Annual PRIMaRE Conference, Cornwall, UK
- ICOE 2022: International Conference on Ocean Energy, Donostia/San Sebastian, Spain

2.1.1 Governing Equations

DFlow FM is a hydrodynamic flow solver which solves the 2D depth averaged or 3D non-linear shallow water equations derived from the Navier-Stokes equations for incompressible free fluid flow. The system of equations consists of the horizontal momentum equations, the continuity equation, the transport equation, and a turbulence closure model. The full description of the equations is described by Lesser et al. (2004). Tidal generating harmonic forces can be applied across the grid along with boundary conditions to provide model input around open boundaries. (Deltares, 2019). The earlier Delft3D-FLOW model has been continually developed since the first release in 1995 and is used widely to model a variety of coastal (Xia et al., 2010), estuarine (Trihartono et al., 2015), river (Lesser et al., 2004) and other hydrodynamic processes. The D-Flow FM model allows the advantages of simulating these processes on an unstructured computational space enabling a higher resolution output on areas of interest without suffering the loss of computational speed required by increasing the resolution of the whole grid.

SWAN (Simulating WAves Nearshore) is a third-generation spectral wave model developed at TU Delft in The Netherlands. The model was developed to predict the wave spectrum in coastal and shallow water zones. SWAN, like other spectral wave models determines the evolution of the action density in space and time. The model incorporates the effects of wave-current interaction, wave breaking, white-capping, triad interaction and quadruplet interaction. A full description of the model is available in the SWAN technical documentation (TUDelft, 2010).

2.2 Description of models

2.2.1 Spatial grid

The flow model is constructed on a Cartesian grid (Eastings and Northings) covering the entirety of the English Channel. The Western boundary runs from the coast of Ireland to a point Southwest of the coast of Brittany. At the Eastern end of the channel the boundary runs East-West from Suffolk in the UK to close to Amsterdam in The Netherlands. There is also a smaller open boundary across the Irish Sea. The flow model is run over a mixed resolution unstructured blended triangular-rectangular grid. The mesh was created using RGDGRID, a tool developed by Deltares to work with the Delft3D suite of models. The mesh consists of 279464 cells. For sections of the grid furthest offshore which are mostly of lower interest and lower spatial variability, 2km square cells are used. In the coastal regions the grid is formed of triangular cells with variable resolution ranging from 2km up to as fine as 20m in the areas of greatest interest (see Figure 2.2).

The SWAN model consists of a regular 2km square grid covering the same region as the flow domain, the extent of the grid is shown as the yellow box in Figure 2.1. Higher resolution nested grids are included around the sites of interest. Two main areas of interest are used in this study. The PTEC site, off the Isle of Wight, and the Alderney Race. The nested areas are shown in Figure 2.3 and described in Table 2.1.

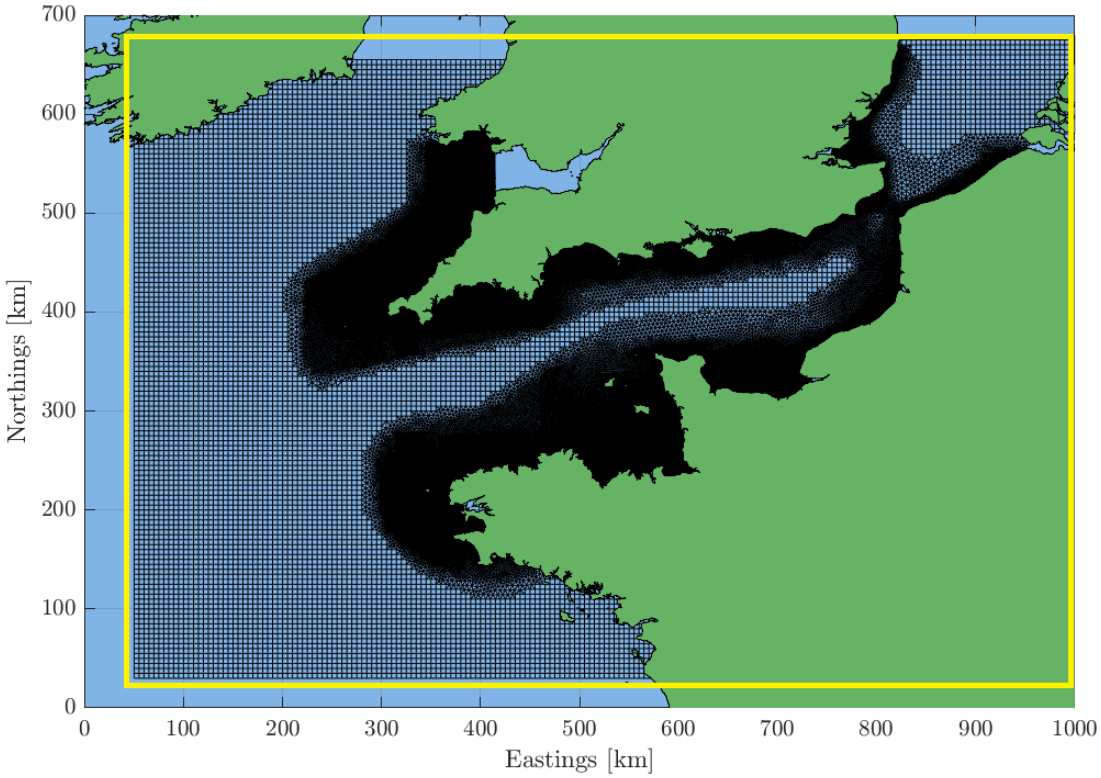

Figure 2.1. Computational domain of the flow model (black grid). Extent of regular SWAN wave grid (yellow box).

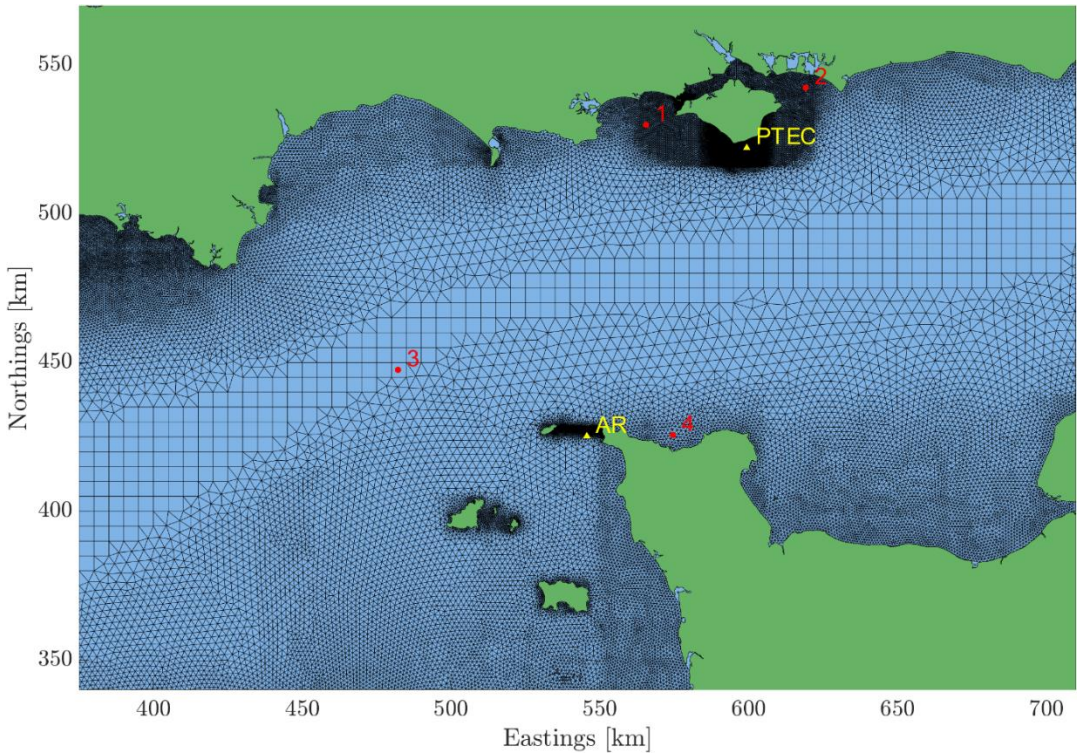

Figure 2.2. Zoom of computational domain of the flow model showing location of PTEC and Alderney Race (yellow).

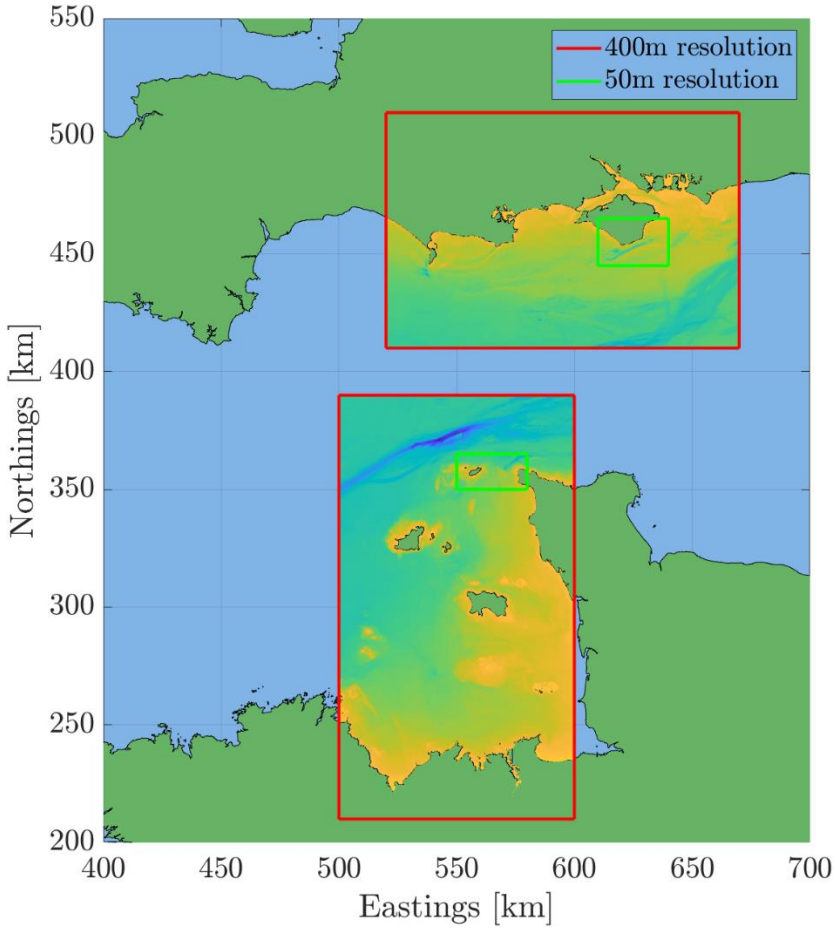

Figure 2.3. Locations of nested grids for SWAN model.

Table 2.1. SWAN grid resolutions

Site	Grid resolution
English Channel	2km
Channel Islands	400m
Alderney Race	50m
Isle of Wight	400m
PTEC	50m

2.2.2 Temporal settings

The model results span 32 years for both the flow and wave models, covering the period from 1st January 1990 – 31st December 2021. This long dataset contains a large range of conditions including more than one complete 18.6 year lunar tidal cycle. This means that the largest astronomical tidal range and flow speed are captured within the flow data. The wave conditions are a random stochastic process, so it is necessary to have a long dataset in order to fully assess all the conditions. In order to undertake extreme analysis, many storm events are required. The longer the dataset available the lower the uncertainty in the extreme value models.

The computational time-step of the flow model is calculated by the solver based on a Courant condition. However, it is limited to a maximum value of 30 seconds, which is sufficient to capture all the physical processes in the model. The wave model has a computational time step of 20 minutes, this was decided as an acceptable balance between model accuracy and computational runtime.

The various time varying inputs are shown in Table 2.2Table 2.2. Summary of DELFT 3D – FM model inputs, where the time step of the input quantity is greater than the computational time step, values are interpolated by the solver.

Table 2.2. Summary of DELFT 3D – FM model inputs

Inputs	Source	Spatial Resolution	Time Step
Bathymetry	Mixed*	1 – 15 arcsec	-
Wind forcing	ERA-5	20km regular grid	1 hour
Air pressure	ERA-5	20km regular grid	1 hour
Harmonic boundary	TPXO-09	On open boundaries	Continuous
Wave boundary conditions	ERA-5 WAM model	0.36-degree regular grid	1 hour

2.2.3 Other numerical settings

The SWAN wave model allows the user to set the acceptance criteria for model convergence. Stricter convergence criteria should result in more accurate model output however it may significantly increase computational time. The SWAN code is set to accept 98% convergence criteria or to continue after 25 iterations.

2.2.4 Inputs and Boundary Conditions

The following is a description of inputs and boundary conditions provided to the models.

2.2.4.1 Bathymetry (both flow and wave models)

Bathymetry for the models are drawn from a combination of sources. Areas around the UK are sourced from Digimap at 1 arc-second resolution (EDINA, 2013). In waters around France the bathymetric data is from the French Hydrographic office (SHOM, 2016) also at 1 arc-second and is compiled as part of the HOMINIM project. A small part of the Southwest corner of the grid was outside the limits of both datasets, this was filled from the GEBCO 2020 global bathymetry map (GEBCO, 2020). The bathymetry is shown in Figure 2.4.

2.2.4.2 Wind and Atmospheric Pressure (both flow and wave models)

The wave model is forced by wind speed data from the ERA-5 global re-analysis dataset from the European Centre for Medium Range Weather Forecasts (ECMWF), this is freely available data with excellent validation and documentation (Hersbach et. al. 2020). This same wind data and atmospheric pressure data are also provided to the flow model. The dataset contains many atmospheric parameters from 1959 - present. The data are provided on a regular grid with a spatial resolution of 20km and a temporal resolution of 1 hour.

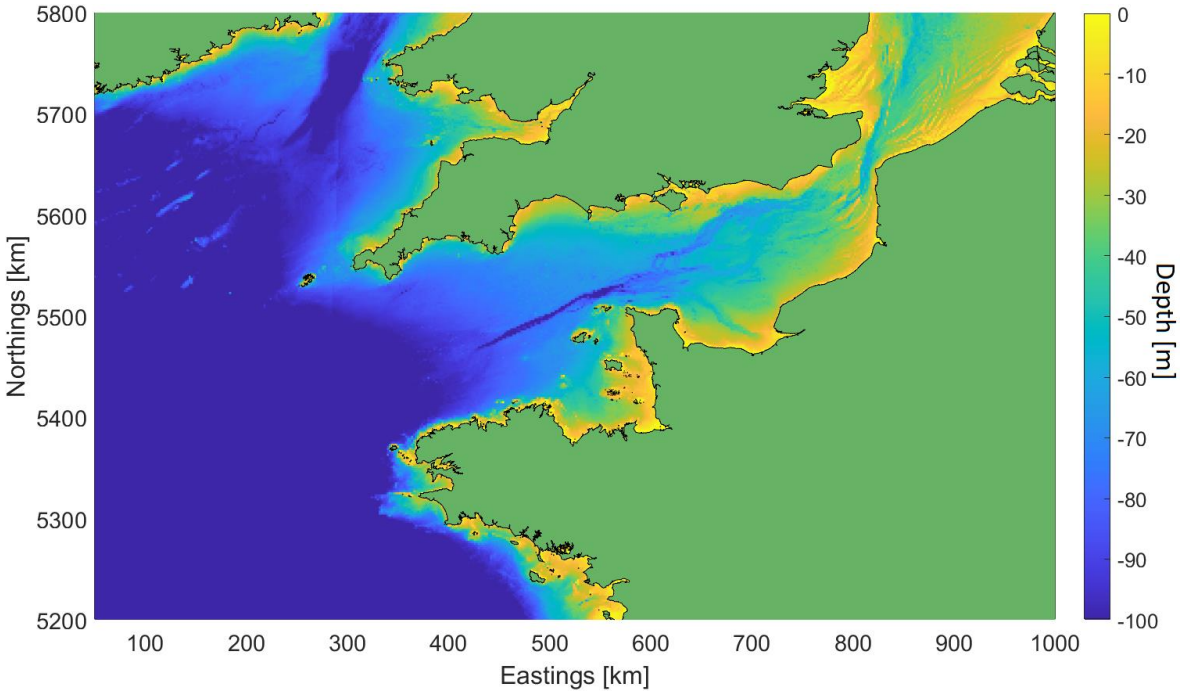

Figure 2.4. Bathymetry across the DELFT 3D – FM domain.

2.2.4.3 Harmonic Water Level Boundary (flow model)

The flow model is forced by time varying water level at the four open boundaries. The water level is calculated from the astronomical harmonic constituents. The amplitude and phase of the 11 largest constituents (M2, S2, N2, K2, K1, O1, P1, Q1, M4, MS4, MN4) are input to the model, then the water level is calculated internally. Data is sourced from the TPXO-9 model system (Egbert, et. al. 1994). As all of the model boundaries are far from the areas of interest there is no requirement for velocity data to be included on the boundary conditions and the water level boundaries are sufficient.

2.2.4.4 Wave boundaries (wave model)

At the open boundaries the model is forced by wave parameter values (Hs, Tp, Dir, Dspr) from the ERA-5 dataset, interpolated along the boundary points at 1 hourly resolution. The ERA-5 data are derived from a WAM global wave model. A full description of these input wave data from ERA-5 is given online at the ECMWF website (Hersbach et. al. 2020).

2.2.4.5 Physical Parameters

Bottom friction was input as a constant with a coefficient of friction equal to 0.023. While it is possible to input spatial varying friction values to the model this was not implemented in this work. Water temperature was set at 12^{o}C and salinity to 35ppm.

2.2.5 Outputs

Both models provided detailed output at 120 pre-set locations within the domain. These included the locations of interest for the project as well as locations of validation instrumentation. At these locations the flow model provides the depth average flow velocity, water level and bottom shear stress data at 5-minute resolution. The wave model provides 45 fields including wave height, period and direction quantities at 20-minute resolution.

In addition to the detailed output the models also provide a smaller number of key quantities across the whole domain. The flow model gives flow speed and direction at all 279,464 cells of the grid on a 10-minute timescale. The wave model provides 6 quantities across the domain every hour. Some examples of spatial output are shown in Figure 2.5 and Figure 2.6.

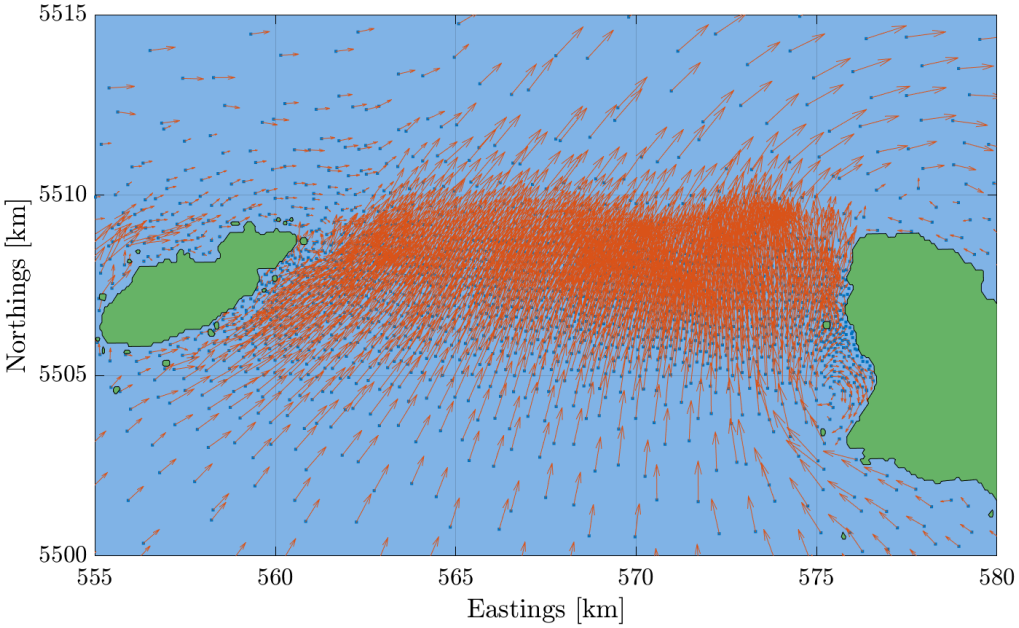

Figure 2.5. Example of the modelled flow through the Alderney Race from DELFT 3D – FM model.

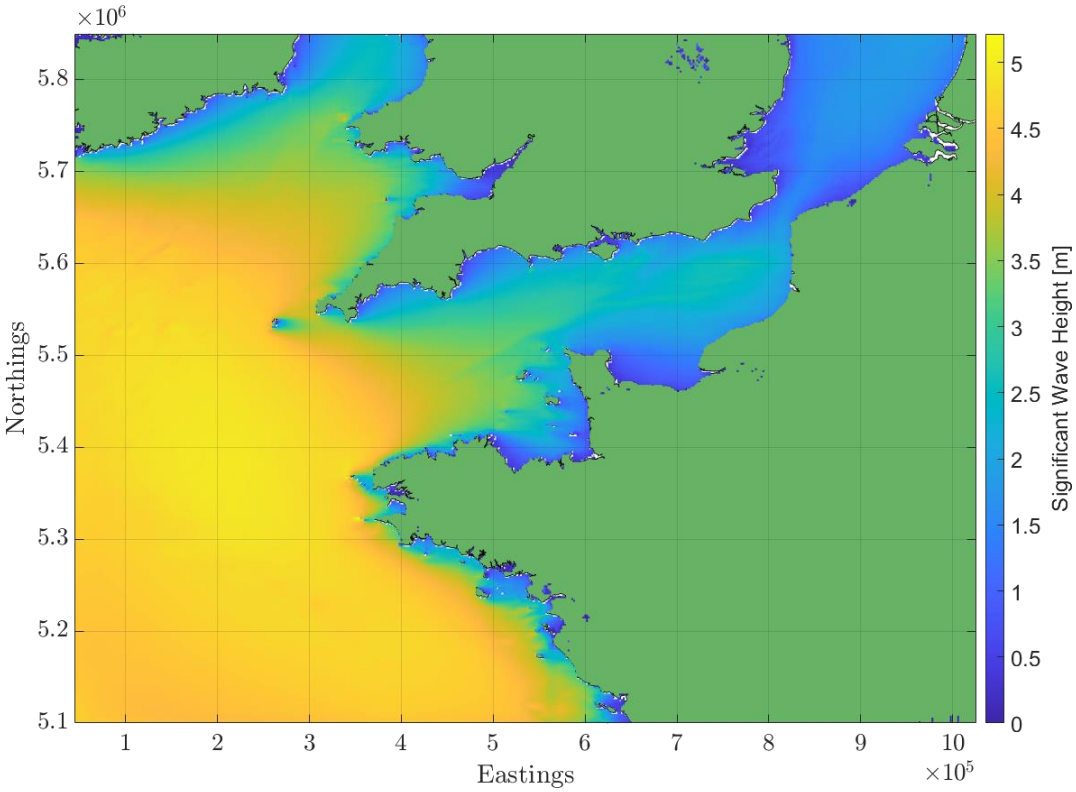

Figure 2.6. Average significant wave height across the domain for 2020 from SWAN model.

3 Thetis: University of Plymouth

3.1 Overview of model and intended use

Thetis is an open source, unstructured grid coastal ocean model built using the Firedrake finite element framework. The Ramsey Sound *Thetis* model has been utilised within the TIGER project by the University of Plymouth for three main purposes; (a) to establish the spatial variability in the tidal resource across the Sound, (b) to quantify the power performance of tidal stream turbine arrays positioned in the Sound, and (c) to aid Cambrian Offshore South West with operations planning for the retrieval of the in-situ Delta Stream turbine and re-deployment of a tidal stream turbine at the site. In addition to these three primary purposes, the University of Plymouth have conducted *Thetis* modelling to (d) generate tidal stream power time series data from sites across the UK as inputs for energy system modelling, (e) optimise the shape of tidal stream turbine arrays (in collaboration with Orbital Marine Power and Black & Veatch), and (f) help establish the practical viability of tidal stream energy development at sites surrounding Ramsey Sound (in collaboration with the ORE Catapult). Table 1 provides a summary of these activities. Outputs from each task are summarised below.

Table 3.1. Summary of Thetis *modelling tasks undertaken by the University of Plymouth.*

Task	Deliverable	Description	Publications/outputs
1. Site and turbine modelling	T1.7.2	-Assess impact of turbine siting on energy yield. -Long duration tidal resource modelling. -Drone surveying of the tidal flow speeds	Coles DS et al. (2021a), Thiébot et al., (2022) Fairley et al., (2022) (See section 1.2.6.1)
2. Array modelling	T1.7.2 / T3.2.1 / T3.2.2	-Array optimisation/assess impacts of arrays on the tidal flow.	Array energy yield estimates reported to the ORE Catapult (see Section 3.2.6.2)
3. Operations planning	T1.7.2	-Provide detailed tidal predictions for operations access.	Results reported to Cambrian Offshore (see Section 3.2.6.3)
4. Energy system modelling	T3.4.3	-Provision of tidal stream power time series used as inputs to energy system modelling.	Coles et al. (2021b), Pennock et al. (2022), Todeschini G et al. (2022), Frost C., (2022) (See Section 3.2.6.4)
5. Array shape optimisation	T3.2.2	-Optimisation of Orbital O2 array shape at sites mimicking Alderney Race and St Catherine's Point (Isle of Wight.	Results reported to Orbital Marine Power and Black & Veatch (See Section 3.2.6.5)
6. Resource assessment – surrounding sites	T3.2.1	-Site prospecting to establish the suitability of site close to Ramsey Sound for tidal stream energy development.	Results reported to ORE Catapult (See Section 3.2.6.6)

3.1.1 Governing equations

Thetis solves the non-conservative form of the non-linear shallow water equations:

$$\frac{\partial \eta}{\partial t} + \nabla.(H_d \tilde{\boldsymbol{u}}) = 0, \tag{1.1}$$

$$\frac{\partial \eta}{\partial t} + \tilde{\boldsymbol{u}}.\nabla\tilde{\boldsymbol{u}} - \nu\nabla^2\tilde{\boldsymbol{u}} + f\tilde{\boldsymbol{u}}^{\perp} + g\nabla\eta = -\frac{\tau_b}{\rho H_d} \tag{1.2}$$

$$\frac{\tau_b}{\rho} = gn^2 \frac{|\tilde{\boldsymbol{u}}|\tilde{\boldsymbol{u}}}{H_d^{1/3}}, \tag{1.3}$$

where t is time, η is water elevation, H_d is total water depth, $\tilde{\boldsymbol{u}}$ is the depth averaged velocity vector with $\tilde{u}$ and $\tilde{v}$ denoting the easterly and northerly flow components respectively, ν is the kinematic viscosity, g is acceleration due to gravity and ρ is the density of seawater. The expression $f\tilde{\boldsymbol{u}}^{\perp}$ describes the Coriolis force, where $\tilde{\boldsymbol{u}}^{\perp}$ is the velocity vector rotated counter-clockwise over 90°, $f = 2\Omega\sin(\zeta)$, Ω is the angular frequency of the Earth's rotation and ζ is the latitude. Bed shear stress is described by τ_b, and n is the Manning coefficient. A wetting and drying formulation described in Karna et al., (2011) is used to model intertidal processes.

Wind and wave effects are not included in the model. The model is run in depth-averaged mode in order to achieve acceptable computational efficiency to run simulations for the range of purposes set out in Table 1. This prevents the models from being able to resolve the boundary layer flow in the vertical plane, which has been deemed acceptable given the accuracy of the model in two dimensions (see Mackie et al. (2021), and the additional computational efficiency this provides.

The *Thetis* model utilises a discontinuous Galerkin finite element spatial discretisation (DG-FEM) through the choice of a P_{1DG} – P_{1DG} velocity-pressure finite element pair. A semi-implicit Crank-Nicolson time stepping approach is applied. The nonlinear discretised shallow water equations are iteratively solved with Newton's algorithm using the PETSc library (Balay et al., 2016).

3.2 Description of model

3.2.1 Spatial settings

The *Thetis* model of the Ramsey Sound uses an unstructured mesh that has been generated using *qmesh*. Figure 3.1 shows the domain extent, which covers a large section of the Irish Sea, as well as incorporating parts of the Celtic Sea and Northern Channel. The spatial resolution of the mesh is 8 km at its outer extremities, and refined to around 250 m around coastlines to capture intertidal processes, and to 25 m within the Ramsey Sound to resolve complex flow features around bathymetric features such as Horse Rock and the Bitches.

3.2.2 Temporal settings

The *Thetis* model adopts a time step of 100 s. In general the time period covered by the model is 1 month. This allows harmonic analysis to be conducted to extrapolate the modelled data out to 1 year to estimate annual energy yield. When the model is run to aid with operations planning (Task 3), the model is typically run for 1 week to cover the entire neap tide period

when operations can take place on site. The model output variables are written at 10 minute resolution to capture the temporal variability of the modelled flow speeds and directions.

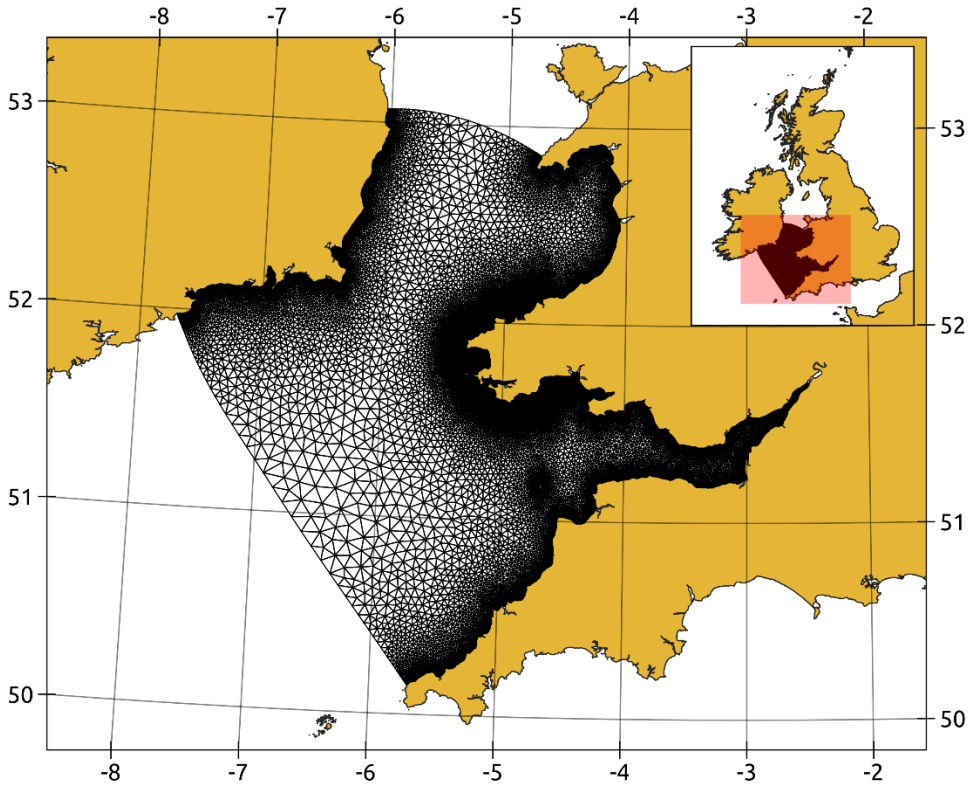

Figure 3.1. Domain and computational mesh for Thetis model of Ramsey Sound and surrounding seas.

3.2.3 Representation of tidal turbines

Task 2 simulates tidal stream turbine arrays within the Ramsey Sound. The added turbine array drag coefficient is parameterised using a turbine array drag coefficient, C_a, which is added to the existing parameterisation of sea bed drag in the momentum equations (Eq. 1.2). The turbine array drag coefficient is parameterised using Equations 1.4-1.5:

$$\lambda = \frac{A_t n}{A_a}, \tag{1.4}$$

$$C_a = \frac{1}{2}\lambda C_{d,} \tag{1.5}$$

where λ is the array density, which is defined as the ratio of the total swept area of the array to the plan area of the array. A_t is the swept area of a turbine rotor, n is the number of turbines in the array, and A_a is the plan area of the array. C_a is the turbine array drag coefficient and C_d is the drag coefficient of a single turbine. The turbine array drag coefficient is applied uniformly over the array plan area. This approach is often referred to as the continuous array drag approach, which is different to the discrete turbine drag approach where each individual turbine is assigned its own drag term. The continuous drag approach cannot simulate local blockage effects caused by the wakes/bypass flow of upstream turbines impinging on downstream turbines, for example. These impacts were minimised in the *Thetis*

modelling by upholding a relatively low array density, to maintain high spacing between turbines, as recommended by Coles et al, (2016).

The array plan area was derived based on a range of practical constraints that determine the viability of turbine positioning, based on work conducted by the ORE Catapult. These constraints included depth (LAT), bathymetric gradient, flow speeds, shipping lanes, and conservation areas. Figure 3.2 shows the resulting array plan area. Simulations were run to quantify the performance of the array when 20 – 80 turbines are distributed evenly over the array plan area.

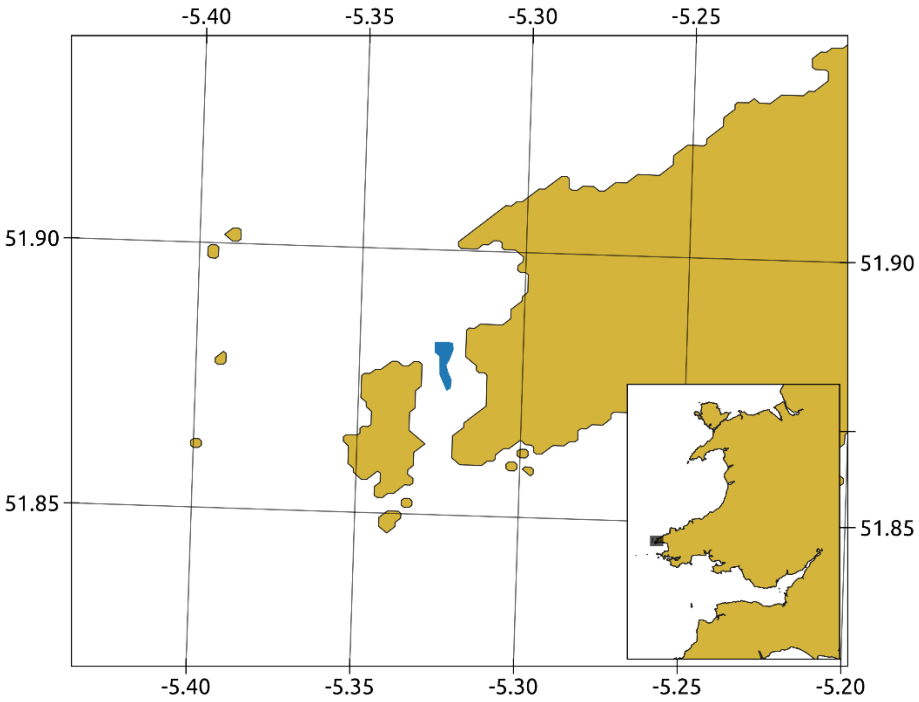

Figure 3.2. Array plan area (blue) within the Ramsey Sound.

3.2.4 Other numerical settings

The Manning coefficient, n, which is used to quantify bed shear stress (Eq. 1.3), is varied across the domain depending on the spatial distribution of different bed material, using Equations 1.7-1.9 (Soulsby, 2005);

$$k_s = 2.5 d_{50}, \tag{1.7}$$

$$z_0 = \frac{k_s}{30}, \tag{1.8}$$

$$n = 0.04 \sqrt[6]{k_s}, \tag{1.9}$$

where k_s is the Nikuradse parameter for sand grain roughness, d_{50} is the associated grain size, and z_0 is the roughness length. Based on data published by the British Geological Survey, associated grain size varies significantly, from 768 – 2048 mm for bedrock, to 0.0625 – 0.125 for silt, clay and mud, resulting in a wide range of Manning coefficient implemented across the domain. Regions of the domain where survey observations are unavailable are estimated to have the properties of "fine gravel", with a grain size d_{50} of 6 mm.

3.2.5 Inputs and Boundary Conditions

The Ramsey Sound *Thetis* model is driven by tidal elevation data extracted from the European Shelf 2008 model (Egbert et al., 2010) at two open boundaries located in the Irish Sea and Celtic Sea. The model uses a variety of bathymetric data; the majority of the domain uses Edina Digimap Service data with a spatial resolution that varies between 18 – 120 m (Seazone Solutions Ltd, 2014). Bathymetry data obtained from the UK Hydrographic Office, with a 2 m resolution (Bangor University, 2017), is used over an 11 x 12 km region that includes the Ramsey Sound.

3.2.6 Outputs

3.2.6.1 Site and turbine modelling (Task 1)

Depth averaged flow speeds were extracted from the *Thetis* Ramsey Sound model at locations DS, a, b and c (shown in Figure 3.3a). DS is the location of the Delta Stream device. The data extraction locations were chosen based on their suitability for tidal stream energy extraction (i.e. depth greater than 15 m and time averaged flow speeds exceeding 1.5 m). The depth averaged flow speeds over two flood-ebb cycles are shown in Figure 3.3b.

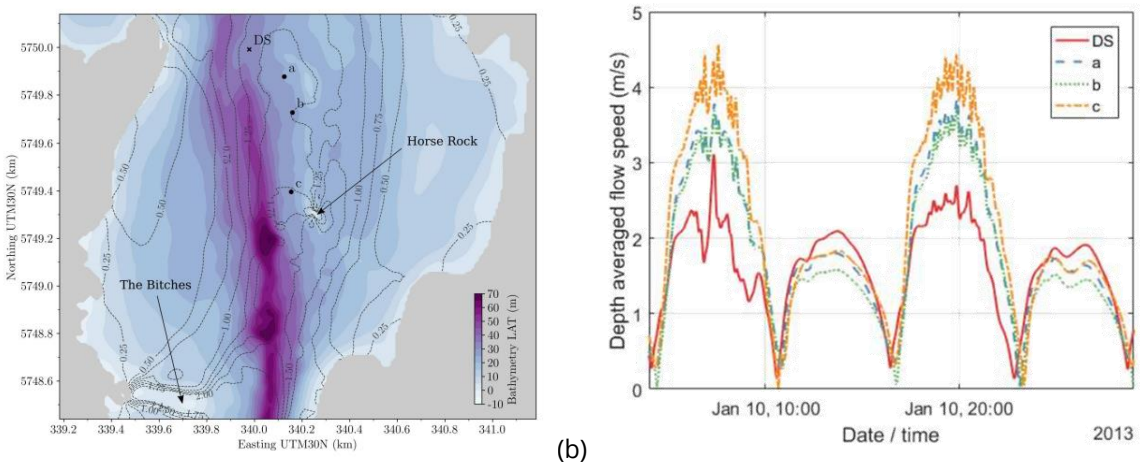

(a) (b)

Figure 3.3. (a) Thetis data extraction locations in the Ramsey Sound, and (b) depth averaged flow speeds at locations DS, a, b, and c over two flood-ebb cycles.

The depth averaged flow speeds were used to estimate the annual energy yield of turbines located at each location. Energy yield estimates were used to estimate cost of energy extracted at each of the four locations, based on a simple cost model developed at the University of Plymouth. The *Thetis* and cost models were used together to estimate the rotor diameter and rated power of the turbines required to minimise cost of energy at each of the four locations. Results from this work are published in Coles et al. (2021), and summarised in Table 3.2 below. The main conclusions drawn from this work are:

- There is a high degree of flood-ebb tidal asymmetry at the flour locations (albeit less pronounced at the DS location), with significantly reduced flow speed magnitudes during flood tides, caused by the wake formed by Horse Rock.
- Given the high spatial variation in tidal stream resource in the Ramsey Sound, there is significant potential to minimise CapEx per unit energy generation by optimising the rated power and rotor diameter of the turbine(s), and their micro-siting.

Table 3.2. Estimated annual power performance and CapEx of turbines at locations DS, a, b and c in the Ramsey Sound

Location	Rated power	Rotor diameter	Turbine CapEx	Annual energy yield	CapEx/MWh
DC	0.4 MW	15 m	2.4 m	1.2 GWh	82 £/MWh
A	0.6 MW	13 m	2.3 m	1.6 GWh	58 £/MWh
b	0.6 MW	13m	2.3 m	1.5 GWh	64 £/MWh
c	0.7 MW	12 m	2.2 m	1.9 GWh	49 £/MWh

The Ramsey Sound *Thetis* model has also been used to quantify the impacts of the 18.6 year lunar nodal cycle on the energy resource at Ramsey Sound. Results from this work are published in Thiebot et al., (2022). The model has also been used to help plan drone surveys of the Ramsey Sound, for the purpose of quantifying the performance of techniques for tidal stream resource assessment (Fairley et al., 2022).

3.2.6.2 Array modelling (Task 2)

Thetis modelling has been used to quantify the performance of arrays located in the Ramsey Sound that use 0.5 MW, 15 m rotor diameter turbines. The array plan area is shown in Figure 3.2. Table 3.3 summarises the estimated annual energy yield and capacity factor of the arrays. Results show that whilst the annual energy yield of the array increases by 200% as the number of turbines is increased from 20 to 80, there is a 25% reduction in the array capacity factor. Given that operational projects are requiring capacity factors of 0.4 to achieve financial close (Black & Veatch, 2020), these results indicate that Ramsey Sound is highly unlikely to be able to facilitate large scale array development. Results from this work are being used by the ORE Catapult to include in their site development report for the Ramsey Sound (deliverable T3.2.1).

Table 3.3. Summary of annual energy yield estimates for arrays with 20-80 turbines in the Ramsey Sound.

Number of turbines	Array capacity	Annual energy yield	Capacity factor
20	10 MW	34.8 GWh	0.40
40	20 MW	63.3 GWh	0.36
60	30 MW	87.4 GWh	0.33
80	40 MW	103.6 GWh	0.30

3.2.6.3 Operations planning (Task 3)

The *Thetis* model has been utilised to establish the dynamics of the flow around slack water at the Ramsey Sound. The purpose of this work is to aid Cambrian Offshore, who are tasked with recovering the in-situ Deltastream turbine, which was installed by Tidal Energy Ltd in 2015. Figure 3.4 provides an example of the elevation, flow speed and direction outputs from *Thetis* that have been provided to Cambrian Offshore by the University of Plymouth.

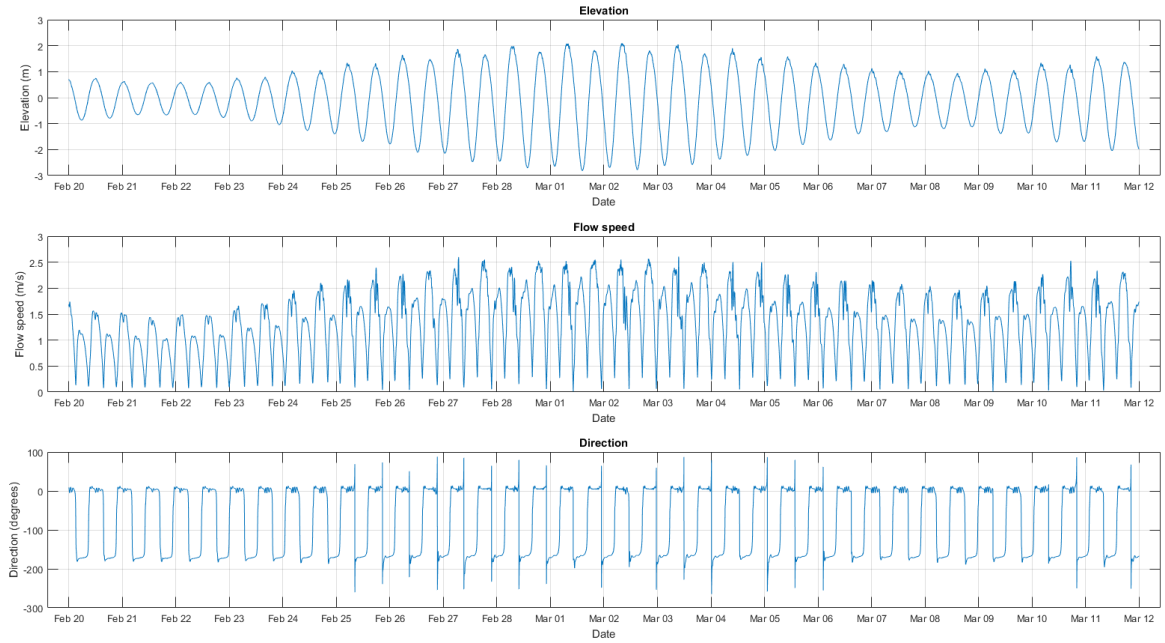

Figure 3.4. Example Thetis outputs provided to Cambrian Offshore to aid operational planning.

3.2.6.4 Energy system modelling (Task 4)

A variety of *Thetis* regional scale models covering high tidal stream resources have been used to derive power time series data for projects across the UK. The spatial extent of the models is shown in Figure 3.5. This power time series derived from the *Thetis* outputs have been used as inputs to energy system modelling (Frost, 2022, Pudjianto et al., 2022, Pennock et al., 2022, Coles et al., 2021c).

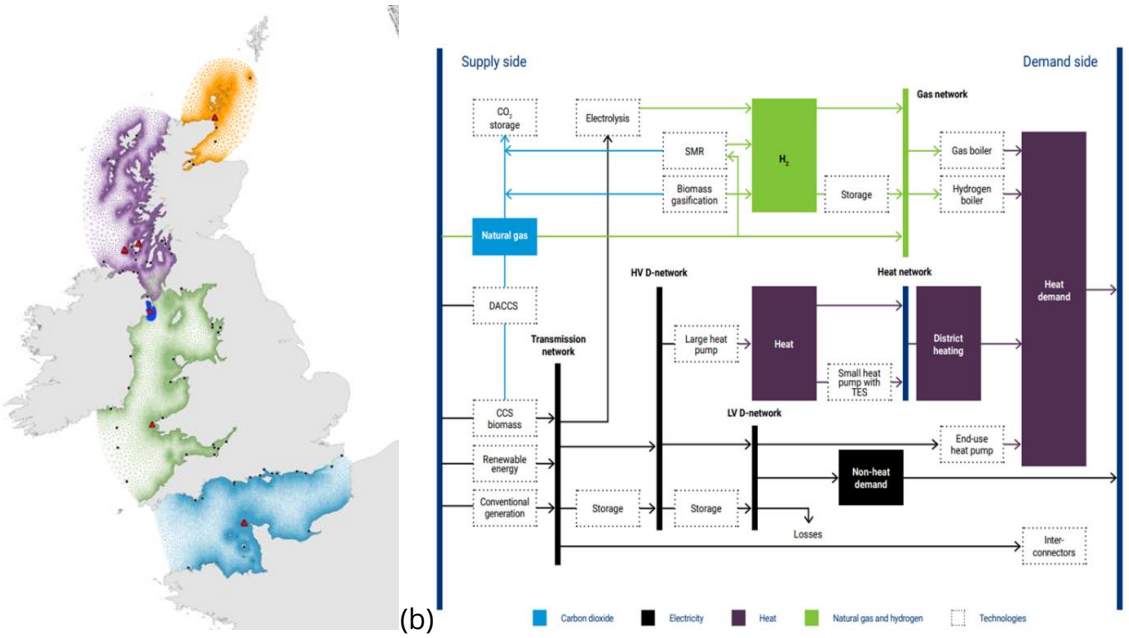

Figure 3.5. (a) Overview of regional scale Thetis domains around the UK covering the Pentland Firth and Orkney Waters (orange), West Scotland (purple), Irish Sea (green) and English Channel (blue), (b) Integrated whole energy system (IWES) model (Pudjianto et al., 2022)

3.2.6.5 Array shape optimisation (Task 5)

Thetis modelling has been undertaken to establish the sensitivity of array annual energy yield to array shape, using the continuous drag approach to array modelling. This work is being undertaken for Orbital Marine Power, so array drag is parameterised using the drag characteristics of the O2 device. Figure 3.6 provides an illustration of the different array shapes that have been simulated within *Thetis*, with characteristics summarised in Table 3.4. This work has initially used the Alderney Race as a case study site.

Table 3.4. Summary of energy yield estimates from Thetis for arrays of varying shape within the Alderney Race.

No. rows	Turbines per row	Array width [m]	Array length [m]
2	48	9640	195.5
4	24	4792	586.5
6	16	3176	977.5
8	12	2368	1368.5

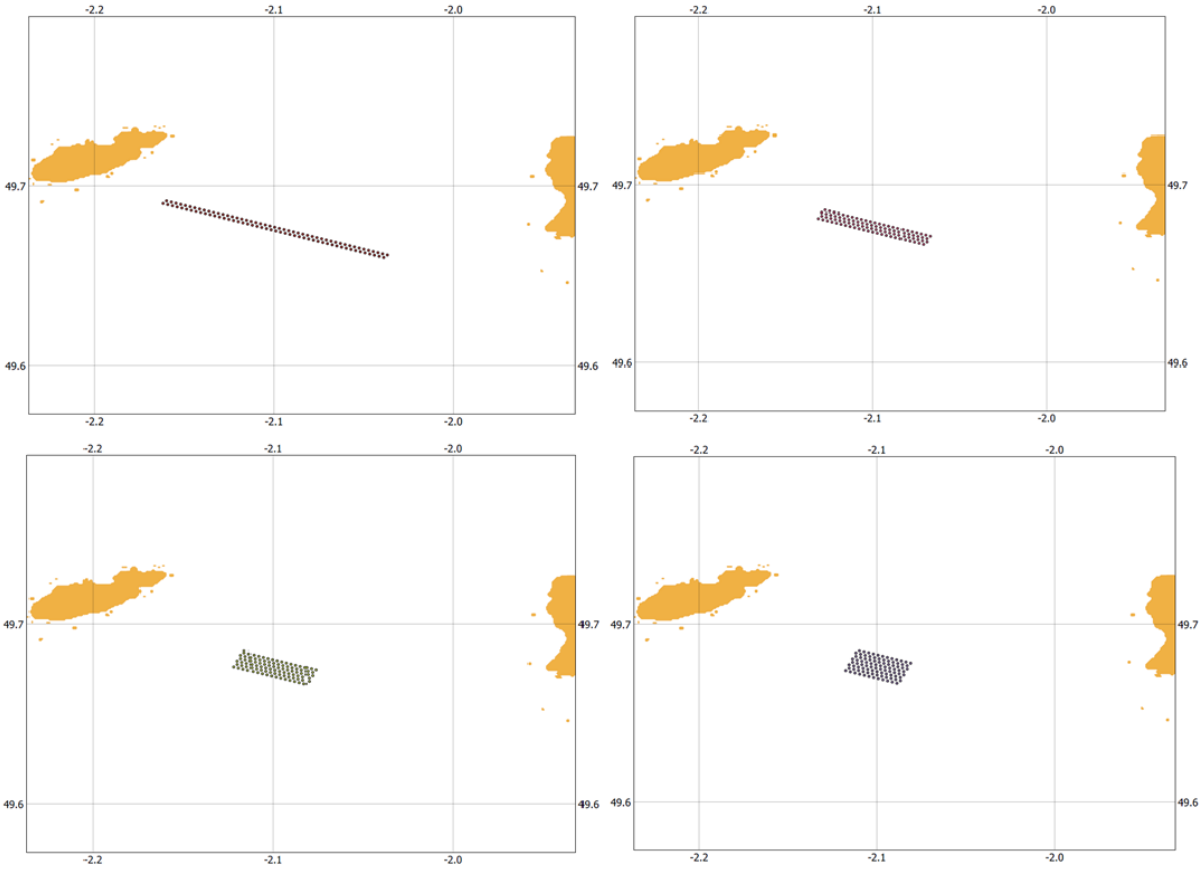

Figure 3.6. Summary of array shapes simulated in Thetis.

3.2.6.6 Resource assessment – surrounding sites (Task 6)

The *Thetis* model has been used to simulate the tidal flows at sites surrounding the Ramsey Sound. This work has been undertaken to help establish the viability of tidal stream energy development in the Pembrokeshire region, and has been undertaken in collaboration with the ORE Catapults, who have extended their practical constraint modelling work undertaken

at the Ramsey Sound to the surrounding regions. Figure 3.7 shows the practical constraint mapping, which has highlighted St David's Head, North Bishop and Ynes Bery West as potential sites for tidal stream energy development, based on consideration such as depth, sea bed slope, flow speeds, shipping lanes and conservation areas.

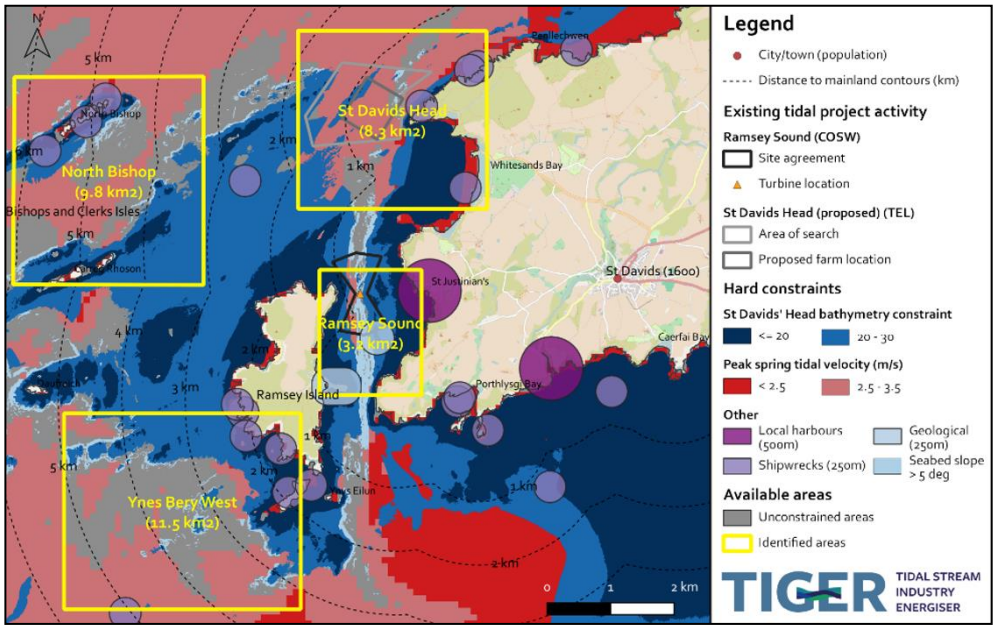

Figure 3.7. Practical constraint mapping of the Ramsey Sound, St Davids Head, North Bishop and Ynes Bery West, based on flow speed outputs from Thetis *modelling.*

4 Palabos LBM-LES: University of Caen Normandy

4.1 Overview of model and intended use

Palabos is an open-source software that implements the lattice-Boltzmann method (LBM) (Latt et al., 2021). It solves the Boltzmann equation on Cartesian grids and includes a sub-grid model (static Smagorinsky model (Malaspinas et al., 2012)) to perform large-eddy simulations (LES).

The model is used for the simulation of turbulent tidal flows at high temporal and spatial resolutions (respectively ~0.005s and ~0.3m) and over short spatial and temporal extents (respectively ~0.5km² and ~30min). The purpose is to characterise the turbulence generated at the seabed. This simulation characteristics result in heavy meshes (~200 million mesh nodes) and require adequate computational means (500 GB to 1 TB of available random access memory, 15000 to 50000 CPU hours).

The model cannot handle temporal variations of the sea level, waves and variations in the overall flow direction. It should be used over areas and timescales where the time averaged flow direction is roughly uniform. It can be used to provide information for studies assessing the flow-turbine interaction.

4.2 Description of model

4.2.1 Spatial settings

The grid is 3-dimensional and Cartesian. The simulation domain is split into zones of different mesh resolutions. These resolutions are necessarily proportional to the finest resolution by a power of two factor. Typical simulations can cover around 0.5km² for typical tidal flow site depths. The domain must be long enough for the turbulent process to be able to fully develop and reach the surface (~1km) (Mercier et al., 2020a). The domain must be wide enough to prevent near-boundary issues and in order not to constraint the flow (~0.5km) (Mercier et al., 2021b).

The grid resolution must be fine enough to capture the unsteady phenomenon generated near the seabed. Typically, the volume near the seabed must have a resolution around 0.3m and the volume near the sea surface can be coarser (0.6m). The sites of interest can be refined for a better mesh resolution. However, a given obstacle (including the full seabed) must be fully contained in a domain of constant mesh resolution.

An illustration of the mesh for the Paimpol-Bréhat site is shown in Figure 4.1. The mesh resolution is indicated by squares of various sizes. Each square edge consists of 28 mesh nodes. The illustration highlights the difference of resolution between a refined zone near the seabed and a coarser zone near the surface. The mesh resolution relative to the seabed obstacles is visible in Figure 4.2, were each square denotes a mesh node. The refined zone follows the variations in elevation of the seabed.

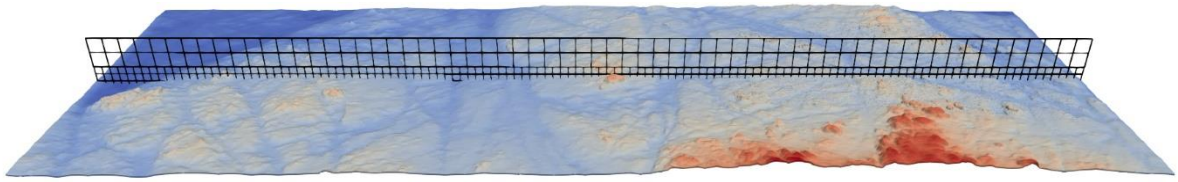

Figure 4.1. Domain bathymetry and overview of the mesh zones. The black square edges consist of 28 mesh nodes.

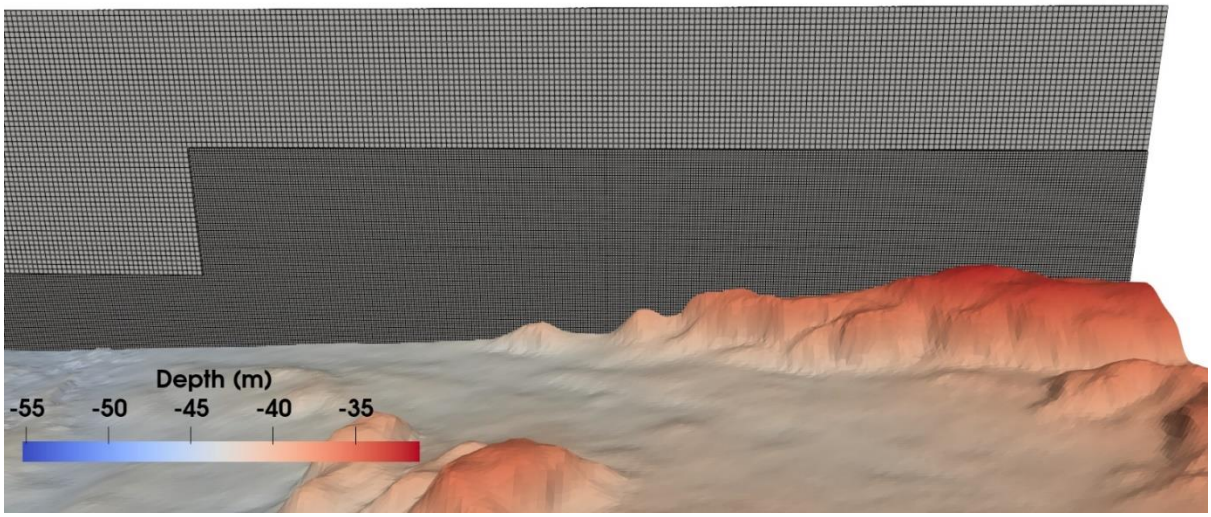

Figure 4.2. Detail of the Palabos LBM-LES mesh for the Paimpol-Bréhat site.

4.2.2 Temporal settings

The model can cover periods of time of the order of a few tens of minutes. This period is chosen as it is long enough to extract converged turbulent statistics (typically 10 minutes in established flow regimes). It should not be much longer because the model does not handle variations in the sea elevation or in the overall flow direction.

The time step is fixed and is proportional to the mesh resolution. It thus differs from one refinement zone to another. Near the seabed, it is typically around 0.005 second. It must be small enough to guarantee the numerical stability: the Courant–Friedrichs–Lewy (CFL) number should be less than 0.1. Typically, we chose a CFL number of 0.075.

The output time step is customisable and depends on the application. For example, a unique output of the whole simulation domain at the end of the simulation for the analysis of average quantities, or high frequency outputs, possibly over constraint zones, to feed in other simulation models or to investigate turbulence phenomena.

4.2.3 Representation of tidal turbines

Turbines are not represented in Palabos in the scope of the TIGER project. It is however possible. The most adequate model is the actuator line method (Grondeau et al., 2019), as it would generate realistic unsteady wakes that can be captured by the LBM-LES model. Blade-resolved CFD would be too computationally expensive due to the Cartesian mesh (Grondeau

et al., 2020; Grondeau et al. 2022). Actuator disk theory could be used (Nguyen et al., 2016) or alternatively Blade Element Momentum Theory (Khaled et al., 20221) would also be feasible.

4.2.4 Inputs and Boundary Conditions

The water level is constant in Palabos simulations. Its value must be provided, from measurements or regional simulations. The top boundary condition is a free-slip, supplemented with a zone of increased viscosity to prevent numerical instabilities. Thus, wind or wave effects cannot be included in this model.

The flow velocity is ideally provided by ADCP measurements. This velocity is reached in the simulation either through the convergence of the flow velocity around a target value in the case of periodic longitudinal boundaries, or by the choice of the inlet boundary condition. In any case the velocity fluctuates at the beginning of the simulation, due to the generation of turbulence, until it reaches an established flow regime. In the case of periodic boundaries, a volume force is applied on the whole simulation domain and is controlled by the flow velocity: the force increases at the beginning of the simulation because the increasing level of turbulence slows down the flow. When both the flow velocity and the volume force reach a steady state, the flow regime is considered to be established. This occurs typically after 10 to 20 minutes of simulated time. In the case of an imposed inlet velocity, turbulence should be injected using the synthetic eddy method (Poletto et al., 2013). In this case, the flow characteristics should only be studied far enough from the inlet, to let the seabed-generated turbulence reach the upper part of the water column.

The bathymetry should be fine enough for the model to capture turbulent phenomenon occurring in the vicinity of the seabed macro-roughness (typically ~1m). It must be provided to the model in the form of a .stl file of length and width slightly shorter than the simulation domain, and a thickness higher than 2 to 3 mesh nodes. The seabed is modelled as a no-slip boundary condition (Bouzidi et al., 2001).

4.2.5 Outputs

Various output can be extracted from the simulations, including instantaneous quantities (velocity, vorticity, lambda2 criterion, relative pressure) and time-averaged quantities (velocity, Reynolds tensor). Reductive operations can also be performed over user-defined domain, such as the calculation of the maximum, minimum or spatial average of a given quantity.

The outputs can be saved at single points (which is recommended if a high output frequency is required), or on user-defined 2D or 3D sub-domains of any dimensions, potentially the whole simulation domain. In the case of large volume of output, it is recommended to moderate the frequency of extraction to avoid flooding the computer memory.

A study of the effects of the spatial and temporal variations of the flow characteristics was reported in Mercier and Guillou (2022). It reveals the large impact of the bottom morphology on the hydrodynamic characteristics at the turbines' location in a farm in the Paimpol-Bréhat site (Figure 4.6). Moreover, a visualisation of the time evolution of the turbulent eddies in such

a flow was is shown in Figure 4.7 for a site in the Alderney Race, illustrating the formation of large boils over the area (Mercier and Guillou, 2021).

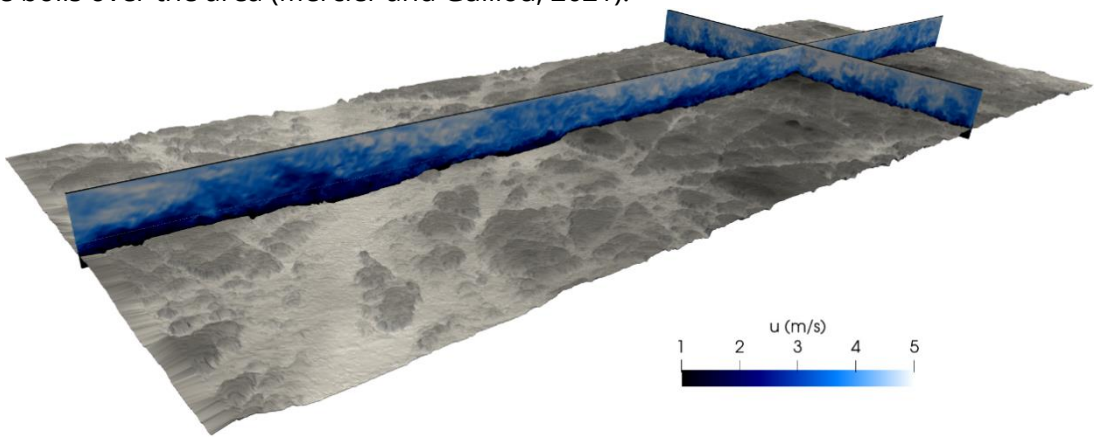

Figure 4.3. Visualisation of the instantaneous longitudinal velocity in the Raz Blanchard using Palabos LBM-LES (Mercier et al., 2021b).

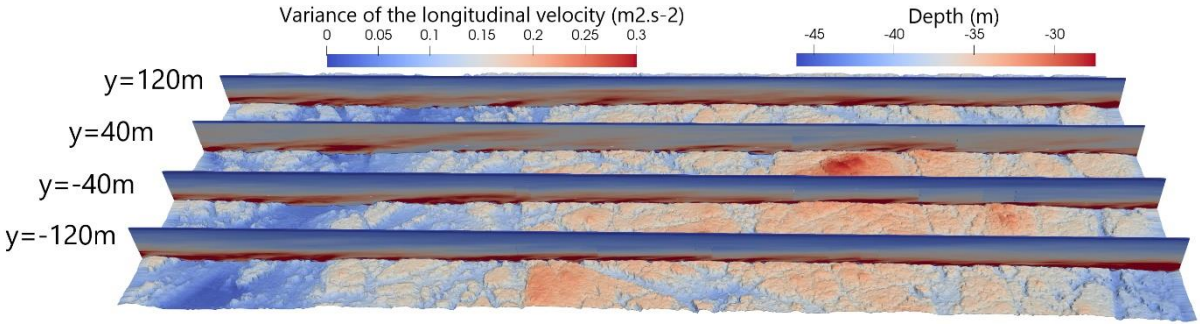

Figure 4.4. Visualisation of the variance of the longitudinal velocity in the Raz Blanchard using Palabos LBM-LES (Mercier et al., 2021b).

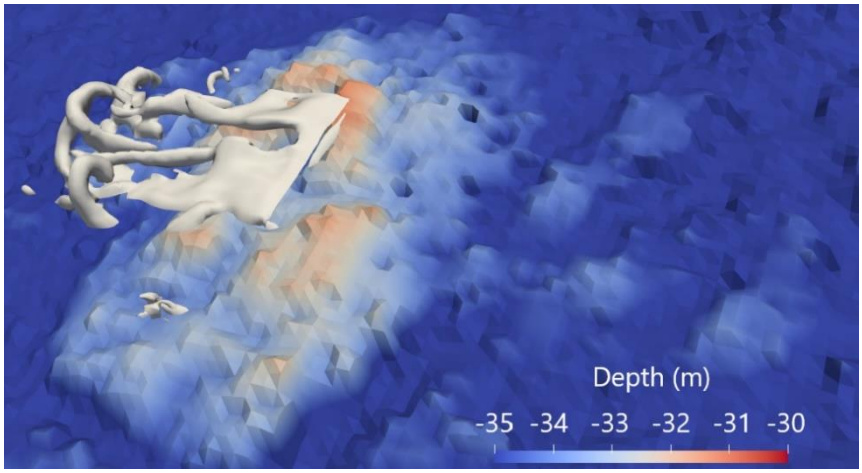

Figure 4.5. Lambda2 visualisation of vortices in the wake of a seabed roughness in the Raz Blanchard using Palabos LBM-LES (Mercier et al., 2020a)

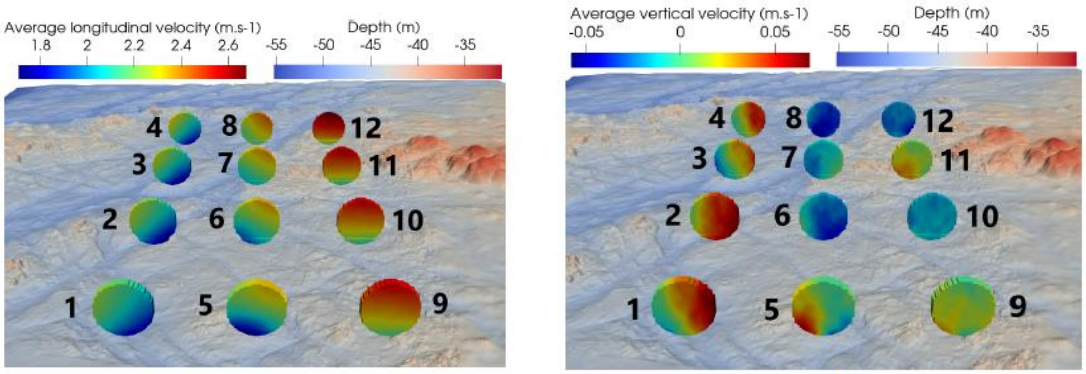

(a) Longitudinal velocity. (b) Vertical velocity.

Figure 4.6. Time-averaged velocity over the disks representing the turbines at the Paimlpol-Bréhat site using Palabos LBM-LES (Mercier and Guillou, 2022).

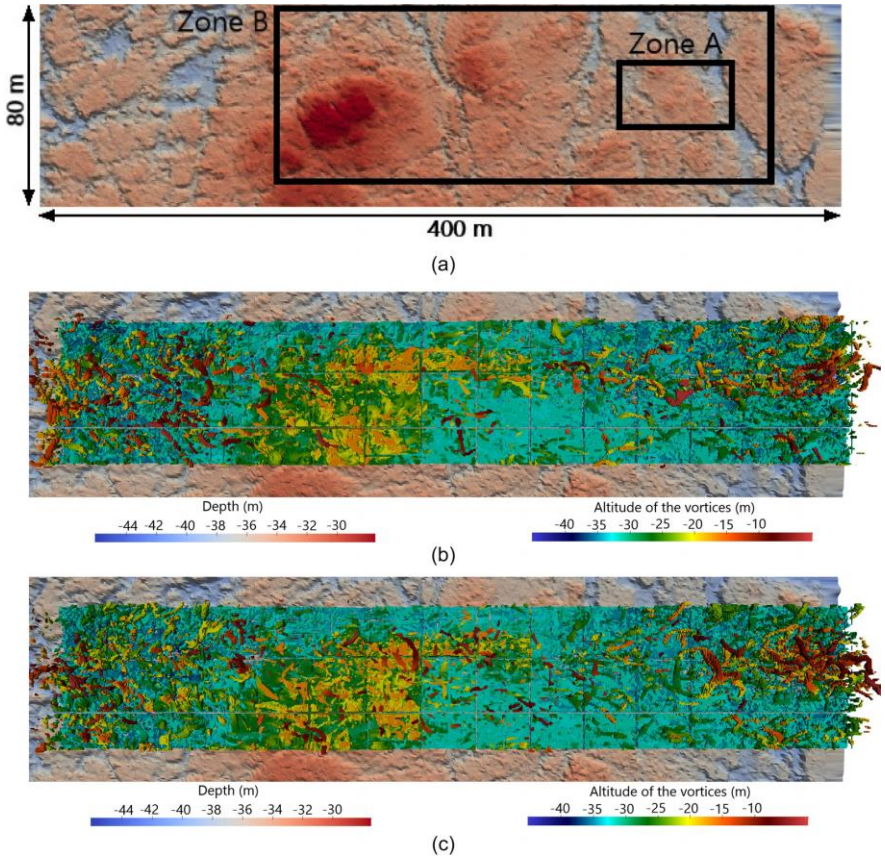

Figure 4.7. Turbulent structure visualization on a reduced area. (a) Detail of the bathymetry. (b) Visualization of a vortex trail. (c) Visualization of a large coherent flow structure using Palabos LBM-LES (Mercier and Guillou, 2021)

5 Telemac: University of Caen Normandy

5.1 Overview of model and intended use

Telemac is an open source model of free surface flows. It solves the shallow water equations (Telemac2D) or the Reynolds-Averaged Navier-Stokes (RANS) equations (Telemac3D) using the finite element method. In addition to the standard versions of Telemac2D/3D, UCAEN develops an "in-house" version of the code permitting to perform Large Eddy Simulation (LES) (Bourgoin et al., 2019, 2020). The LES version of the code permits to characterise both the time-mean and the fluctuating part of the current velocities.

Within the TIGER project, Telemac is used to simulate the tide propagation, the resulting currents and hence the tidal resource. The LES version is used to characterize the ambient turbulence. We study three tidal-stream energy sites: Raz Blanchard, Paimpol Bréhat and Gulf of Morbihan.

In addition to characterizing ambient flow conditions, we use different techniques to simulate turbines. For large (regional) scale studies, we simulate turbines with an enhanced friction term spread out over the tidal array (Thiébot et al., 2015). For wake-field studies (regional and turbine scales), we represent each turbine independently with an actuator disk formulation (Thiébot et al., 2016, 2020, 2021, Djama Dirieh et al., 2022).

Within the TIGER project, the following models have been used:

- Telemac2D to characterize the resource of the Raz Blanchard and to analyse the effect of energy extraction on the resource using an enhanced friction term. Results will feed into the techno-economic analysis of the site being conducted by ORE Catapult.
- Telemac2D to assess the resource of the Gulf of Morbihan.
- Telemac2D and 3D to assess the resource of the Paimpol-Bréhat site.
- Telemac3D to characterize the hydrodynamics and resource of the Alderney Race. Outputs are used by UoM for a cross-comparison of different models and by SIMEC Atlantis to aid the deployment and recovery of an ADCP.
- Telemac3D to assess the energy yield of the Raz Blanchard considering different turbine deployment scenarios (Thiébot et al., 2021, Djama Dirieh et al., 2022)
- Telemac3D-LES to characterize the hydrodynamics of the Alderney Race, focussing in particular on the turbulence (Guillou et al., 2021).

Telemac2D focuses on comparable scales as Delft (UoEx) or Thetis (UoP). In the configurations used in TIGER, waves and meteorological forcing are neglected (in contrast to the work being carried out at UoEx). For turbine modelling, the enhanced friction approach is used in a similar way in Thetis (UoP). The Telemac3D model presented here, includes a representation of tidal turbines as actuator disks, to simulate turbines within a regional model.

5.2 Description of model

5.2.1 Spatial settings

Telemac uses unstructured mesh layouts. For Telemac2D and 3D, a cell size ranging from 10 km to 10 m is used. With Telemac3D-LES, a cell size of up to 1 m is used in the studied zone. A comparable cell size (1m) is also used when implementing actuator disks in Telemac3D.

A Telemac2D model covering the English Channel (Figure 5.1) has been created. It includes the Raz Blanchard and the Paimpol-Bréhat sites. Another domain is used for the Gulf of Morbihan (Figure 5.2). Information about existing model configurations are summarised in Table 5.1.

Table 5.1. Tidal-stream energy sites and model (X indicates that a model configuration exists). The cell sizes are indicated between brackets. For the Raz Blanchard, the cell size is refined up to 1m when using actuator disks.

	Raz Blanchard	Paimpol Bréhat	Gulf of Morbihan
Telemac2D	X (10 km – 100 m)	X (10 km – 100 m)	X (10 km – 10 m)
Telemac3D	X (10 km – 100 m)	X (10 km – 100 m)	
Telemac3D-LES	X (10km – 1m)		

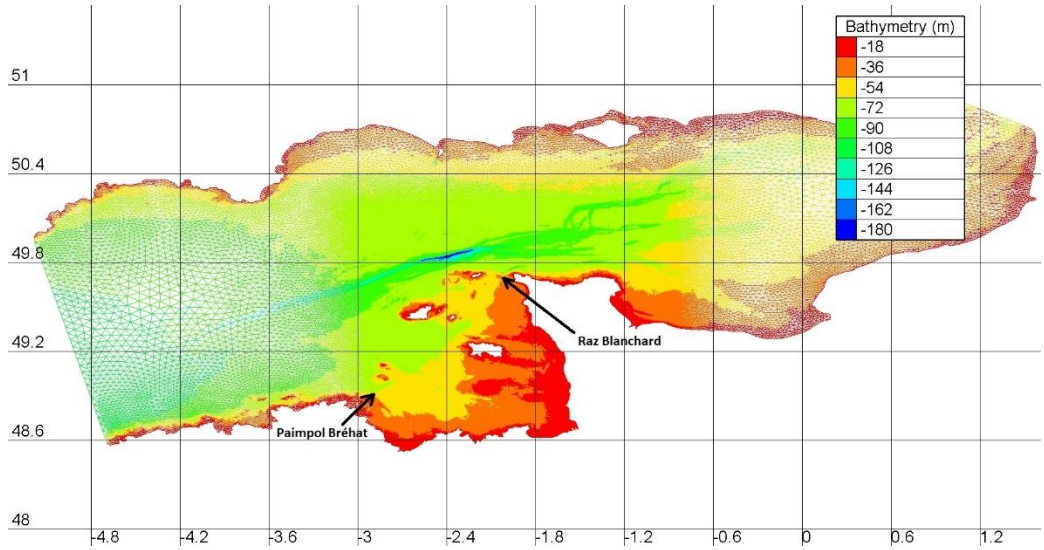

Figure 5.1. Telemac computational domain used for the Raz Blanchard and the Paimpol Bréhat sites.

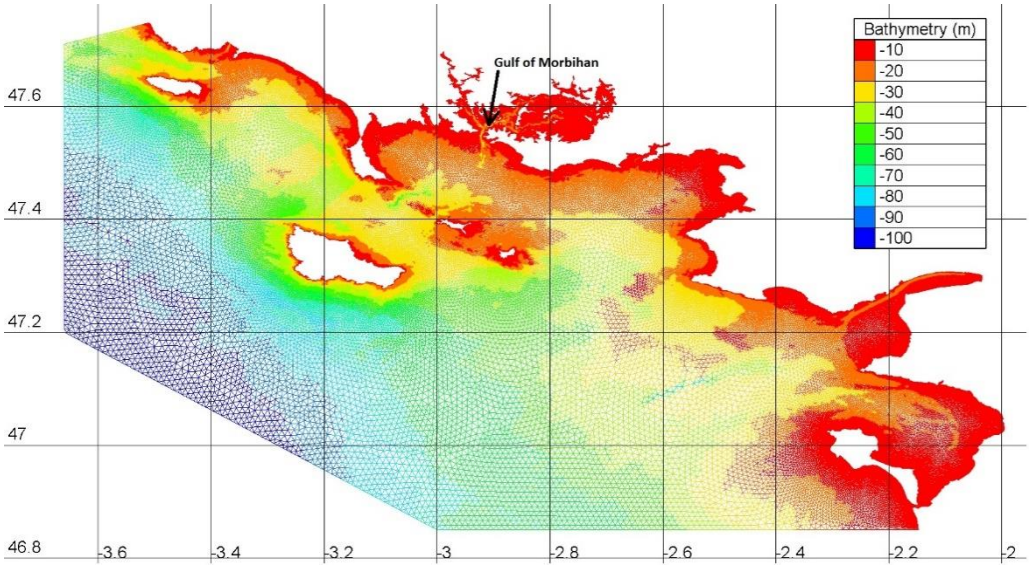

Figure 5.2. Telemac computational domain used for the Gulf of Morbihan.

5.2.2 Temporal settings

The Telemac model configurations used in TIGER are massively parallelized. They are run using hundreds of cores. Simulations are run on the CRIANN supercomputer (Normandy region). According to the available computational resource, simulations are run over periods of up to one year for Telemac2D and 1 month for Telemac3D. For the LES version of Telemac, only two tidal cycles are simulated due to the computational requirements.

The time step is set such that the CFL number is smaller than 1. The results are extracted every 10 or 15 min for RANS simulations (Telemac2D and Telemac3D). For LES, the results are extracted every 1 seconds at specific locations (where ADCP are deployed for instance) to compute turbulence proxies (e.g. velocity variance).

5.2.3 Representation of tidal turbines

In Telemac2D, the turbines are represented with an enhanced friction term spread out over the zone occupied by the tidal array (Thiébot et al., 2015). In Telemac3D, turbines are represented by actuator disks (Thiébot et al., 2016, 2020, 2021, Djama Dirieh et al., 2022). For the large scale investigations using Telemac2D, the scenarios of energy extraction in the Raz Blanchard have not yet been defined. For the simulations with Telemac3D and actuator disks, either a single fence of turbines has been studied (Figure 6.3; Thiébot et al., 2021) or two arrays containing up to 30 turbines deployed with either a staggered or an aligned layout (Figure 6.4; Djama Dirieh et al., 2022). Telemac3D-LES is run without turbines.

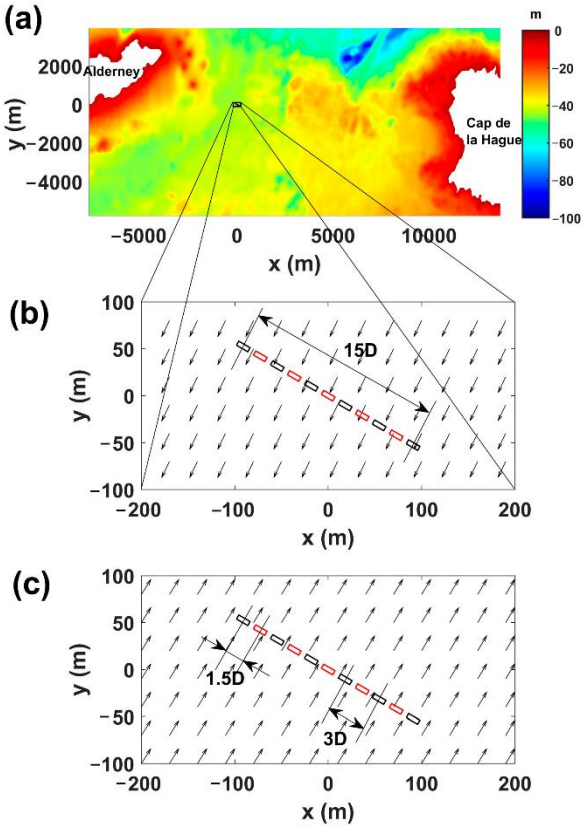

Figure 5.3. Scenario of turbine deployment simulated with actuator disk in Telemac3D (Thiébot et al., 2021).

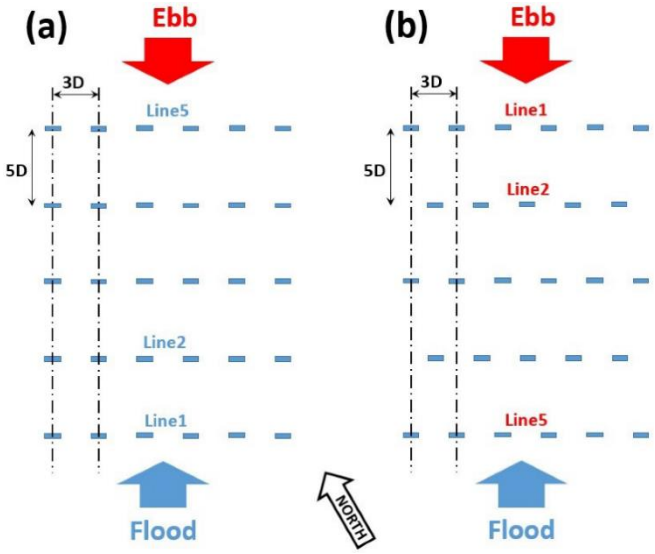

Figure 5.4. Scenario of turbine deployment studied with actuator disks (Djama Direih et al., 2022): (a) aligned and (b) staggered layout.

5.2.4 Inputs and Boundary Conditions

The input data are the bathymetry, the bed roughness (estimated from sediment maps) and tidal constituents. The TPXO database is used to predict sea level and current velocity at the domain boundary. Meteorological and wave effects are not included in the models.

5.2.5 Outputs

For Telemac2D, the outputs are (time-mean) depth-averaged current velocities and water depth. For Telemac3D, the outputs are (time-mean) water depth and current velocities at different vertical elevations. For Telemac3D-LES, the outputs are the same as in Telemac3D, but the fluctuating part of the current velocity (velocity variance) can also be extracted. As an example, the correlation between the bottom morphology and the turbulence at 10m above the bottom is shown in (Figure 5.5). Moreover the components of the Reynolds tensor are also available (Bourgoin et al., 2020).

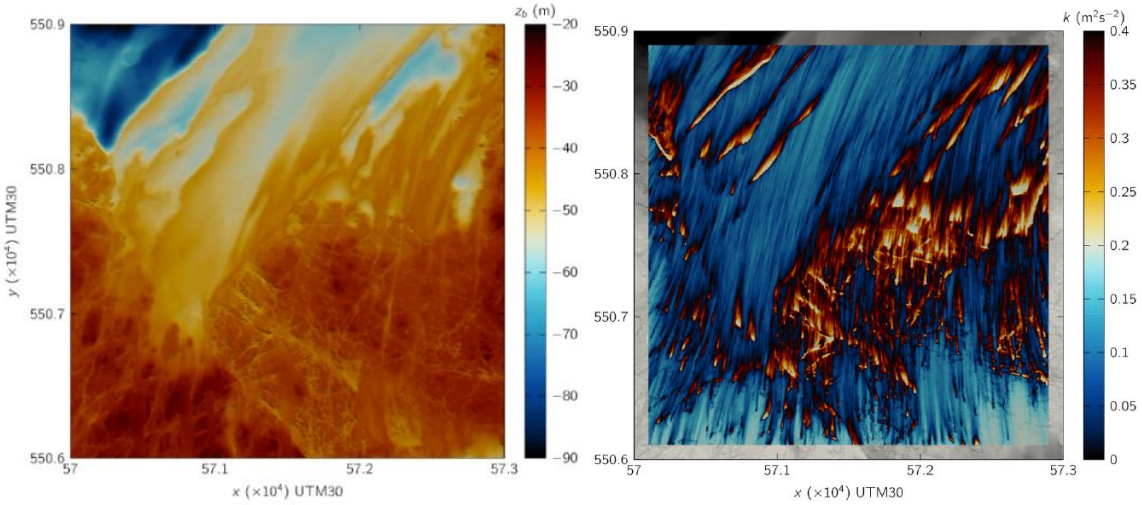

Figure 5.5. Left: Bathymetry over an area in the Alderney Race. Right: Spatial distribution of instantaneous turbulent kinetic energy at 10 m above the seabed on flood peak (Bourgoin et al., 2020).

The model can provide data about current velocity and turbulence intensity, as provided in the Alderney Race in Guillou et al. (2021). This work showed the impact of the seabed variation on the hydrodynamic and turbulence characteristics (Figure 5.6 and Figure 5.7) and reveals the effects on the turbines.

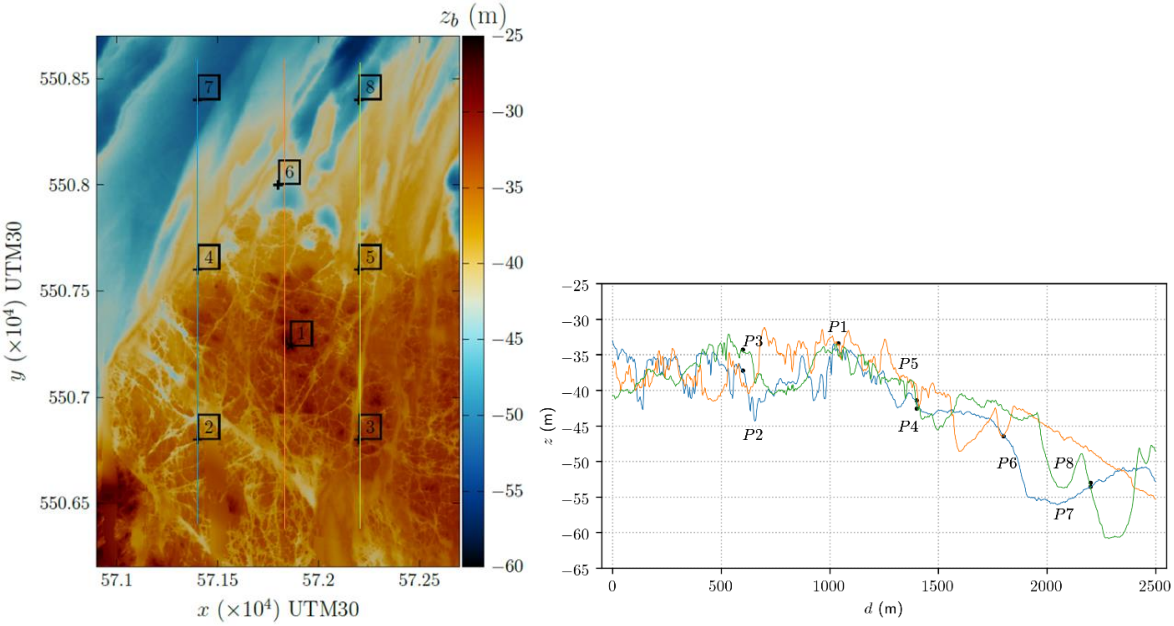

Figure 5.6. Left: Seabed elevation relative to mean sea level. Right: Bathymetry profiles along North-South coloured lines shown on left.

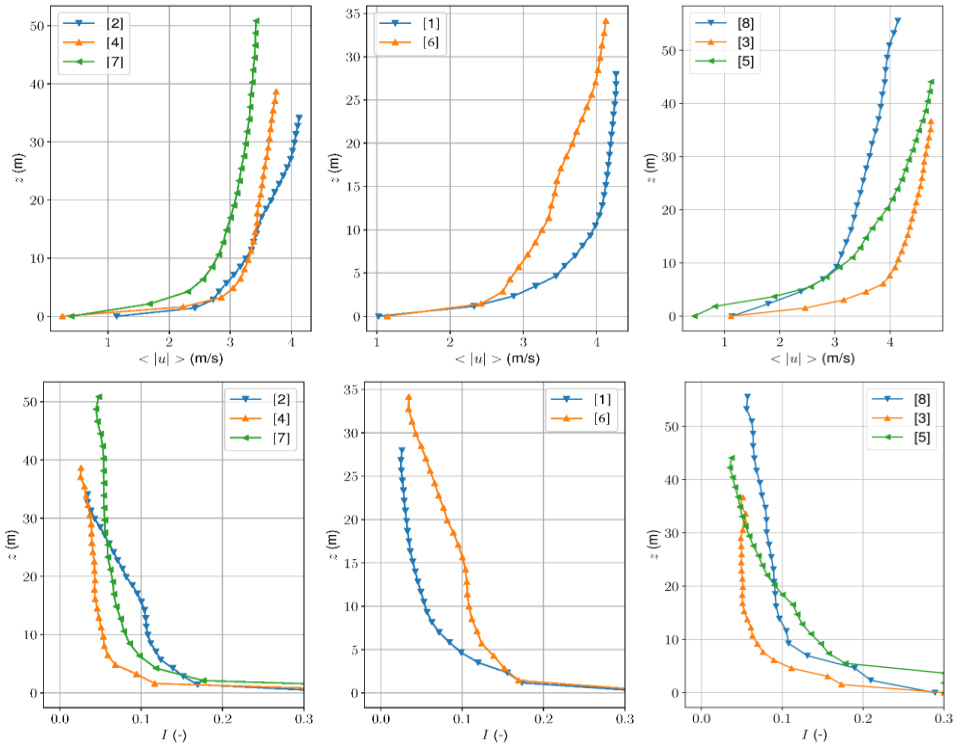

Figure 5.7. Vertical profiles of velocity magnitude (top) and turbulence intensity (bottom) at flood peak, for locations shown in Figure 5.6.

6 DOROTHY: University Le Havre Normandy

6.1 Overview of model and intended use

The in-house simulation code DOROTHY is based on a Lagrangian Vortex Particle Method (Pinon et al. 2012; Choma Bex et al. 2022). The Vortex Particle Method uses a Lagrangian resolution of the fluid domain, discretized into fluid particles representing the vortex perturbation of the flow. The particles are advected using Runge-Kutta time stepping schemes. Redistributions of the fluid particles on a regular Cartesian grid are carried out every few iterations to maintain a homogeneous distribution of the particles over the flow domain. The main governing equations of this method are the Navier-Stokes equations, with the assumptions that the flow is incompressible:

$$div\ \vec{u} = 0$$
$$\overrightarrow{rot}\ \vec{u} = \vec{\omega}$$
$$\frac{\partial \vec{\omega}}{\partial t} + (\vec{u} \cdot \vec{\nabla})\vec{\omega} = (\vec{\omega} \cdot \vec{\nabla})\vec{u} + \nu\Delta\vec{u}$$

where u is velocity, t is time, ω is vorticity and ν is kinematic viscosity.

The current implementation also includes a Large Eddy Simulation type diffusion model, implemented via a Particle Strength Exchange (PSE) model. Until recently, DOROTHY exclusively used a panel method for a simplified zero-thickness representation of the turbine blades (Pinon et al. 2012). However the computation of loads with this method has proven difficult and required improvements to the representation of the turbine blades.

In the meantime and over the course of the TIGER project, a new representation of the turbine blades has been implemented using the lifting line method. Details of the lifting line are available in Katz and Plotkin (2001), while the implementation within the Vortex Particle Method is close to the implementation of the lifting line within vortex panel methods such as the ones described in Shaler et al. (2020) or van Garrel (2003). The model is referred to as the Lifting Line Vortex Particle Method (LL-VPM).

The lifting line method relies on the fact that lifting bodies generate a circulation. By including the circulation, it is then possible to build the vortex perturbation of the flow generated by the blade. Once the flow velocity $\overrightarrow{v_{rel}}$ is known, including the induction from the previous time steps, efforts on the blade profile are estimated using lift and drag coefficients. This workflow is illustrated in Figure 6.2. The main equations driving the lifting line are:

- The blade circulation: $\Gamma_{B,k} = \frac{1}{2}\, c\, |\overrightarrow{v_{rel}}|\, C_L$
- Trailing circulation: $\Gamma_{T,k} = \Gamma_{B,k+1} - \Gamma_{B,k}$
- Spanwise circulation: $\Gamma_{S,k} = \Gamma_{B,k}(t) - \Gamma_{B,k}(t - dt)$
- Particles vorticity weight: $\overrightarrow{\Omega_{T,k}} = \Gamma_{T,k} dt\, \overrightarrow{v_{rel}}$ and $\overrightarrow{\Omega_{S,k}} \simeq \Gamma_{S,k} \overrightarrow{dr}$

where $\Gamma_{B,k}$, $\Gamma_{T,k}$, $\Gamma_{S,k}$ are respectively blade, trailing and spanwise circulations for a blade section k, c is its chord, C_L is its lift coefficient, dt is the timestep duration, dr is the radial section length, $\Omega_{T,k}$ and $\Omega_{S,k}$ are respectively the trailing and spanwise particles vorticity weights for the given blade section k.

Figure 6.1 shows how the common lifting line associated to vortex panels is translated into vortex particles in DOROTHY. Blade spanwise and trailing circulation are represented with particles placed at the center of the represented filament. Blade and spanwise circulation are in a direction along the blade, the trailing circulation corresponds to the circulation along the velocity flow.

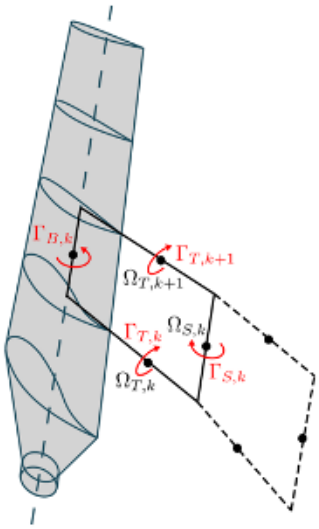

Figure 6.1. Representation of a blade inside the Lifting Line Vortex Particle Method code with the circulations and vortex particles.

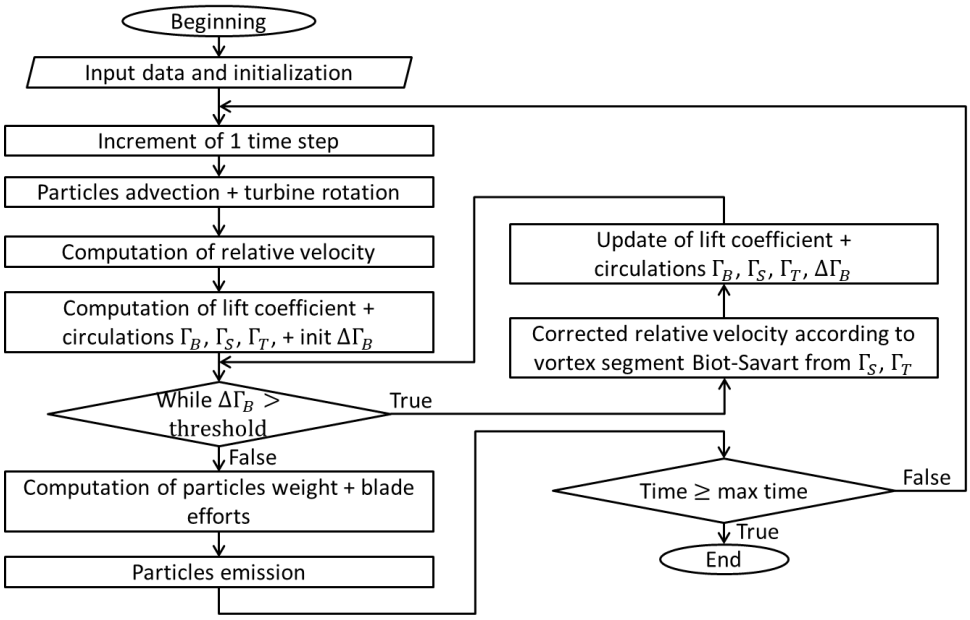

Figure 6.2. Lifting Line Vortex Particle Method flowchart.

This simulation code also includes a possibility for the representation of ambient turbulence (Pinon et al. 2017 , Choma Bex 2020 (a)), with a choice of two alternative formulations for the computation of added velocity disruptions (Choma Bex 2020 (b)): Jarrin's Synthetic Eddy Method (SEM) or Poletto's Divergence Free Synthetic Eddy Method (DFSEM) adaptation. These methods have been integrated into the Lagrangian code as an added term applied to the upstream velocity throughout the entirety of the chosen study space. They allow for the artificial reproduction of any turbulence intensity, Reynolds stress tensor, and integral length scale of turbulent behaviour in the flow.

The simulation code DOROTHY is an in-house code developed by members of the laboratory Laboratoire Ondes et Milieux Complexes of Université le Havre Normandie and IFREMER[1]. It is not a commercial code and not fully open source, although its sources may be shared within the contexts of various collaborations under the conditions of non-disclosure type agreements.

The model can be used for both performance evaluation and wake characterisation. Examples of this on the large scale configuration of the NEPTHYD project (now belonging to Normandie Hydroliennes) were presented in Slama et al. 2021 (a) and Slama et al. 2021 (b), including a four-turbine array in various inflow conditions with high levels of ambient turbulence.

More detailed studies of the fluctuation of loads along turbine blades in different inflow conditions are currently under consideration. This would allow for a better understanding of the impact of velocity fluctuations induced by different factors such as ambient turbulence, wake interaction, or shear profiles in the incoming flow on the fluctuation of loads at different points along the blades, which can be closely correlated with material fatigue.

[1] See https://wwz.ifremer.fr/code_dorothy/

Compared to blade element momentum theory, the advantage of the in-house LL-VPM is to have inherently 3D effects in the wake and a lower computational cost. Compared to LL coupled with other vortex panel methods, the advantage of the in-house LL-VPM is the ability of the code to have wake interactions between turbines, as DOROTHY has a Vortex Blob representation of the particles.

Compared to blade resolved CFD, the advantage of the in-house LL-VPM is having loads and interactions between turbines at a lower computational cost. Nevertheless, the pressure distribution is, for instance, not available from the LL-VPM model.

6.2 Description of model

6.2.1 Spatial settings

As a Lagrangian method, the VPM does not use any spatial grid. Nevertheless in order to preserve a homogenous distribution of fluid particles, redistributions are carried out at regular intervals.

According to the lifting line description shown in Figure 6.1, there are $N_{blade}(2N_{section}+1)$ emitted particles per timestep, where $N_{section}$ is the number of sections in which each blade is divided and N_{blade} the number of blades in the turbine. In the TIGER simulations with ambient turbulence there are more than 150 000 particles. Their size depends on the timestep, the turbine angular velocity, and the upstream flow velocity. The spatial domain for a simulation with ambient turbulence is a box of 8 times the radius (R) of the blade around the turbine and 24R behind. Outside this box size, particles are slowly dissipated. But as it is Lagragian, at the beginning of the simulations, shed and advected particles do not fill the whole simulation domain.

Spatial and temporal convergence studies of the base Vortex Particle Method of DOROTHY combined with the historical panel method have been carried out and presented in Pinon et al. 2012. More thorough convergence studies of the newly implemented lifting line alternative are still under way.

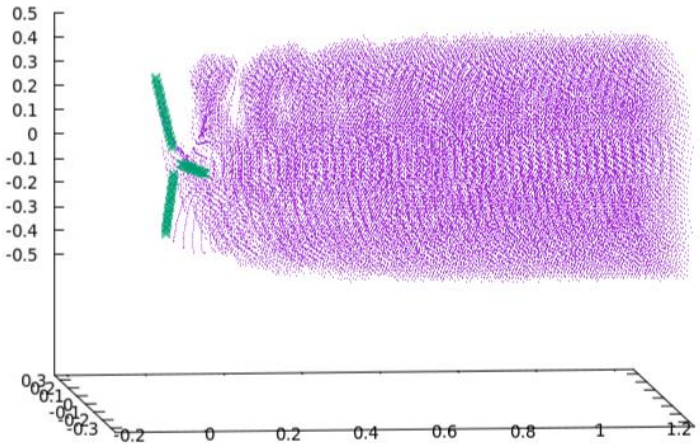

Figure 6.3. Spatial representation of the blade bound circulations and of the emitted particles, using Lifting Line Vortex Particle Method model.

6.2.2 Temporal settings

The time period is chosen by the user depending on the simulation objectives. It is commonly considered that, for a single turbine, the induction generated by the wake is steady after reaching 4 times the radius (R) of the blade. Then, if the simulation objective is to focus on the load of a single turbine, the time period should be at least $4R/U_\infty$, , where U_∞ is the upstream flow velocity. If some wake interactions are being considered, the advection time of the wake between the turbines should be taken as the reference time scale.

In the case of high ambient turbulence, longer time periods can also be considered for statistical studies of turbulence-induced fluctuations. The time step for calculation is fixed. For a horizontal turbine, the time step is chosen so that the angular discretization is less than 10° per time step: then $dt \leq \Omega/(10 \cdot \pi/180)$, where dt is the timestep and Ω is the turbine angular velocity.

The time step for all the output quantities can be chosen. Usually output loads are stored each time step of the simulation and the position and weight of particles are stored each 20 time steps. The storage frequency can be user defined instead, if required.

6.2.3 Representation of tidal turbines

In the scope of the considerations of the TIGER project, the new lifting line model is used exclusively over the panel representation, which is also still available in the simulation code. As presented in the previous sections, within this lifting line representation, the turbine blades are one dimensional and represented solely by their position and circulation generating profile. To this end, this model requires a distribution of radial position along the blades with their associated chord, twist angle and profile which can differ from section to section. Each type of profile also requires polar curves which can be Reynolds-number dependent. Polar curves are tabulated values of lift and drag coefficients for a given range of angle of attacks. These are stored as an array which gives the lift and drag coefficient for each angle of attack and a given blade profile at a given Reynolds number.

An array of four turbines was considered as a demonstration case, with the NEPTHYD proposed layout of three upstream turbines and one downstream turbine (Slama et al. 2021 (a) and Slama et al. 2021 (b)). The turbine model used for these simulations was that of IFREMER, close to the TGL model which also served as a basis for the Alstom Oceade turbines considered at the time for this project.

For the sake of comparison with other academic partners within the TIGER project, the open TGL model provided by Scarlett (2009) is currently under investigation. Wind turbine models such as the NREL-5MW reference turbine are also considered for validation purposes and convergence studies.

6.2.4 Other numerical settings

The simulation is deemed to be numerically converged when the temporal variation of the loads is below 0.5% of the actual load value.

6.2.5 Inputs and Boundary Conditions

A constant upstream flow velocity and the rotational velocity of each turbine are fixed. Fluid density and kinematic viscosity are also given. Ambient turbulence parameters (Reynolds tensor and Taylor length scale) are given for the Jarrin SEM or Poletto DFSEM.

Bathymetry effects are neglected at present. A first prospect would be to take into account velocity profiles in the water column. Wind and waves are also not considered in the current model. The use of linear (Airy) wave theory to account for orbital velocity is currently under consideration.

6.2.6 Outputs

Various outputs are available, which can be stored every n time steps. These include:

- Position and vorticity weight of all the emitted fluid particles
- For each blade section:
  - Bound, trailing and spanwise circulations;
  - Local velocity, Reynolds number and angle of attack;
  - Local C_L and C_D coefficients giving lift and drag;
  - As different projections of lift and drag: $x-axis$ and $\theta-axis$ forces plus normal and tangential to blade forces.
- Integrated values:
  - Global angle of rotation the turbine;
  - Global loads: thrust, torque and associated coefficients C_T and C_P.

Post-processing the output particle data allows to generate a map of the vorticity and velocity in the wake. With all these outputs the interaction between several turbines can be assessed. The evolution of loads along the blade over the time can also be studied. The results presented below are taken from Choma Bex et al. (2022). The radial distribution of normal force density f_n, presented in Figure 6.4, shows a good agreement for the 3 methods, which gives confidence in the LL-VPM model. However, the radial distribution of tangential force density, f_t, presented in Figure 6.5, shows some discrepancies. Nevertheless, differences of the same order of magnitude for equivalent methods are presented in similar benchmarks. BEM and LL-VPM seem to underestimate f_t mainly close to the blade root. In this region, the angles of attack can be high, thus, blade sections can be close to stall domain. Some phenomenon that can occur in this domain are not well described by C_L, C_D polar curves whereas CFD method represents them with greater accuracy.

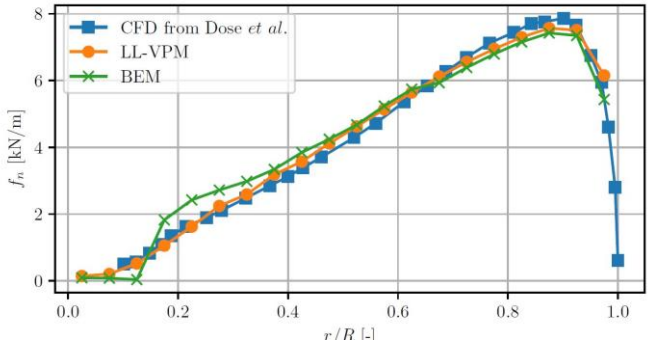

Figure 6.4. Radial distribution of normal force across a blade of the reference offshore wind turbine case NREL 5 MW. The Lifting Line Vortex Particle Method is compared to a steady BEM and a blade resolved CFD from the literature. Figure reproduced from Choma Bex et al. 2022.

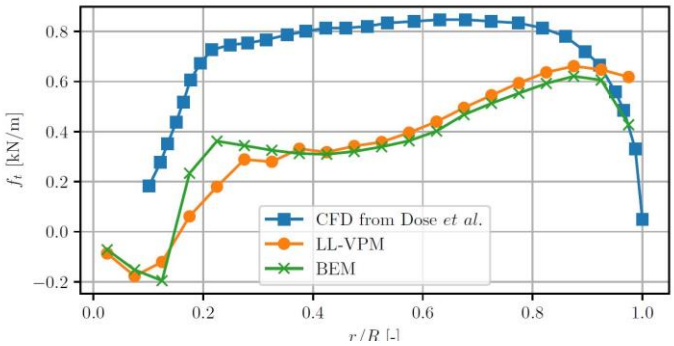

Figure 6.5. Radial distribution of tangential force across a blade of the reference offshore wind turbine case NREL 5 MW. The Lifting Line Vortex Particle Method is compared to a steady BEM and a blade resolved CFD from the literature. Figure reproduced from Choma Bex et al. 2022.

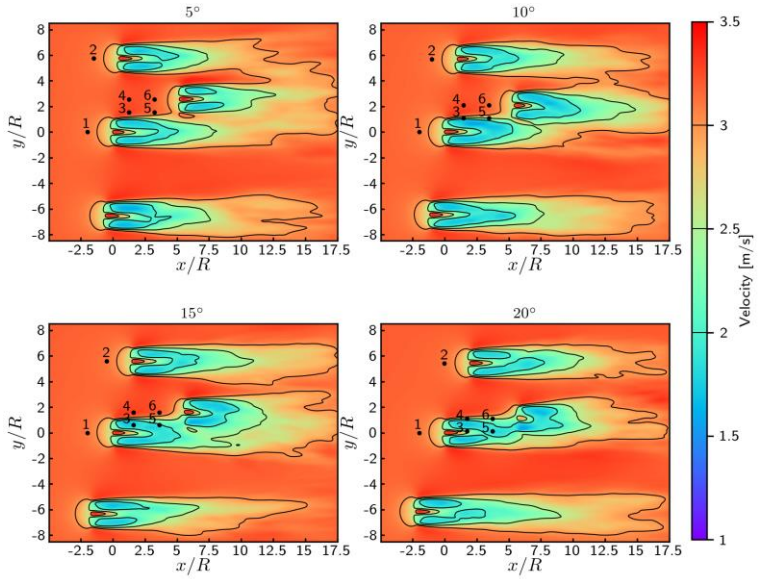

Figure 6.6. Wake characteristics of 4 tidal turbines projected to be installed in the Raz Blanchard, modelled with the Lifting Line Vortex Particle Method. This has been computed for a turbulence intensity of 10 % at different yawed flows showing the influence of the central upstream turbine on the downstream one. Figure reproduced from Slama et al. 2021.

7 MIKE 21: University of South Brittany

7.1 Overview of model and intended use

To investigate tidal stream energy potential at the Gulf of Morbihan TIGER site, a two-dimensional depth-averaged numerical model, was developed using the MIKE 21 Flow Model (MIKE 21HD), and used to simulate the tidal hydrodynamics in the area of interest.

MIKE 21 Flow Model (Mike 21HD) uses an unstructured triangular mesh to discretize the aquatic environment and is based on the Reynolds-Averaged Navier-Stokes (RANS) equations, using the Boussinesq assumption and hydrostatic pressure. It is a two-dimensional model for free-surface hydrodynamic calculations that simulates water level and flow variations, averaged over the water column, within the model domain. The MIKE 21 hydrodynamic model is used to simulate many hydraulic phenomena including tides, wind and wave induced currents, and surges. MIKE 21 HD also considers foreshore immersion and emersion phenomena (DHI, 2012).

Within the TIGER project, MIKE 21 HD is used to simulate the tide propagation and the resulting currents (hence tidal resource) at the Gulf of Morbihan.

7.2 Description of model

7.2.1 Spatial settings

In this study, the computational domain starts outside the Gulf of Morbihan on a grid similar to the one used for the TELEMAC modelling with a cell size ranging from 10 km to 10 m (c.f. Figure 5.2).
In the Gulf of Morbihan, we used two complementary bathymetries: the Litto-3D bathymetry from SHOM (2003-2004) which has a global coverage of the Gulf with a resolution of 10 X 10 m and the 2014 bathymetry carried out by UBS in the sector of the entrance of the Gulf of Morbihan with a point density of 1 X 1 m (Figure 7.1). The combination of the two bathymetries was used to produce the final bathymetry for the computational domain of the MIKE 21 model, which is presented in Figure 7.2.

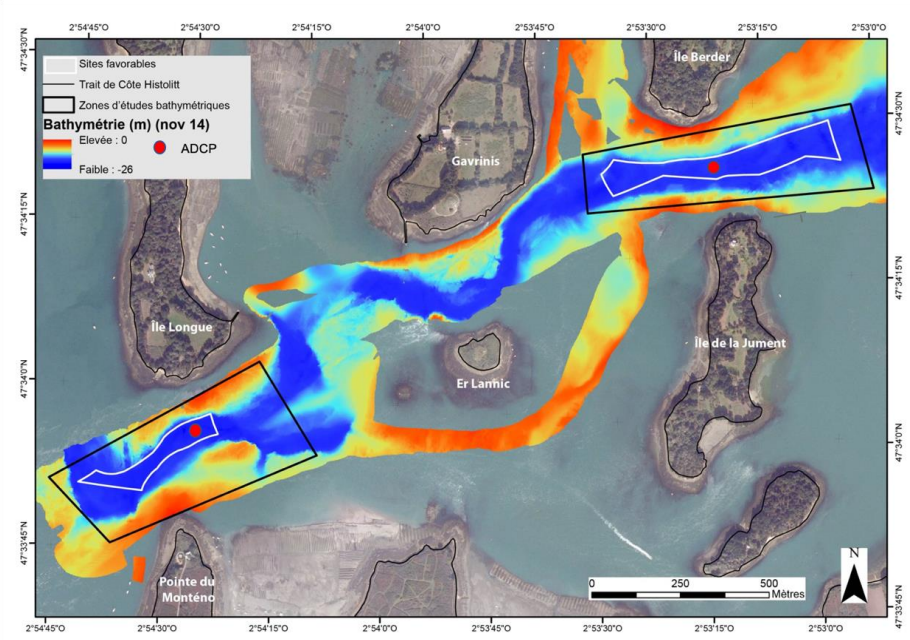

Figure 7.1. Bathymetry of the entrance of the Gulf of Morbihan (UBS-2014) with the location of the two ADCP's deployed between December 2014 and January 2015.

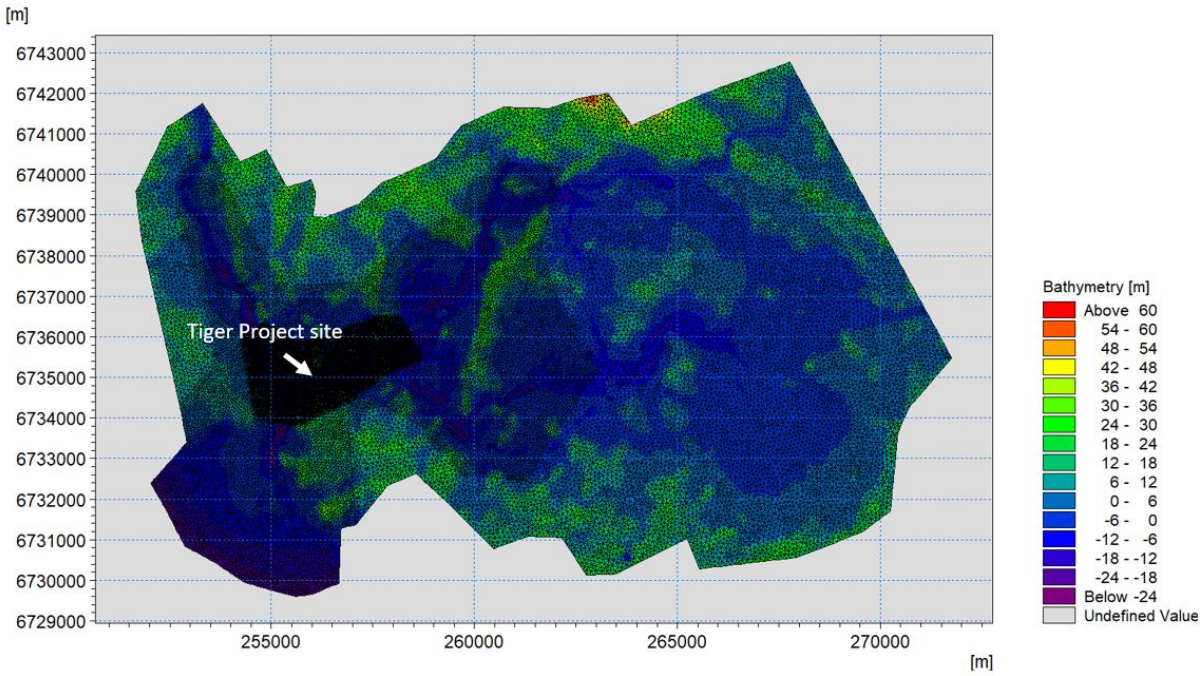

Figure 7.2. Computational mesh for MIKE 21 model.

7.2.2 Temporal settings

The Mike 21 model configuration used for the TIGER project covers a period of one month. This period was chosen to allow for optimal model calibration by incorporating measurements made by the two ADCPs deployed between December 2014 and January 2015 (Figure 7.3).

This allows harmonic analysis to be conducted to extrapolate the modelled data out to 1 year, to estimate annual energy yield. The model output variables are extracted at 10 minutes resolution to capture the temporal variability of the modelled flow speeds and directions.

7.2.3 Representation of tidal turbines

Turbines are not represented in the MIKE 21 model used for TIGER.

7.2.4 Inputs and Boundary Conditions

The input data are the bathymetry, the bed roughness (estimated from sediment maps) and tidal constituents. Meteorological: wind data and atmospheric pressure data, were collected for the Vannes area from Météo-France. To achieve viable results for water surface elevations and stream velocities, differences between model results and measurements have to be minimized to an acceptable level.

Additional hydrodynamic measurements from the two ADCPs deployed at the site (Figure 7.1) were integrated into the model to optimally calibrate the simulations. These are measurements of water level and current speed and direction (Figure 7.3).

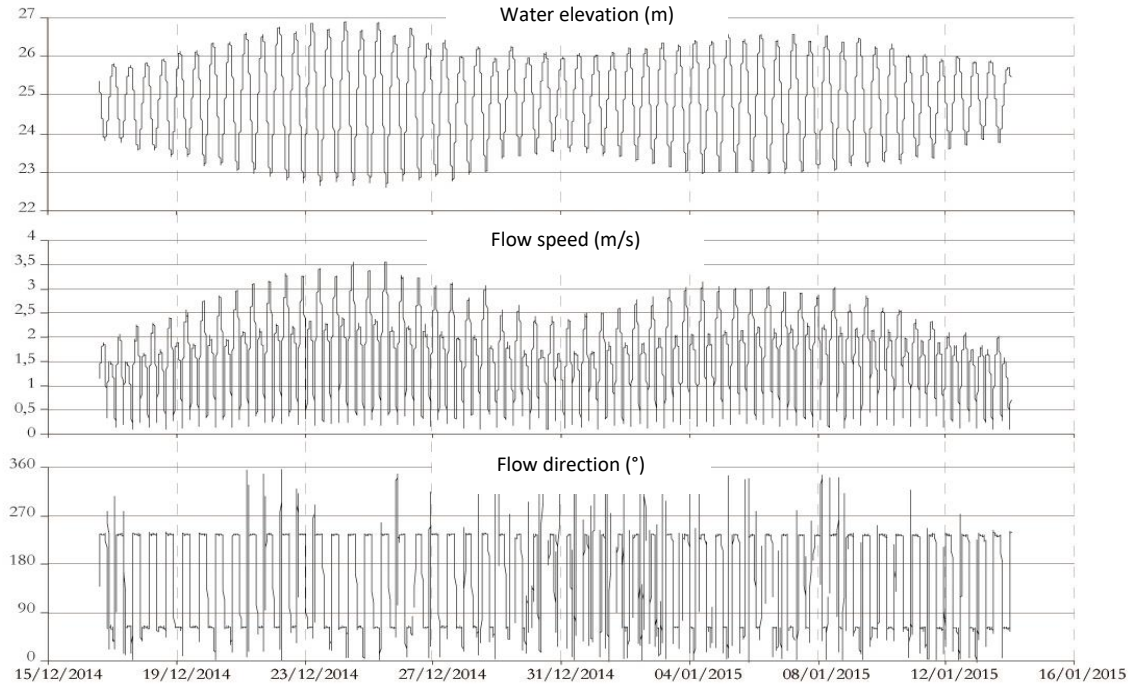

Figure 7.3. Example of the data used for model calibration: time series of hydrodynamic measurements obtained by the ADCP deployed in the TIGER site in the Gulf of Morbihan (Ile Longue site).

7.2.5 Outputs

For the MIKE 21 Flow Model, the outputs are (time-mean) depth average current velocities and water depth with a time step of 10 minutes. Data can be output over the entire Gulf of Morbihan (Figure 7.4). A zoom over the TIGER project site is shown in Figure 7.5.

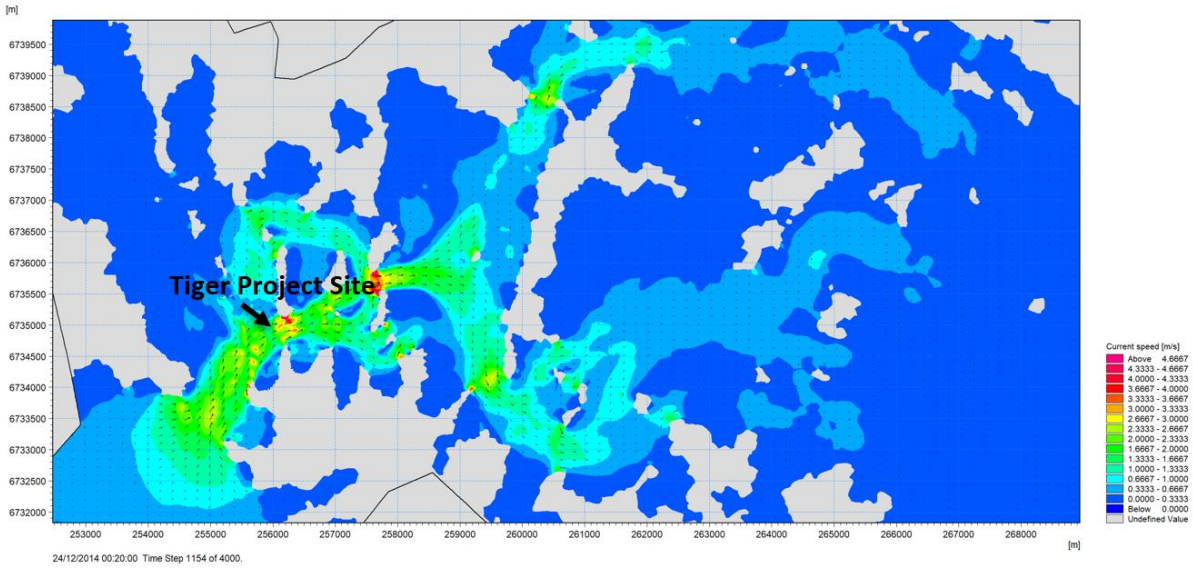

Figure 7.4. Example map of current velocities and directions from MIKE 21 model.

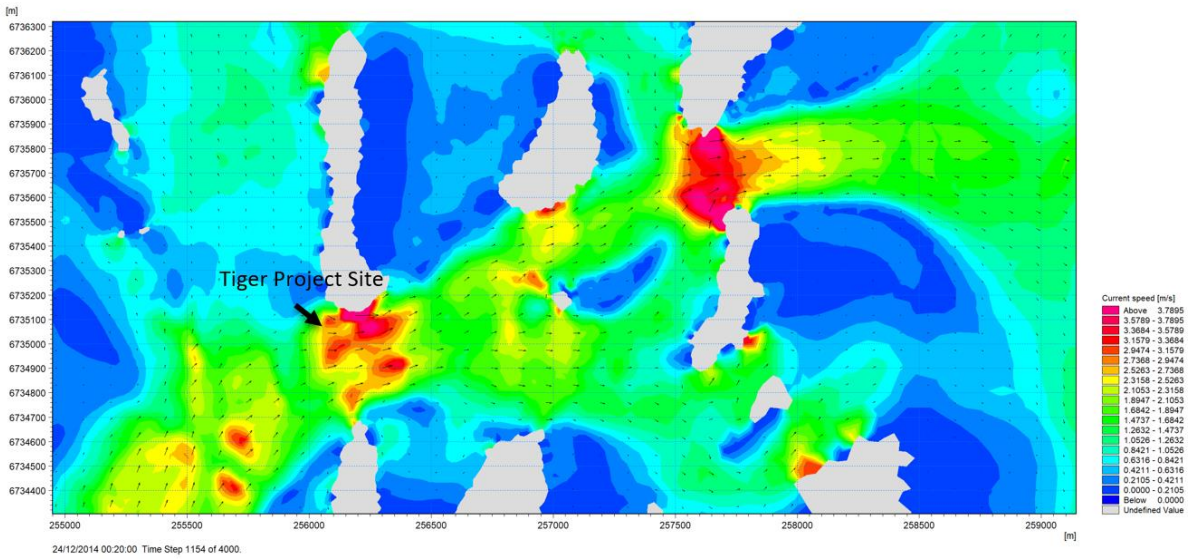

Figure 7.5. Zoom of Figure 7.4 over the TIGER project site.

The power density over the TIGER project site (to the west) and another site to the east with strong currents (Berder Island site), is shown in Figure 7.6. The values shown are the mean power density per unit area of cross-sectional flow, averaged over a tidal period, defined as $P = \frac{1}{2}\rho U_{avg}^3$, where P is theoretical mean power density, ρ is density of seawater and U_{avg} is depth-averaged current speed. Table 7.1, summarizes the calculation of mean power density in the Gulf of Morbihan TIGER site.

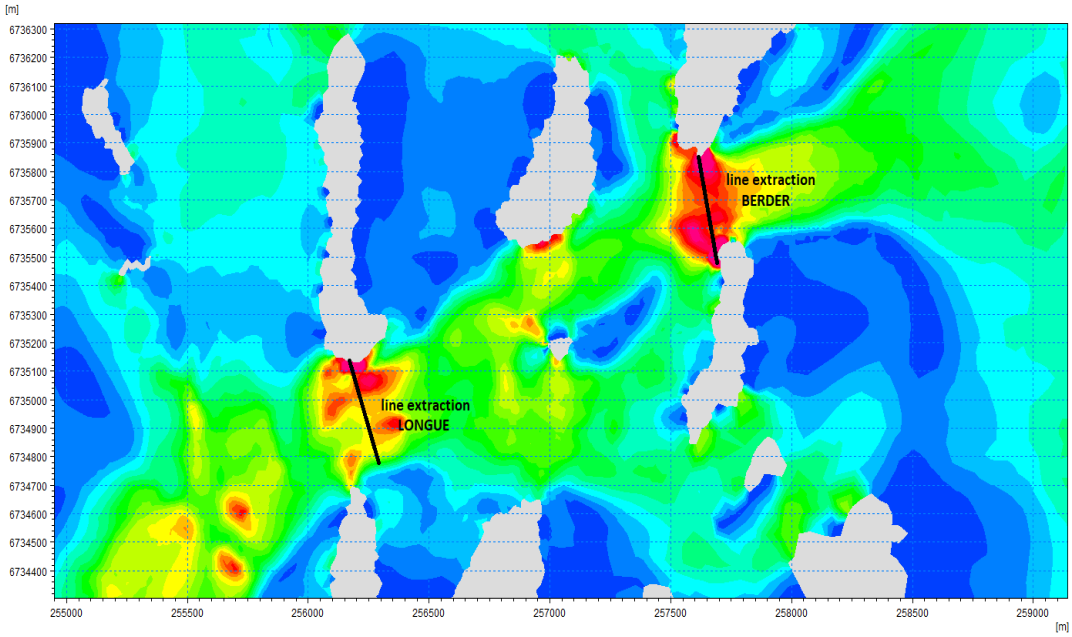

Figure 7.6. Lines extraction for the Power Density calculation at two sites in the Gulf of Morbihan.

Table 7.1. Calculation of mean power density for TIGER project site of the Gulf of Morbihan.

	Flow velocity [m/s]	Power density [kW/m^2]
Max	5.04	65.6
Min	0.007	0
Mean	1.82	3.1

8 DOFAS: University of Manchester

The DOFAS model has been applied to the simulation of horizontal and vertical axis wind and tidal stream turbines operating in turbulent flows. Turbines can be represented in DFOAS with various methods, namely: a direct-forcing immersed boundary method for a geometry-resolved approach, an anisotropic actuator line method, and a non-rotating actuator disc for horizontal axis turbines. Wall-functions can be adopted as boundary conditions when coarse mesh resolutions are adopted, e.g. in application to real-scale devices. A Large-Eddy Simulation turbulence closure model is used with various sub-grid scale models available: Smagorinsky, WALE and the one-equation model. Turbulent velocity fields are thus well-resolved, including the wakes of turbines or turbulence due to shear profile development over a bed of flat- or defined-bathymetry. The development distance of turbulent flows in a channel can be reduced by introduction of turbulence at the inflow, either via a precursor simulation (such as a periodic channel or using internal mapping) or via a synthetic turbulence method, e.g. Synthetic Eddy Method (SEM).

An accurate prediction of the velocity deficit and turbulence in a turbine's wake is of importance to the arrangement of tidal turbine arrays. This code is used for the analysis of the turbulent flows that occur at tidal sites due to the development of a boundary layer over its bottom bed that can be either flat or rough, the analysis of turbulent flows co-existing with ocean waves, and the loading and downstream wake effects of turbines exposed to such flows. Within the TIGER project, DOFAS has been used for the following:

- Simulation of turbulent flows in constant-depth channels without surface waves, with surface ocean waves and downstream turbines (in the wake region) to generate time-varying velocity field onset to a rotor plane to input to BEM models (see Section 9).

- Simulation of unsteady conditions in the wake of a single rotor system based on the TGL rotor and a twin-rotor system based on the Orbital Marine Power O2 system. In this study the impact of the approaching flow vertical distribution with uniform and log-law characteristics was analysed. Artificial turbulence was superimposed at the inlet using an anisotropic Synthetic Eddy Method with idealised turbulence length-scales. Simulations are run on 384 processors requiring four days to complete using University of Manchester's computational shared facility (CSF).

- Development of the code for simulation of waves co-existing with a turbulent flow resulting in unsteady turbine loading due to wave-induced kinematics and with a particular focus on the impact of waves on the rate of wake recovery. This analysis focused on a laboratory scale channel of 0.45 m depth and turbine of 0.27 m diameter due to availability of published experimental data. Four different regular wavelengths were analysed to assess impact on turbine loadings and wake dynamics.

Several academic publications are available concerning the use of the DOFAS model for different aspects of turbine and wake simulation including:

- Ouro, P., L. Ramirez, & M. Harrold (2019). *Analysis of array spacing on tidal stream turbine farm performance using Large-Eddy Simulation*. Journal of Fluids and Structures 91, 102732.
- Ouro, P. & T. Stoesser (2019). *Impact of Environmental Turbulence on the Performance and Loadings of a Tidal Stream Turbine.* Flow, Turbulence and Combustion 102, 613–639.
- Ouro, P. & T. Nishino (2021). *Performance and wake characteristics of tidal turbines in an infinitely large array.* Journal of Fluid Mechanics 925, A30.
- Ouro, P, P. Stansby & T. Stallard (2021). *Investigation of the wake recovery behind a tidal stream turbine for various submergence levels.* 14th EWTEC, Plymouth, United Kingdom.
- Ouro, P, H. Mullings & T. Stallard (2022). *Establishing confidence in predictions of fatigue loading for floating tidal turbines based on large-eddy simulations and unsteady blade element momentum.* Trends in Renewable Energy Offshore. RENEW conference, Lisbon, Portugal.
- Stansby, P. & P. Ouro (2022). *Modelling marine turbine arrays in tidal flows.* Journal of Hydraulic Research 60, 187–204.

The model has also provided input to presentations and posters at the following local and international events:

- EWTEC 2021: 14th European Wave and Tidal Energy Conference, Plymouth, UK.
- PRIMaRE 2022: 9th Annual PRIMaRE Conference, Cornwall, UK.
- ICOE 2022: International Conference on Ocean Energy, Donostia/San Sebastian, Spain
- RENEW 2022: 5th International Conference on Renewable Energies Offshore, Lisbon, Portugal.

8.1 Description of the Model

DOFAS is an open-source in-house Large-Eddy Simulation CFD code that resolves the spatially-averaged incompressible Navier-Stokes equations in rectangular Cartesian grids adopting a staggered storage of velocities. The advancement in time is performed with a fully-explicit standard fractional-step method to couple pressure and velocity fields, the latter solved iteratively with a low-storage three-step Runge-Kutta method. DOFAS approximates the convective and diffusive fluxes by either a central difference scheme or a 5th order WENO, and the Poisson pressure equation is solved with a multi-grid method. DOFAS is fully parallelised with Message Passing Interface (MPI) to perform simulations on multiple processors with proven effective scalability up to 100k cores on ARCHER2 (UK Tier 1 HPC facility), with the option to adopt OpenMP for alleviating the computational load from resolving Lagrangian particles.

8.1.1 Spatial Settings

Multiple simulations have been conducted with different turbine dimensions, blockage relative to channel cross-section, wave properties and mesh configurations. Details of the spatial resolution and configuration of different parts of the domain are specific to the simulation and are reported in relevant publications. Typical spatial resolutions are determined by the number of grid cells across the rotor diameter, being 50 times the average

number considered. For the main types of turbine simulation conducted the following dimensions are representative.

For a generic 'full-scale' geometry based on the TGL geometry and O2 system each rotor has a diameter of *O*(20 m) and a hub-to-hub spacing of 25 m. The computational domain has a uniform mesh resolution of 0.375 m in the three spatial directions and is 1152 m long, 480 m wide and 42 m deep, for a total of approx. 250 million cells. The turbine geometry is represented with the actuator line method following the aerofoil geometry and hydrodynamic properties either published (TGL) or provided. The nacelles are also simulated with the immersed boundary method.

For simulations based on experiments with 0.27 m diameter rotor: the computational domain of the open-channel is 14 m long, 3.0 m wide and 1.2 m deep, within which the mean water depth is defined as 0.45 m. A level-set method is employed to describe free-surface motion and velocities induced by the action of waves with air density defined above the free surface and water density below. The turbine is represented by the actuator line method with a resolution of 0.005 m uniform in all three axes across the domain. The synthetic eddy method is adopted to generate artificial turbulence with an intensity of 10% that is superimposed at the inlet, onto a logarithmic velocity profile.

8.1.2 Temporal Settings

The time step of the CFD simulations is defined to a sufficiently low value to ensure the Courant-Friedrich-Lewy (CFL) condition is satisfied. For simulations with a turbine, the time step is set such that the distance advanced by the actuator points defining the rotor is less than the cell dimension. For a horizontal axis turbine, the distance of actuator point movement per time step is proportional to angular speed and radial position. Prior to analysis of wake conditions, time-steps were selected to satisfy these constraints and ensure accurate prediction of mean thrust and power coefficient at the operating point of interest. For the simulations compared to experimental data a time step of 0.001 s is adopted, as it provided a good match with experimental measurements of mean thrust and power coefficient. For the full-scale turbine simulations, a fixed time step of 0.0475 s is adopted as it provides a close match with the BEM data for the power and thrust coefficients.

8.1.3 Representation of Tidal Turbine

For the analysis conducted in TIGER using DOFAS turbines are represented using an actuator line method with an anisotropic force projection in which the Gaussian spreading function is varied depending on the actual chord length of each actuator point. The actuator line method implemented in DOFAS has a negligible computing cost, with this being very similar when simulating one turbine or 60 devices.

8.1.4 Inputs and Boundary Conditions

The Navier-Stokes equations are solved using an LES turbulence closure, which resolves the large to medium turbulent scales and thus allows for resolving time varying instantaneous velocity. To reduce the distance over which a turbulent boundary layer develops downstream of the inlet velocity fluctuations are defined at the inflow using a Synthetic Turbulence method.

Free-surface flows can also be simulated with DOFAS adopting a level-set method with the capability of generating waves. This level-set method requires the resolution of an advection equation that is solved with a three-step total variation diminishing Runge-Kutta method and a 5th-order WENO scheme for approximating the level-set function fluxes. At the inflow plane the depth variation of kinematics and the surface elevation are defined by either linear wave theory or 2nd-order Stokes theory. Towards the outflow plane an absorption layer is imposed over which wave amplitude is reduced such that water depth is constant at the outflow boundary. An example of such a domain is shown in Figure 8.1.

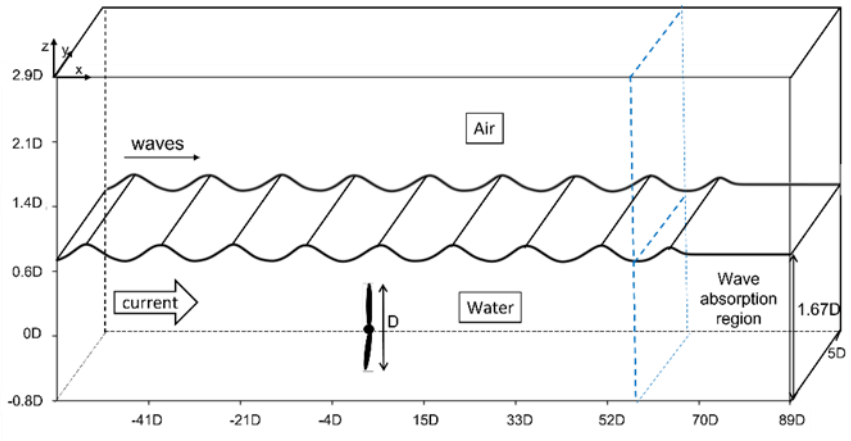

Figure 8.1. Typical configuration of domain used for DOFAS simulations with turbulent inflow defined by synthetic eddy method and free surface waves modelled with level-set method. The rotor geometry and channel characteristics are based on the conditions studied experimentally by Stallard et al. (2015).

8.1.5 Outputs

The outputs that DOFAS generates from these simulations are: first-order mean velocities, second-order turbulence statistics such as Reynolds stresses, third- and fourth-order flow statistics, mean water level, velocity time series at selected spatial locations, and instantaneous values of the flow field to be post-processed for analyses such as Proper Orthogonal Decomposition. For simulations including one or more turbines, outputs also include mean and time-varying loading and power, and the previously listed flow properties throughout the wake region, enabling characterisation of the steady and unsteady structure downstream of one or more turbines.

8.1.5.1 Unsteady Onset Flows due to Channel Flow and Turbine Wakes

Some examples of the types of output for a tidal stream system in a channel flow are shown in the following figures. Further details are given in the referenced papers.

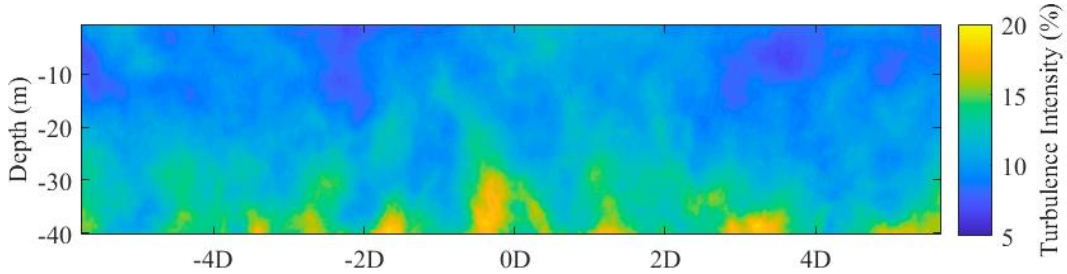

Figure 8.2. Example contour plot of vertical plane of turbulence intensity through the water depth of a flat bed tidal periodic tidal channel obtained by large eddy simulation with DOFAS (Ouro et al., 2022).

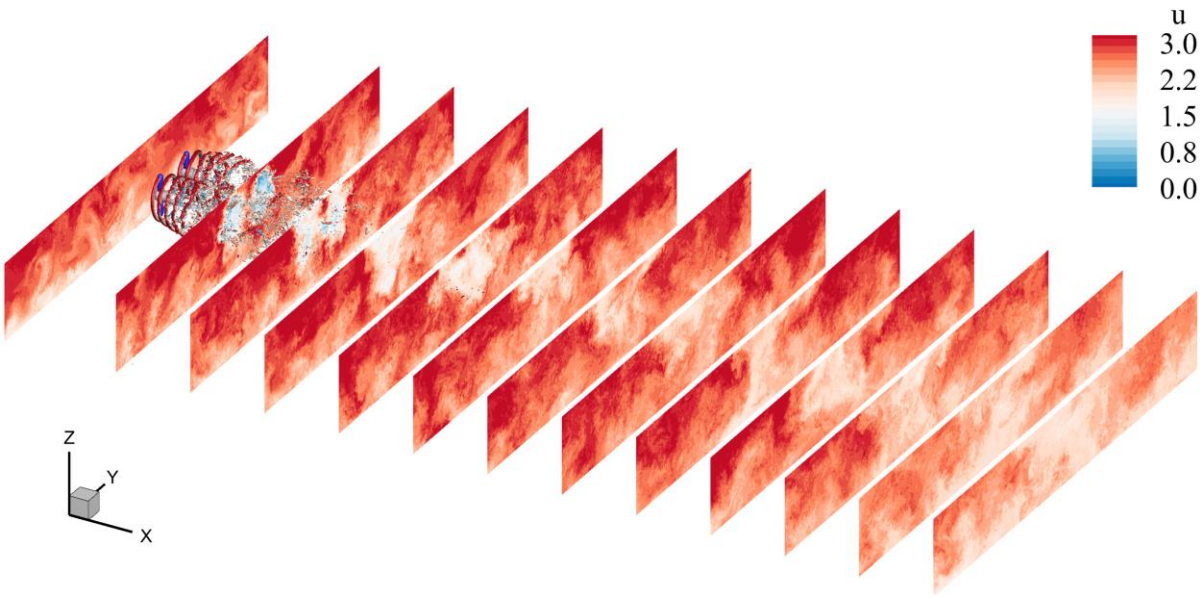

Figure 8.3. Example contour plot of vertical (yz-) planes of streamwise velocity downstream of a twin-rotor tidal stream system generated from the DOFAS model of the two-rotor tidal turbine with turbulent structures represented using the Q-criterion. (image source: Ouro et al., 2022)

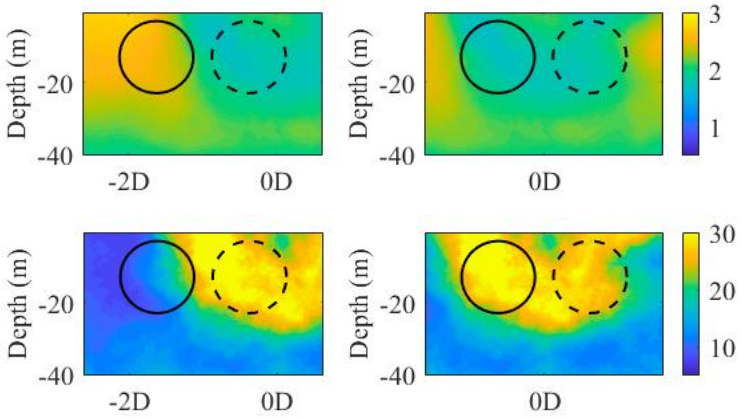

Figure 8.4. Example of onset flow fields to rotors at a plane 6D downstream of a two-rotor tidal stream system obtained by LES simulation with DOFAS. Streamwise velocity in m/s (top) and turbulence intensity [%] (bottom) with the circles indicating regions over which time-varying velocity is extracted to provide inflow to BEM analysis of unsteady loading. (Image adapted from Ouro et al., 2022)

8.1.5.2 Flow and wake modelling with turbulence and waves

The action of waves coexisting with approach flow turbulence and the impact of these environmental conditions on turbine loading has received some attention to-date, through engineering models and CFD of various fidelity. However, few studies have been undertaken regarding the effect of wave-induced velocity and turbulence on the form, characteristics and recovery rate of the wake behind a tidal turbine. Developments and analysis using DOFAS have included mean power and thrust coefficients, near wake and far wake velocity deficit and turbulence levels, and wake expansion ratio of a turbine in a turbulent channel flow, both without and with the presence of waves.

An example is given here for a case comparable to laboratory experiments. The time averaged thrust coefficient for a tip speed ratio (TSR) of 5.5 is 0.86 due to turbulent flow only, without waves. This is comparable to experimental data for the same rotor, and the mean value is not significantly altered for the simulations with waves. Since wake generation is driven by momentum extraction this similarity of thrust coefficient is expected to result in formation of a similar mean wake. Figure 8.5 and Figure 8.6 compare time-averaged streamwise velocity and turbulence intensity at 8D downstream of a rotor with and without waves. Whilst a similar wake form is observed in the presence of waves the vertical profile is affected by the presence of surface waves and the resultant wave induced kinematics through the depth. The simulation without waves presents a lower disk averaged velocity and disk averaged turbulence intensity (0.39 m/s and 11%) than the simulation with waves (0.40 m/s and 16% turbulence and wave-induced intensity) which would affect downstream turbine loading.

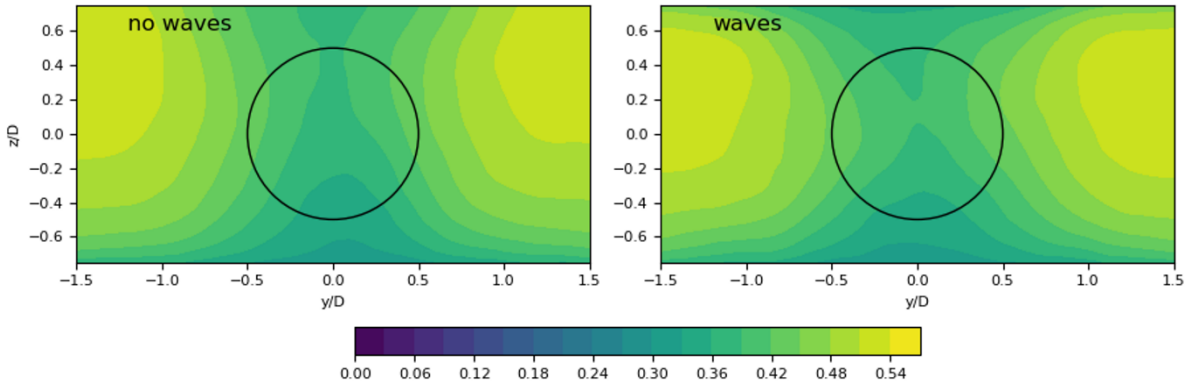

Figure 8.5 Example contour of streamwise time averaged velocity at 8D downstream the turbine without waves (left) and with waves (right), from DOFAS model. The circle indicates the rotor area and position.

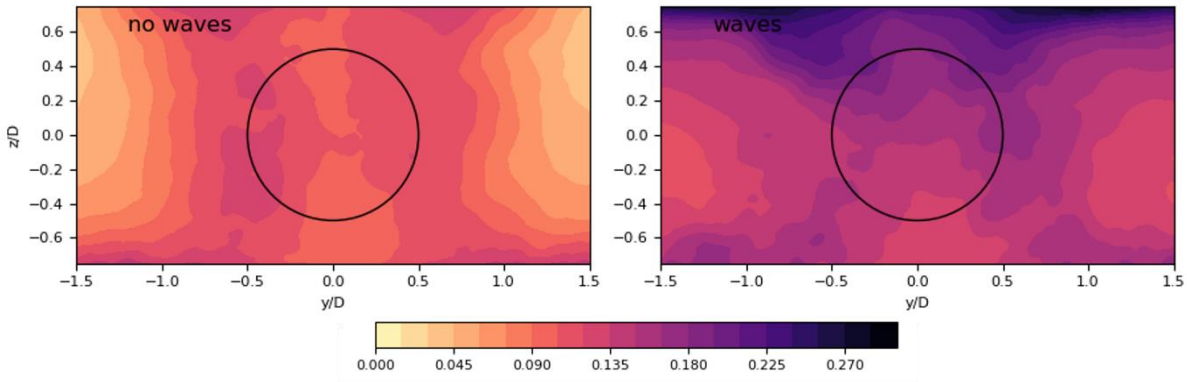

Figure 8.6. Example of streamwise turbulence intensity at 8D downstream the turbine without waves (left) and with waves (right), from DOFAS model. The circle indicates the rotor position and area.

Comparison to experiments and detailed analysis of the in-wave cycle variation of flow characteristics is being documented for publication. Extension of the methodology to analyse specific irregular wave-series and wave-fields that are oblique to the rotor plane and hence axis of the wake, which are known to occur at many sites, is also progressing.

9 Unsteady BEM: University of Manchester

9.1 Overview of Model and Intended Use

The University of Manchester has developed an in-house blade element momentum (BEM) method which can be utilised to determine loading and power output of a device experiencing both steady and unsteady operating conditions. The main application of the method is prediction of blade loading spectra from which an indicator of aggregated fatigue loads, a damage equivalent load (DEL), is obtained.

Design standards stipulate a 'normal' operating point which contributes to fatigue measured at a site as a ten-minute condition (Peacock, 2011). These conditions vary with onset flow velocity, shear, turbulence and waves. Each of these types of unsteady conditions has been investigated during the TIGER project, using measurement data acquired at different TIGER sites, with a particular focus on Raz Blanchard. Prior to availability of ADCP data from this site, analysis and development of methods has been undertaken using flow data and model predictions from the EMEC site. Throughout, a key focus of this work is on using an efficient BEM to determine the impact of spatial variation of conditions at a single site and between sites on the fatigue loading experienced by both single turbine and an array of turbines. The characterisation of the spatial variation of conditions at a site will also be used to better inform and validate channel-scale models.
During TIGER, several different tidal devices have been modelled, including a laboratory scale turbine for which load data is available from prior publications (Payne et al. 2018), a publicly available geometry of a 'full-scale' turbine (Scarlett et al., 2019) and with a study conducted with turbine developers Orbital Marine Power (OMP) (e.g. Ouro et al. 2022). The tidal device modelled consists of two rotors each with two blades, following the design of a full-scale floating device by OMP. In addition a blind modelling study has been conducted between ULHN and UNIMAN to assess the level of fidelity required in the inflow to device scale models and the uncertainty in the loading and power production from the different methods, for the cases listed in Table 9.1.

Table 9.1. Cases considered in blind modelling study.

Turbine Models / Onset Flow Conditions	LES-ALM (UoM)	LL-VPM (ULHN)	BEM (UoM)	BEM (Bladed)
Mean Onset flow speed, TI	TGL	TGL	TGL /O2	O2
Synthesised Turbulence	TGL /O2	TGL	TGL /O2	O2
Synthesised Turbulence + Shear	TGL /O2	N/A	TGL /O2	O2
High-fidelity model of Turbulence + Shear	TGL / O2		TGL / O2	O2

Several academic publications produced using the data from the unsteady BEM model:

- Mullings H, Stallard T. (2019) Assessment of tidal turbine load cycles using synthesised load spectra, including blade-scale fluctuations, *EWTEC 2019 13th European Wave and Tidal Energy Conference*, Naples, Italy.

- Mullings H, Stallard T. (2021) Assessment of dependency of unsteady onset flow and resultant tidal turbine fatigue loads on measurement position at a tidal site. *Energies*, volume Special Issue Tidal Turbines DOI: 10.3390/en14175470.
- Mullings H, Stallard T. (2022) Impact of spatially varying flow conditions on the prediction of fatigue loads of a tidal turbine. *International Marine Energy Journal.* 5(1) 103-111. DOI: https://doi.org/10.36688/imej.5.103-111.
- H. Mullings, T. Stallard (2022) Analysis of tidal turbine blade loading due to blade scale flow, *Journal of Fluids and Structures,* Volume 114, DOI: https://doi.org/10.1016/j.jfluidstructs.2022.103698.
- Ouro P, Mullings H, Stallard T. (2022) Establishing confidence in predictions of fatigue loading for floating tidal turbines based on large-eddy simulations and unsteady blade element momentum, *Trends in Renewable Energies Offshore,* 915-924, DOI: 10.1201/9781003360773-101.

The model has also provided input to presentations and posters at the following local and international events:

- EWTEC 2019: 13th European Wave and Tidal Energy Conference, Naples, Italy.
- EWTEC 2021: 14th European Wave and Tidal Energy Conference, Plymouth, UK.
- SEANERGY 2022: Seanergy Conference and Exhibition, Le Havre, France.
- PRIMaRE 2022: 9th Annual PRIMaRE Conference, Cornwall, UK.
- ICOE 2022: International Conference on Ocean Energy, Donostia/San Sebastian, Spain
- RENEW 2022: 5th International Conference on Renewable Energies Offshore, Lisbon, Portugal.

9.2 Description of the model

9.2.1 Spatial Settings

Unlike resource models the spatial grid is not site specific within this code. The spatial grid here is mainly used to define the onset flow conditions, and as this is not a computationally expensive code the grid can be quite detailed. The grid spacing typically employed for defining the time-varying onset flow-field is of the order of 0.25 m to 1 m for turbines of diameter 20 m. Smaller spacing, e.g. 0.01 m can be employed for finer turbulence length scales and for differing sizes of turbine under consideration.

9.2.2 Temporal Settings

As with the spatial grid, the temporal settings are not restricted due to the computational cost. However, for validation with experiments and to consider quasi-steady intervals of tidal resource specific time periods are used ranging from 60 to 600 seconds. These periods are sampled at high frequency, typically corresponding to the experimental dataset, or to resolve relevant frequencies of unsteady onset flow. For simulations focused on wave-induced kinematics O(10) time steps per wave-cycle are typically employed. For simulations with turbulent onset conditions a higher frequency range is modelled, and this can vary with the turbulence model employed to synthesise the onset flow.

9.2.3 Representation of the Turbine

The Blade Element Model (BEM) extracts the onset flow at 'N' positions along a blade length, at positions that rotate with time, depending on the chosen operating point of the turbine. The onset flow is used to determine the relative onset flow (U_{REL}) and inflow angle (φ) to the blade at each position along the blade, as shown by Equations (9.1) and (9.2).

$$\partial U_{REL}(t) = \sqrt{U_X^2 + (\omega r - U_\theta^2)} \tag{9.1}$$

$$\partial \varphi(t) = \sin^{-1} \frac{U_X(t)}{U_{REL}(t)} \tag{9.2}$$

Where U_{REL} is the relative velocity to the blade which incorporates the longitudinal velocity, U_X is the stream-wise onset velocity which includes an axial induction (a) through $U_X = U_0(1-a)$, where U_0 is the upstream velocity, and the components in the tangential direction, U_θ with the angular velocity ω and each radius, r. The lift force, L, and drag force, D, on each blade segment vary according to Equations (9.3) and (9.4).

$$\partial L(t) = \frac{1}{2} B \rho c U_{REL}^2 C_L \partial r \tag{9.3}$$

$$\partial D(t) = \frac{1}{2} B \rho c U_{REL}^2 C_D \partial r \tag{9.4}$$

where, c is the chord length, ∂r is the radial width of the blade segment, B is the number of blades, ρ is the fluid density, C_L and C_D correspond to the lift and drag coefficients respectively. Using the calculated lift and drag forces for each blade the axial ($F_a(t)$) and tangential ($F_t(t)$) forces along each blade are calculated using Equations (9.5) and (9.6).

$$F_a(t) = \partial L(t) \cos\big(\varphi(t)\big) + \partial D(t) \sin\big(\varphi(t)\big) \tag{9.5}$$

$$F_t(t) = \partial L(t) \sin\big(\varphi(t)\big) - \partial D(t) \cos\big(\varphi(t)\big) \tag{9.6}$$

The axial force ($F_a(t)$) on each segment of the blade leads to the calculation of root bending moment as well as rotor thrust. These results can be used to establish the respective load spectra and hence determine the load cycles enabling the fatigue loads to be predicted for the blades and rotor. This method can be implemented to determine unsteady loading through the use of the varying onset flow.

9.2.4 Other Numerical Settings

Blade element models are typically dependent on input of lift and drag coefficient polar curves. The BEM code used at University of Manchester has been extended to include the contribution from higher frequency blade-scale fluctuations of the lift and drag forces due to the turbulent relative velocity to the blade (Mullings and Stallard, 2022). This has been shown in provide better predictions in the fatigue loading when highly coherent structures are

present in the onset flow, such as observed in field measurements and when modelled using a synthetic eddy method.

9.2.5 Input and Boundary Conditions

The main input conditions to this BEM code include:

- Turbine Geometry (N blades, rotor and hub radius)
- Blade geometry (radial variation of aerofoil section, chord and pitch)
- Section definition, steady (Lift and Drag coefficient variation with angle of attack)
- Section definition, unsteady (Spectrum of Lift and Drag coefficient variation)

Inflow boundary conditions include:

- Gridded domain of time-varying onset velocities across the swept area including:
    - Onset flow (single or multiple/tidal cycles))
    - Shear profiles
    - Turbulence length-scales (streamwise, vertical, transverse)
    - Turbulence intensity (at hub or disc averaged)
    - Turbine position (relative to surface and bed)
    - Wave-induced kinematics

This BEM code operates on the basis of defined inflow velocities. These can range from a simplified set of steady conditions to examine overall performance characteristics to loading from an unsteady onset, defined by a turbulence model (such as Von Karman or Synthetic Eddy Method) and / or with kinematics due to waves (regular or irregular, typically linear waves are assumed) or defined by a precursor CFD simulation (e.g. from DOFAS simulations, see Section 8). Within TIGER, a collaborative study has been conducted looking at the way the inflow can be defined and the uncertainty which occurs by modelling an unsteady onset flow with the same time-averaged properties in several different ways.

9.2.6 Outputs

This code has primarily been used to assess the variation of loading experienced on a blade and rotor of a tidal turbine. Previous work validated the code against the experimental results, as shown in Figure 9.1, with the peak loading predicted to within 2% and the fatigue loading to within 7%.

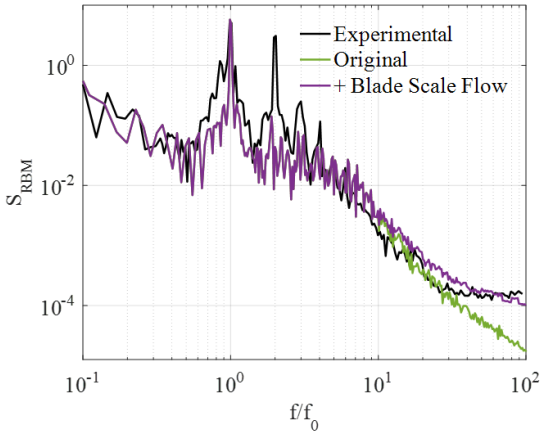

Figure 9.1. Spectra of root bending moment from BEM code with onset flow simulation using a Von Karman spectral model of turbulence and both mean lift and drag coefficients and with inclusion of high frequency force fluctuations due to blade scale flow, showing agreement over the entire frequency range with experiment (Mullings & Stallard 2022)

In addition, the code has been used to analyse the impact of different design conditions, such as series of operating points and the influence of the downstream wake, to quantify variation of fatigue loads with onset conditions and to assess the range of fatigue loads predicted with differing onset flow synthesis method (shown in Figure 9.2). This work is informing analysis of control strategies for mitigating load variation both for single turbines subject to unsteady onset flow, and for turbines in arrays subject to upstream turbine wakes.

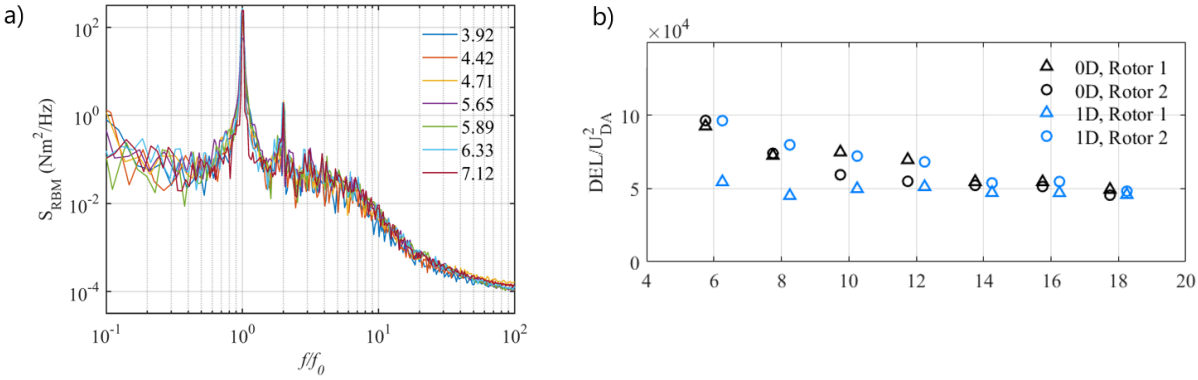

Figure 9.2. (a) Spectra of root bending moment for multiple tip speed ratios (Mullings and Stallard, 2022). (b) Variation in normalised damage equivalent loads for a two turbine system located at different downstream positions, for an inline turbine system and 1 diameter offset system (Ouro et al., 2022).

10 Conclusions

This report has summarised the range of models used in the TIGER project. In many cases, the models have been used to provide information to technology and site developers to aid in their design process. This feeds into one of the key goals of TIGER, which is to accelerate the development of the tidal sector, faster and more effectively than would be possible without Interreg support.

Data from the models has also been used to inform high level strategic techno-economic considerations for the tidal energy industry. In particular, data from several models has been used to support the ORE Catapult in developing their report "Cost Reduction Pathway of Tidal Stream Energy in the UK and France"[2].

This report can be viewed as a companion piece to TIGER deliverable T3.1.2, "Data Collection & Survey Best Practice Report", which discusses general requirements for tidal resource assessment. Deliverable T3.1.2 highlighted the key importance of numerical modelling as part of any resource assessment study. The report has also highlighted the capability of the range of models, regarding different oceanographic inputs, including bathymetry, depth-dependant tidal currents, turbulence, wind and wave effects, as well as the inclusion of the tidal turbine(s) themselves.

As such, the report should assist researchers, practitioners and decision-makers in the selection of suitable modelling approaches and tools to cover the spatial and temporal domain required for their needs. Given the different capabilities and computational cost a combination of two or more modelling approaches to cover the regional, site and turbine domain across years, tidal cycles and turbulence is most likely.

The research, resources and applications presented here and conducted as part of TIGER, will feed into the overall advancement of the sector, by providing the highest quality modelling input for engineering, environmental and financial decision-making.

[2] https://ore.catapult.org.uk/?orecatapultreports=cost-reduction-pathway-of-tidal-stream-energy-in-the-uk-and-france

Annex A - Cross-comparison of resource models and measured data at Le Raz Blanchard

Prepared by University of Manchester

A1 Introduction

The main aim of the study presented in this annex is to quantify the range of unsteady load predictions from methods of determining the onset flow conditions at a site. Within the TIGER project six different sites were looked at, with measurement devices deployed at some and models analysis applied to others. This annex focuses on the Raz Blanchard site off the coast of Normandy in France. This site was chosen as it is one of the most energetic sites in the channel region, with various models already applied to indicate potential power capture for tidal stream turbines.

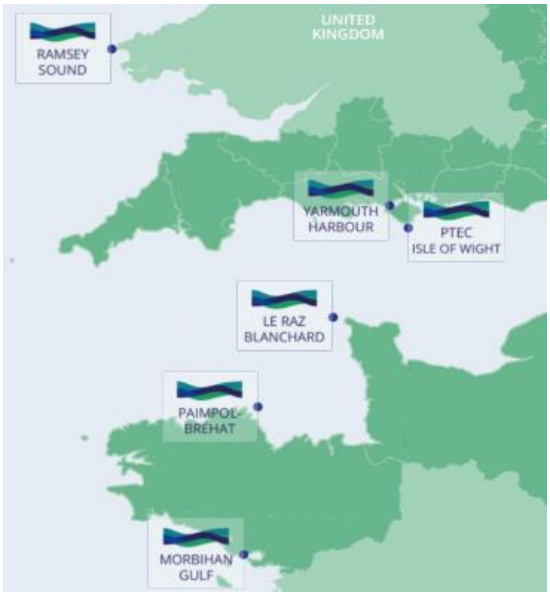

Figure A.1. Sites around the Channel region which are studied within the TIGER project. Obtained from Interregtiger.com

This study is split into three areas. Firstly, a focus on data available at a highly defined test site (EMEC) is presented in Section A2. Section A3 presents the application of the analysis used for the EMEC site to a site within the TIGER project (Le Raz Blanchard), with a comparison of the onset flow conditions, leading into a further comparison to modelled data within the site. A brief overview of the application of these conditions within the device scale models is included. In addition, the influence of the variation of conditions for a single design case (single disk averaged velocity) on the loading is shown.

A1.1 Understanding the Unsteady Resource

In order to plan for tidal array development, a thorough understanding of the resource is required. Using the tides for power generation allows for reliable performance, as the tidal cycles are predictable. This predictability can be defined using tidal constituents which are area specific, in terms of amplitude, but consistent in frequency. Understanding the tides in

a specific area allows for a simple determination of the most appropriate sites for tidal stream energy extraction. One of the easiest ways for calculating the best sites is to use channel models, which rely upon the non-linear shallow water equations. Several of these models have been used in this project across the academic partners. Some of those models have been included in this study at Le Raz Blanchard site to compare with measurement data. A measurement campaign was conducted within this project in order to determine the spatial variability at a tidal site, with multiple devices deployed and measuring over a concurrent time span.

Channel models are very useful in determining the overall power production which can be obtained from a site. Channel models can include turbines as drag terms to provide an idea of the perturbed flow around an array. The interest in this study is to establish the variation of conditions for each design case, where a design case is considered as a specific disk average velocity used to estimate the performance of a turbine or array. The variation of the flow conditions can differ between sites, between locations within a site and also between turbine positions at each location. Here both the measurements and model data will define the variation of conditions for each design case.

A2 Initial Study: EMEC Test Site

An initial study was conducted looking at the EMEC test site, using data acquired within the REDAPT project (Sellar et al., 2016). This data included two ADCPs measuring concurrently, spaced approximately 78m apart, as well as results from MIKE3 channel models which were validated across the site. The influence of turbine position on the loading experienced was investigated with results shown in (Mullings and Stallard, 2021) as well as the variation of load with position and location at a site, results shown in (Mullings and Stallard, 2022). These findings can vary by 0.5% to 30% between position, location and model to measurement. This illustrated the need to have a thorough understanding of the spatial variation of conditions at a site.

For a single design case the unsteady onset conditions are defined by a velocity shear profile, turbulence and wave characteristics. For this study, the disk averaged velocity range is 2.0-2.2 m/s for a turbine considered to be ‘bed-mounted’ and therefore the position will be referred to as ‘near-bed’. Using the measurements from the REDAPT project provides quality assured ADCP data providing vertical profiles of current velocities. Post-processing of data within the ReDAPT project also provided mean wave characteristics and therefore cases where very large waves are present can be removed to see the impact without waves present. The onset flow characteristics have been published in Mullings and Stallard (2021, 2022) an overview is shown here in Figures A2 and A3.

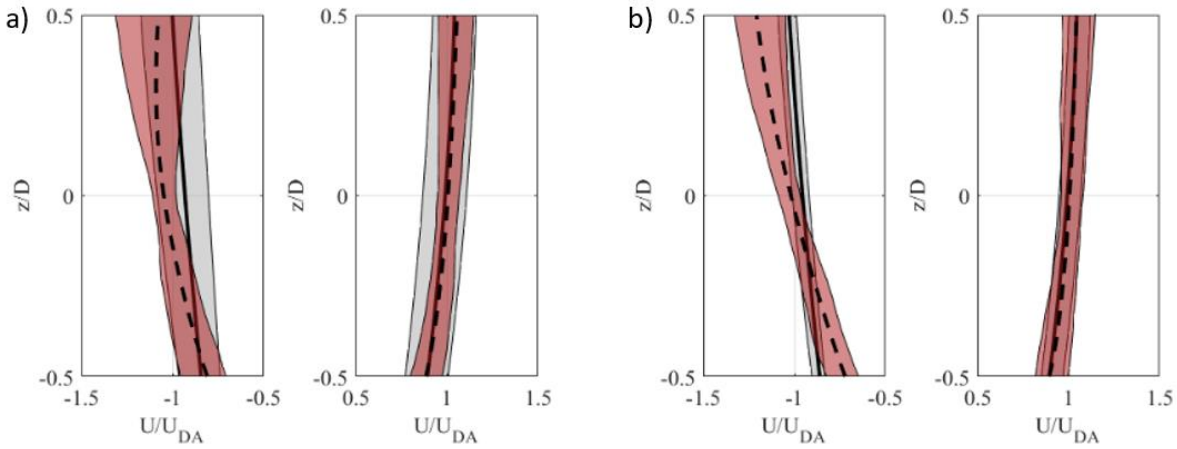

Figure A2. Variation of vertical shear profile, normalised with UDA, for the single design case, mean of the measured profile (black dashed), variation of measured profile (red band), mean of the predicted profile (black solid) and variation of the predicted profile (grey band).

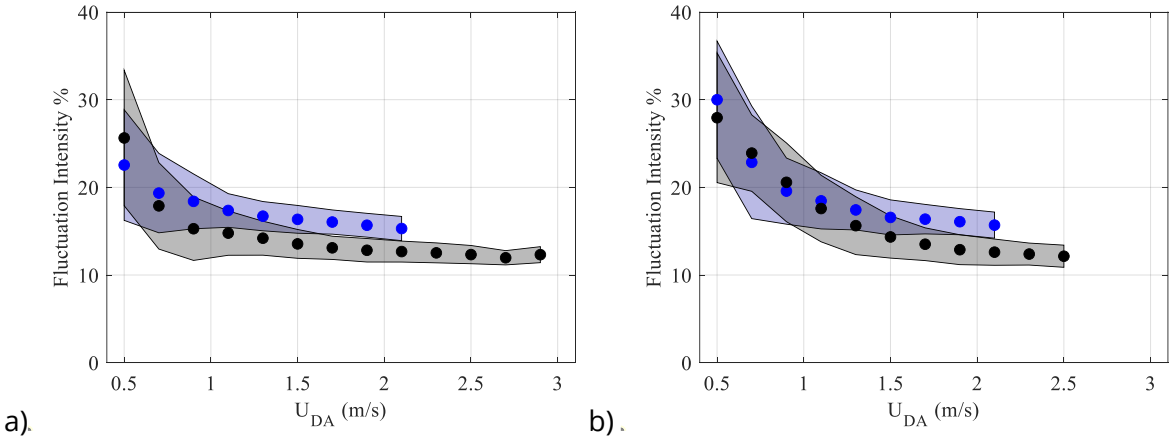

Figure A3. Fluctuation intensity of velocity at two ADCP locations (a and b), for a near-bed turbine for the flood tide (RHS) and the ebb tide (LHS) within the EMEC test site, for a range of disk averaged velocities.

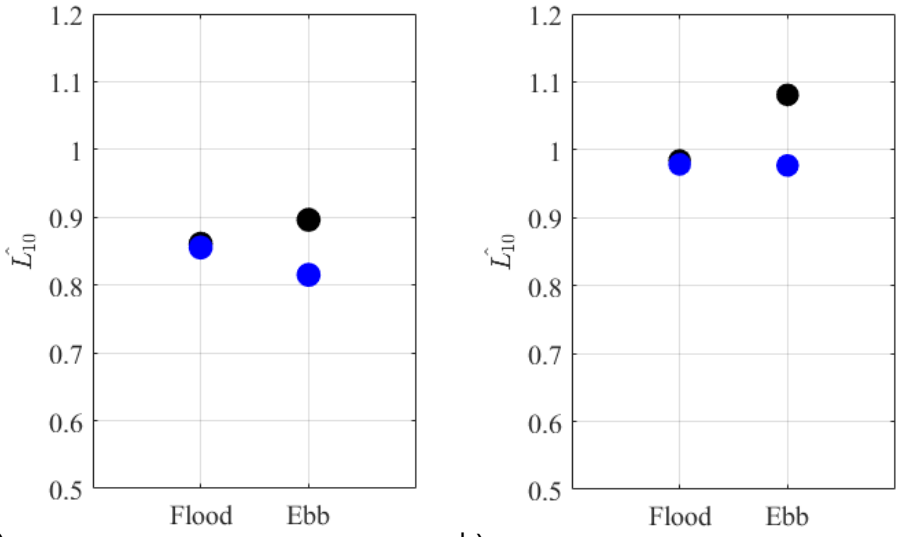

Figure A4. Variation of damage equivalent loading for a turbine experiencing loading at one disk average velocity (2.0-2.2 m/s), one design case, for both flood and ebb tides for location (a) and location (b).

A3 Study Focus: Le Raz Blanchard

With the focus on Le Raz Blanchard, an initial review was conducted to determine the modelling and measurement points that have previously been studied and are shown in Figure A5. The locations chosen in this previous work informed industry and other research projects. In this work the focus area is shown as the highlighted area in Figure A5, this is a region of interest to partner tidal developers, Hydroquest and Normandie Hydrolienne.

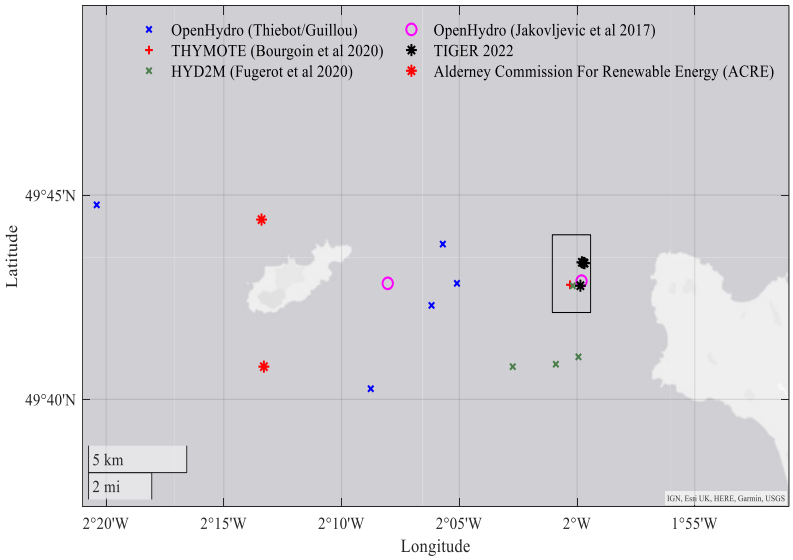

Figure A5. Map showing the region around Le Raz Blanchard where previous/current measurement campaigns are located, area of interest studied here highlighted.

Previously measurement campaigns have been conducted by both research projects, with the aim of validating channel models and by industrial turbine developers. Both sets of campaigns have drawbacks with the distribution of data post-deployment. Therefore, a new

set of ADCP devices were deployed within the TIGER project. These devices are listed in Table 1, along with their location and period of deployment.

Table A1. ADCP device information for deployments in Le Raz Blanchard as part of the TIGER project.

Device Name	Latitude	Longitude	Period of Deployment
NH1 (Teledyne RDI Workhorse Sentinel 600)	49.72258	-1.9965	15/01/2022 1600 19/03/2022 1906
NH2 (Teledyne RDI Workhorse Sentinel 600)	49.72223	-1.9947	14/01/2022 1900 17/03/2022 0700
MU (Nortek Signature500)	49.72216	-1.9954	14/01/2022 1630 31/01/2022 0000

The locations of these ADCPs as well as modelled data points are shown in Figure A6, with various markers illustrating the types of models and locations where data has been acquired. Various TIGER project partners have models set up which encompass the region around this site. These models are listed in Table 2. Together with the measurement campaign, this allows a comparison of conditions as well as the subsequent loading on a device to be determined.

Table A2. Resource models run in Le Raz Blanchard as part of the TIGER project.

Model Type	Project Partner	Number of Data Points
TELEMAC RANS	University of Caen	49
LBM-LES (PALABOS)	University of Caen	9
DELFT3D	University of Exeter	52

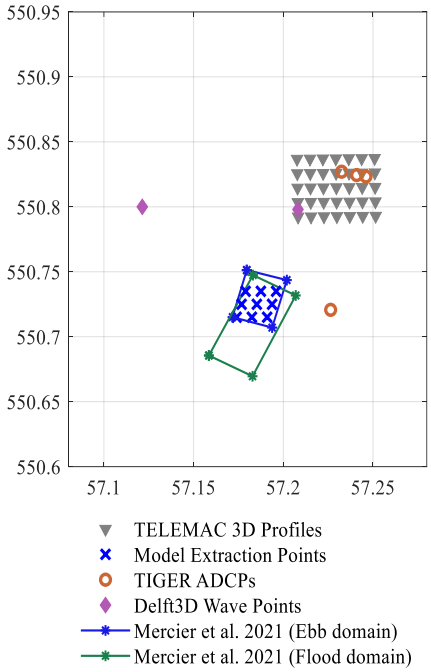

Figure A6. Location of model and measurement points within the area of interest in Le Raz Blanchard.

As with the study of the EMEC site, the onset flow characteristics across the design cases has been investigated for each of the measurement devices. An overview of the variation in characteristics are determined for a bottom mounted turbine is shown in Figures A7, A8 and A10. Initially the vertical profiles from each ADCP for a mean 10 minute time period are used to determine the disk averaged velocity, results are shown in Figure A7, against the percentage occurrence within the time period measured. Across the measured range of ebb flow speeds the disk averages are very similar for the MU and NH1 devices, with NH2 having a greater percentage of higher velocities and therefore a smaller number of lower velocities compared to MU and NH1. For the flood tide there is more variation in the occurrence of the UDAs, with NH2 and MU measuring cases approaching 4 m/s. However, at the low to mid-range of UDA speeds (1.0 -2.5 m/s) MU and NH1 show a very similar measured occurrence. For each ADCP the variation in vertical shear is determined and binned with respect to the disk averaged velocity. This variation is shown in Figure A8. Visually, slight variations between each measurement device can be seen, especially at the higher flow speeds. For a flow speed bin of 2.0 – 2.2 m/s the range of shear profiles for each measurement device is compared in Figure A9 (a-c). In these figures the range of shear for the NH1 ADCP is compared to the shear from the MU device which is closest to the NH1 device (approx.. 87 m) and the NH2 device which is furthest away (approx. 140 m). These distances between the ADCPs compare to about 4 to 7 turbine diameters, at these distances it can be seen that there are slight differences at the top and bottom of the rotor area for a bed mounted turbine. For Figure A9c the MU and NH2 devices are compared which have a distance of 53 m between each device, this is equivalent to just over two and a half turbine diameters, when considering a 20 m rotor. These distances are comparable to the spacing turbines could experience within an array, differences over the range of shear that can be found at the site can contribute to load fluctuations which will not be considered if only one device is used as a reference for the

entire site. These shear profiles will be used and compared to profiles from models of the site.

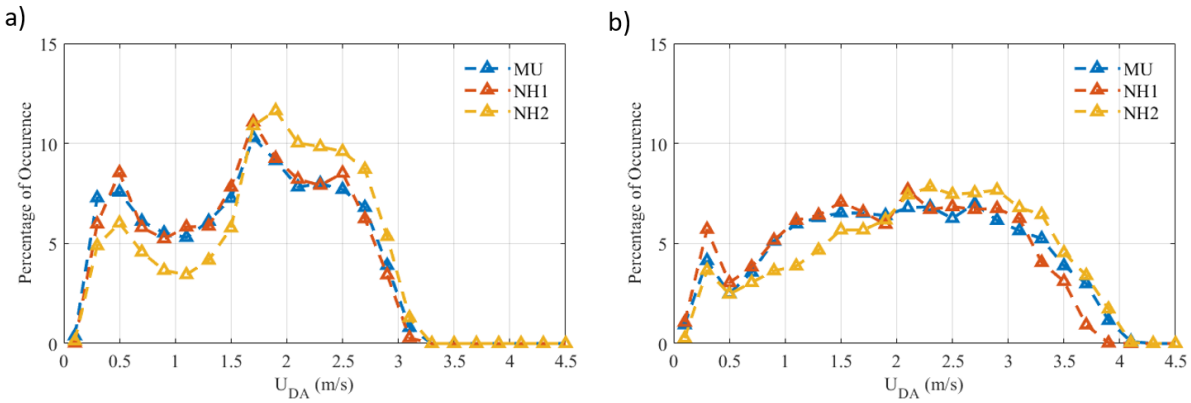

Figure A7. Percentage occurrence of disk averaged velocities for each ADCP, at (a) ebb tide and (b) flood tide.

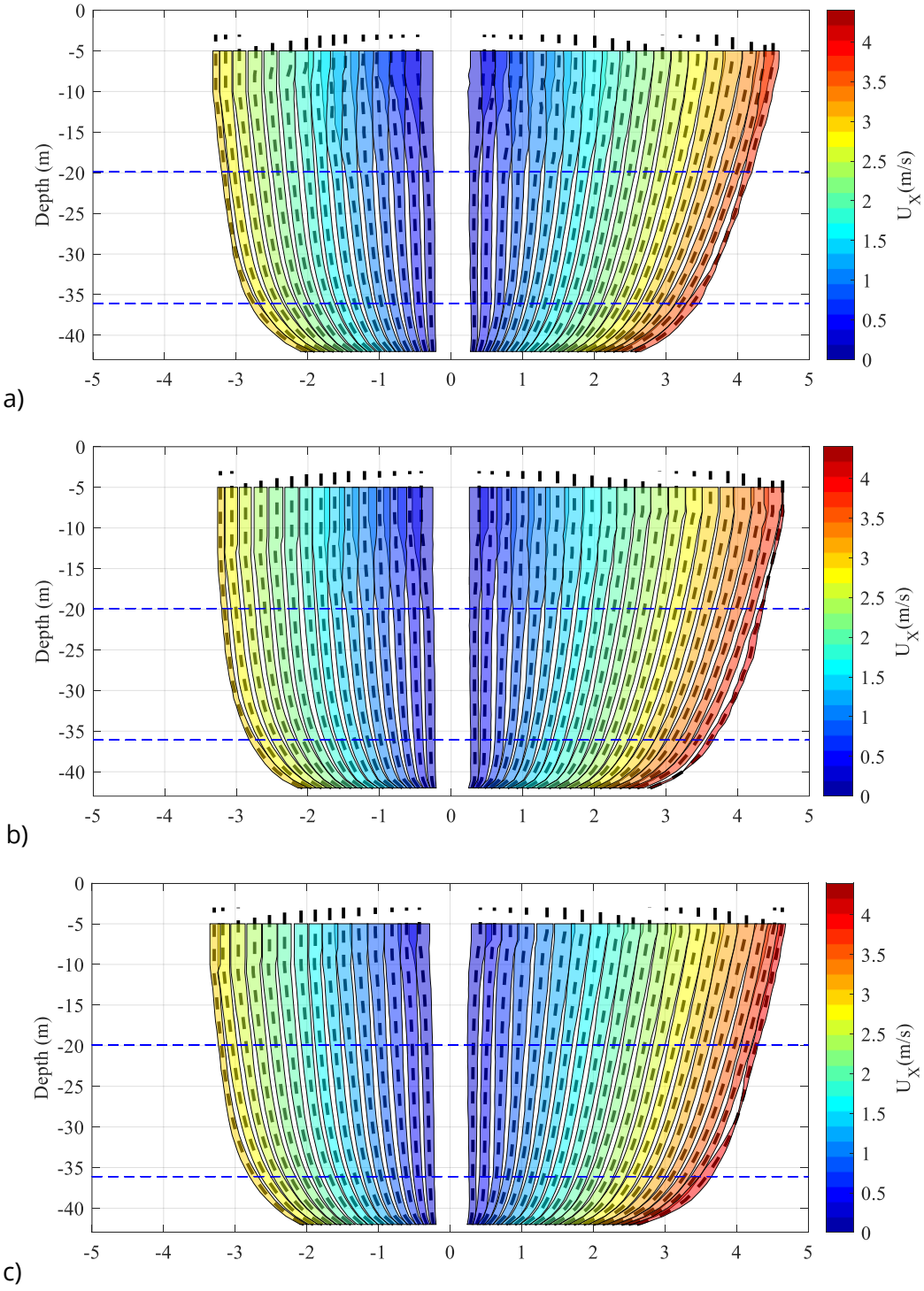

Figure A8. Variation of vertical profiles for each binned UDA for a bed mounted turbine (vertical position highlighted by blue dashed line), profiles given for each ADCP, (a) NH1, (b) NH2 and (c) MU.

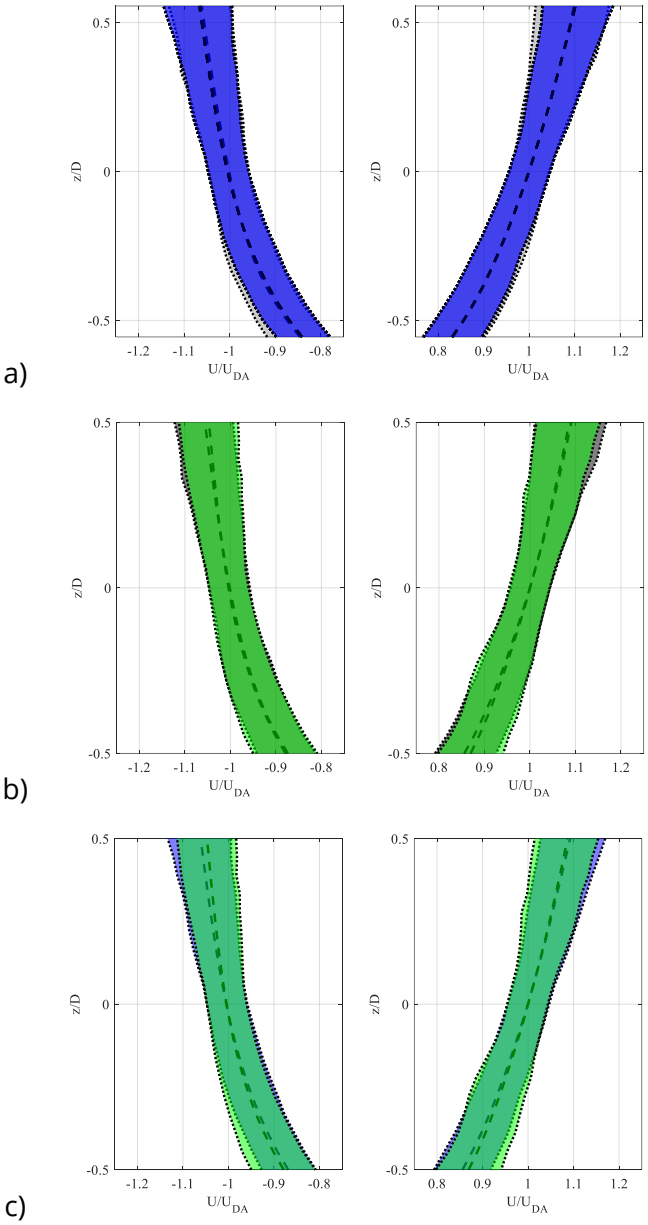

Figure A9. Variation of in vertical shear across the rotor area between the measured values. (a) NH1 (grey band) and MU (blue band). (b) NH1 (grey band) and NH2 (green band). (c) MU (blue band) and NH2 (green band).

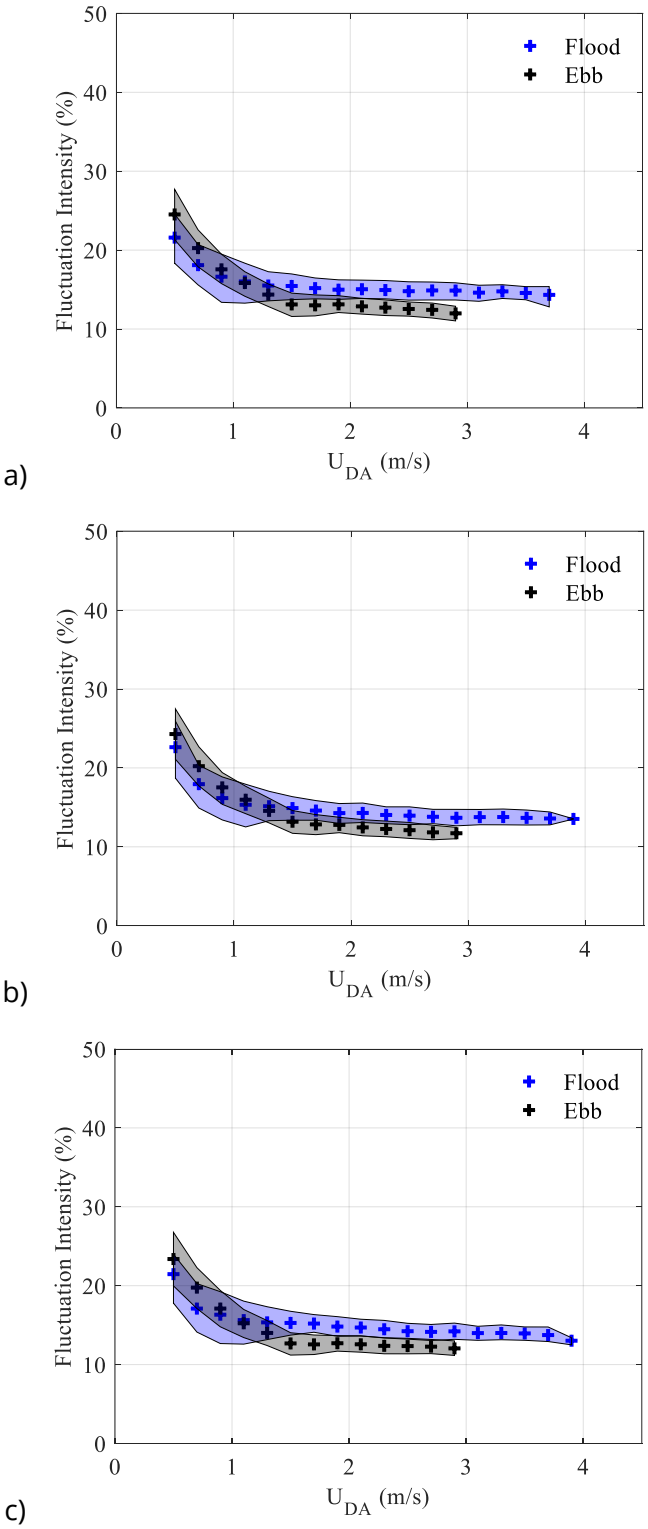

Figure A10. Variation of fluctuation intensity for the flood and ebb tides at each measurement location for a bed mounted turbine.

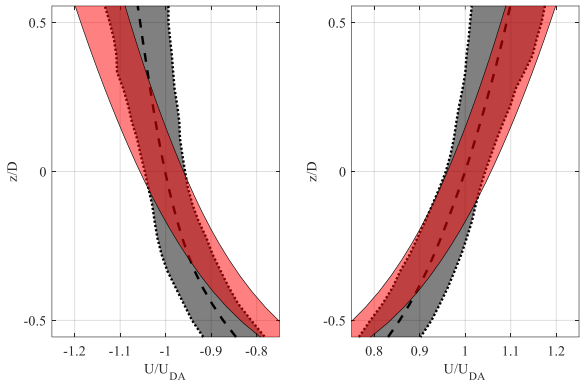

Figure A11. Variation of in vertical shear across the rotor area between the measured values (NH1 grey band) and the TELEMAC RANS data (red band).

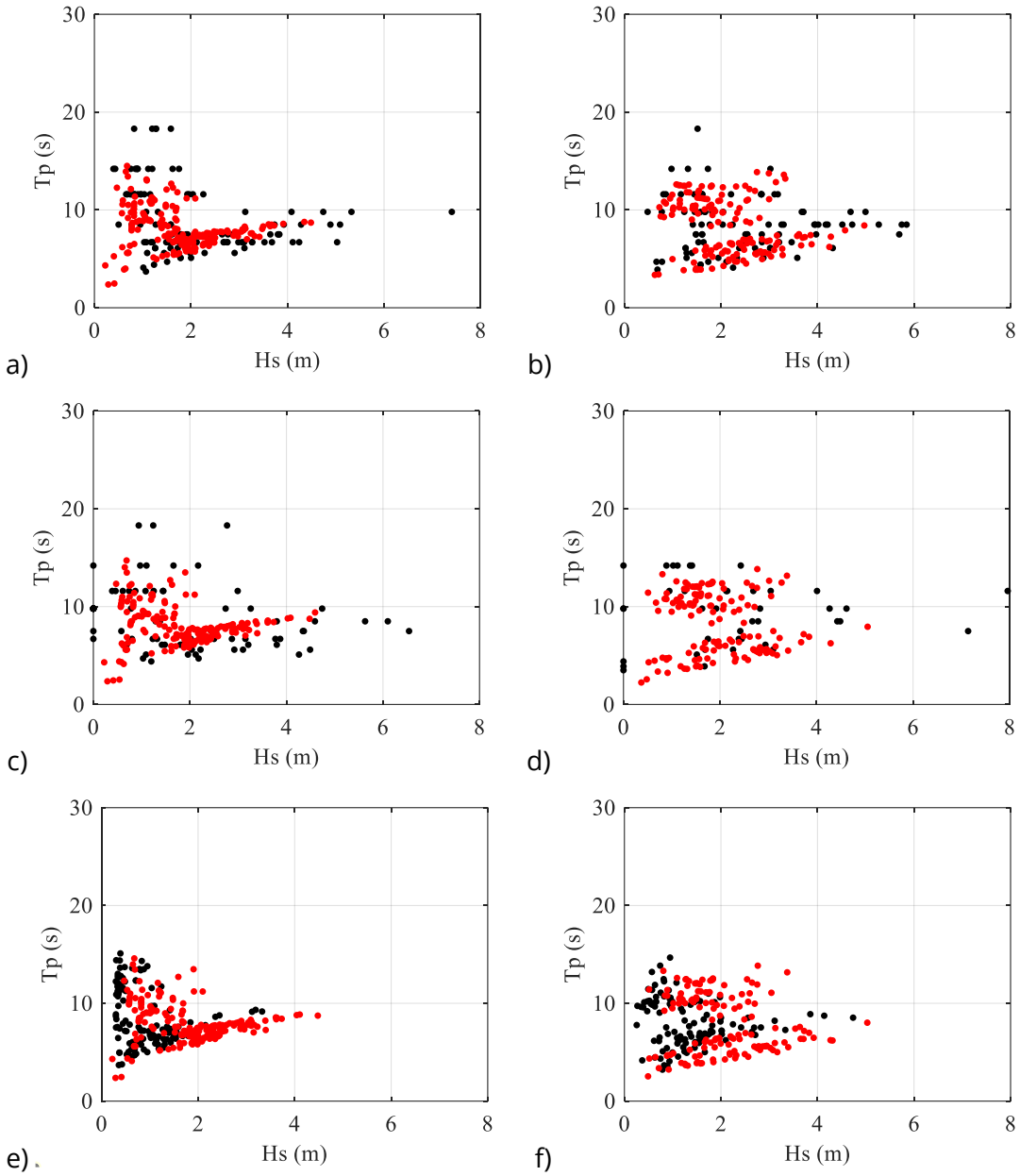

Figure A12. Occurrence of wave conditions for flood (RHS) and ebb (LHS) tides with disk averaged onset flow velocity (2.0-2.2m/s), for three locations with black (measured) and red (modelled) data, for each measurement device, from top to bottom: NH1, NH2 and MU.

In addition to the variation in shear at a site, the design conditions are also affected by fluctuations in velocity, which are caused by disturbances to the flow field and are usually defined through turbulence and wave characteristics. Initial analysis of the ADCP data allows for the calculation of the fluctuation intensity, taking into account all causes of the fluctuations in velocity. Figure A10 shows this intensity across the range of disk averaged velocities measured at the site for both the flood and ebb tides. The model data provided using the TELEMAC RANS model provides the vertical profile of velocity as well as RANS turbulence data (Thiebot et al., 2020), this does provide enough detail model the blade loading, however higher-fidelity models, such as, PALABOS, which is a LBM-LES case resolves large turbulent

eddies providing a better predicted of turbulence with flow speed within the site model. Due to the nature of the LES simulations, they are computationally very expensive to run and therefore model data provided within this project focussed on the design cases where a turbine would experience the highest onset flow. Further work will include the influence of these differences between location on the loading for a design case, as well as the comparison to modelled values of turbulence intensity.

An example a model to measurement comparison is shown in Figure A9, where one U_{DA} bin has been singled out for a single device in the ebb and flood tides. The variation in profile across the vertical rotor area is shown and overlaid with the variation in profile from the TELEMAC RANS model at the same location in the site. The influence of this difference between the measured and model profile for this case will be shown in the next section.

As mentioned determining the fluctuation intensity includes the influence of waves at the site, ongoing work is looking at the separation of these conditions to determine the loading caused by each environmental factor. The measurement data from the ADCP deployments is also compared to model data using the DELFT3D model (Deltares, 2019), with the variation in conditions at flow design case (one UDA case) shown in Figure A12. The overall spread of significant wave height and time period is similar between the cases, with outliers of very high wave height at the NH2 position. This data will be further analysed within the project and the influence on turbine loading determined.

A4 Implication of Spatially Varying Conditions at a Tidal Site

This section gives a brief overview of the impact on loading when cross-comparing site locations and models with measurements. It can be observed from this overview that there is a variation of condition at a site, with location and between models and measurements. The impact of this on fatigue loads is shown here, using the variation in onset flow condition for one chosen design case, with a disk-averaged velocity of 2.0-2.2 m/s, to provide a variation in the fatigue loading that the turbine blades experience. This difference in loading is shown in Figure A13, using the vertical shear profile data from EMEC, and measured in Le Raz Blanchard using NH1. The fatigue loads are calculated using damage equivalent loads, with time varying blade loads calculated using the variety of onset flows as input to a unsteady blade element model. Figure A13 shows the influence of varying turbulence compared to average turbulence. Where there is a 35% difference in flood tide loads and only a 4% difference in ebb tides between the measured site conditions when using the varying turbulence values. This reduces to a 25% difference for the flood and 2.5% difference for the ebb between sites when the average turbulence is used as input to the model. When considering the Raz Blanchard data only with average turbulence applied, there is a 6% difference in the loads predicted for the flood tide and a 15% difference for the ebb tide.

All the loading calculations performed here consider the single design point, ongoing work looks to establish the range of aggregated loads from the variety of conditions which contribute to fatigue, in order to determine a range of uncertainty that can be allowed and to reduce safety factors applied in blade design. Ongoing work will examine the contribution to the loading of the turbulence intensity when be comparing model and measurement values. Successfully capturing the influence from both waves and turbulence will also be demonstrated in further work.

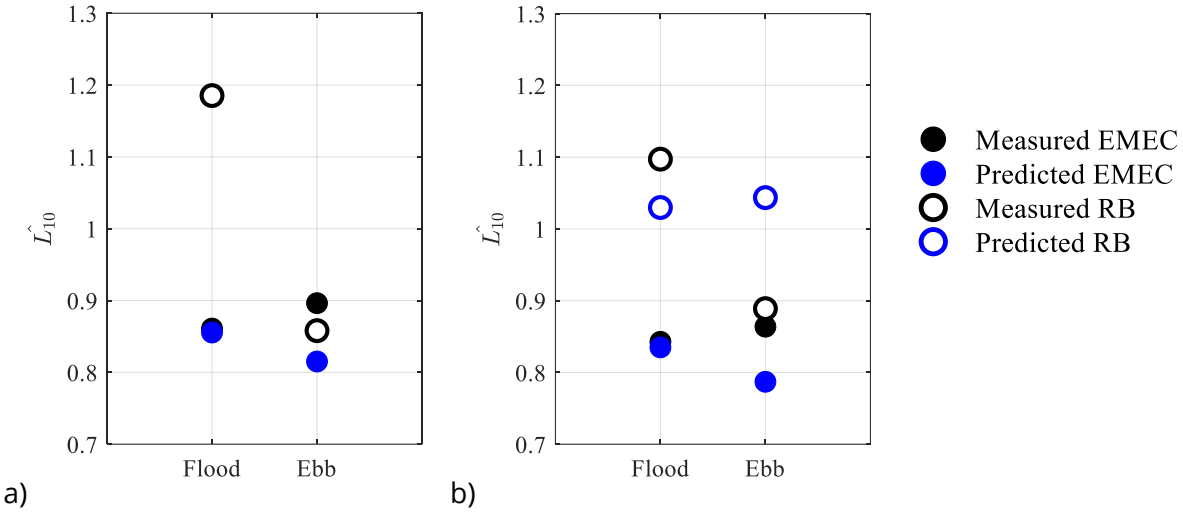

Figure A13. Variation in normalised damage equivalent loads for two tidal sites, flood and ebb tides, using (a) varying turbulence and (b) average turbulence values. Where RB stands for Le Raz Blanchard in the legend.

References

Section 2 – Delft3D FM-SWAN

EDINA Marine Digimap Service. 2013. Arcsecond Gridded Bathymetry [ASC geospatial data]

Deltares, 2019 Delft3D-FLOW: User Manual. Technical report.

Egbert, G. D., Bennett, A. F., and Foreman, M. G. G. 1994. TOPEX/POSEIDON tides estimated using a global inverse model. Journal of Geophysical Research: Oceans, 99(C12):24821–24852. doi: 10.1029/94jc01894

GEBCO Bathymetric Compilation Group 2020. The GEBCO_2020 Grid - a continuous terrain model of the global oceans and land. NERC, UK 2020. doi:10.5285/a29c5465-b138-234d-e053-6c86abc040b9.

Hersbach, H, et al. 2020. The ERA5 global reanalysis. Quarterly Journal of the Royal Meteorological Society vol:146 730, pg1999-2049,

Lesser, G. R., Roelvink, J. A., van Kester, J. A. T. M., and Stelling, G. S. 2004. Development and validation of a three-dimensional morphological model. Coastal Engineering, 51(8–9):883–915, 2004. http://dx.doi.org/10.1016/j.coastaleng.2004.07.014

SHOM. 2016. Service Hydrographique et Océanographique de la Marine.

Trihartono, A., McLellan, B., Putra, S. S., Wegen, M. v. d., Reyns, J., Dam, A. v.,Solomatine, D. P., and Roelvink, J. A. 2015. The 5th Sustainable Future for Human Security (2014) Multi Station Calibration of 3D Flexible Mesh Model: A Case Study of the Columbia Estuary. Procedia Environmental Sciences, 28:297–306, 2015. doi: http://dx.doi.org/10.1016/j.proenv.2015.07.038

TUDelft, 2010. SWAN: Scientific and Technical Documentation. Technical report.

Xia, J., Falconer, R. A., and Lin, B. 2020 Impact of different tidal renewable energy projects on the hydrodynamic processes in the Severn Estuary, UK. Ocean Modelling, 32(1–2):86–104, http://dx.doi.org/10.1016/j.ocemod.2009.11.002.

Section 3 - Thetis

Balay S, Abhyankar S, Adams M.F, Brown J, Brune P, Buschelman K, Dalcin L, Eijkhout V, Gropp WD, Kaushik D, Knepley MG, McInnes LC, Rupp K, Smith BF, Zampini S, Zhang H, Zhang H, 2016, PETSc Users Manual, Technical Report, Argonne National Laboratory

Bangor University, 2017, UKHO Tide Gauge Network Data

Black & Veatch, 2020, Lessons Learnt from MeyGen Phase 1A Final Summary Report, Technical report

Coles DS, Blunden LS, Bahaj AS, 2016. Experimental validation of the distributed drag method for simulating large marine current turbine arrays using porous fences, International Journal of Marine Energy, 16:298-316

Coles DS, Mackie L, White D, Miles J, 2021a, Cost modelling and design optimisation of tidal stream turbines, Proceedings of the 14th European Wave and Tidal Energy Conference (EWTEC), Plymouth, UK, 2139:1-11

Coles DS, Angeloudis A, Goss Z, Miles J, 2021b, Tidal stream vs. wind energy: The value of cyclic power when combined with short-term storage in hybrid systems, Energies, 14:1106

Coles DS, Angeloudis A, Goss Z, Miles J, 2021c, Tidal stream vs. wind energy: The value of cyclic power when combined with short-term storage in hybrid systems, Energies, 14:1106

Egbert G, Erofeeva S, Ray R, 2010, Assimilation of altimetry data for nonlinear shallow-water tides: Quarter-diurnal tides of the Northwest European Shelf, Cont. Shelf Res., 30:668–679

Fairley I, Williamson B, McIlvenny J, King N, Masters I, Lewis M, Neill S, Glasby D, Coles DS, Powell B, Naylor K, Robinson M, Reeve D, 2022, Drone-based large-scale particle image velocimetry applied to tidal stream energy resource assessment, Renewable Energy, 196: 839-855

Frost C., Quantifying the benefits of tidal stream energy to the wider UK energy system, Technical Report, Offshore Renewable Energy Catapult

Karna, T, de Brye, B, Gourgue, O, Lambrechts, J, Comblen, R, Legat, V, Deleersnijder, E, 2011, A fully implicit wetting-drying method for DG-FEM shallow water models, with an application to the Scheldt Estuary, Computer Methods in Applied Mechanics and Engineering, 200 (5):509–524

Mackie L, Evans PS, Harrold MJ, O'Doherty T, Piggott MD, Angeloudis A, 2021, Modelling an energetic tidal strait: investigating implications of common numerical configuration choices, Applied Ocean Research, 108:102494

Miles J, Coles DS, Paine A, Barr S, 2022, Flow characteristics at Ramsey Sound relevant to tidal

device deployment and recovery planning, PRIMaRE poster, Penryn, UK

Pennock S, Coles DS, Angeloudis A, Bhattacharya S, Jeffrey H, 2022, Temporal complementarity of marine renewables with wind and solar generation: Implications for GB system benefits, Applied Energy, 319:119276

Pudjianto D, Frost C, Coles DS, Angeloudis A, Smart G, Strbac G, UK Studies on the Wider Energy System Benefits of Tidal Stream, 2022, in preparation.

Seazone Solutions Ltd, 2014, Edina Digimap Service, Hydrospatial one, gridded bathymetry

Soulsby RL, 2005, Tidal current boundary layers, In: Le Mehaute, B., Hanes, D.M. (Eds.), The Sea, Volume 9: Ocean Engineering Science, 9. Harvard University Press

Thiebot J, Guillou N, Coles DS, Guillou S, 2022, On nodal modulations of tidal-stream energy resource in north-western Europe, Applied Ocean Research, 121:103091

Todeschini G, Coles DS, Lewis M, Popov I, Angeloudis A, Fairley I, Johnson F, Williams AJ, Robins P, Masters I, 2022, Medium-term variability of the UK's combined tidal energy resource for a net-zero grid, Energy, 238(Part A):121990

Section 4 - Palabos

Bouzidi M., Firdaouss M., and Lallemand P., "Momentum transfer of a Boltzmann-lattice fluid with boundaries", Phys. Fluids 13, 3452 (2001).

Grondeau M., Poirier J.-C., Guillou S.S., Méar Y., Mercier P., and Poizot E., "Modelling the wake of a tidal turbine with upstream turbulence: LBM-LES versus Navier-Stokes LES," Int. Mar. Energy J. 3(2), 83 (2020).

Grondeau M., Guillou S.S., Mercier P., and Poizot E., "Wake of a ducted vertical axis tidal turbine in turbulent flows, LBM actuator-line approach," Energies 12, 4273 (2019).

Grondeau M., Guillou S.S., Poirier J.-C., Mercier P., Poizot E., and Méar Y., "Studying the Wake of a Tidal Turbine with an IBM-LBM Approach Using Realistic Inflow Conditions", Energies 15, 2092 (2022).

Khaled F., Guillou S.S., Méar Y., and Hadri F., "Impact of blockage ratio on the transport of sediments in the presence of a hydrokinetic turbine: numerical modelling of the interaction sediments-turbine", International Journal of Sediment Research 36, 696-710 (2021).

Latt J., O. Malaspinas, D. Kontaxakis, A. Parmigiani, D. Lagrava, F. Brogi, M. Ben Belgacem, Y. Thorimbert, S. Leclaire, S. Li, F. Marson, J. Lemus, C. Kotsalos, R. Conradin, C. Coreixas, R. Petkantchin, F. Raynaud, J. Beny, and B. Chopard, "Palabos: Parallel lattice boltzmann solver", Comput. Math. Appl. 81, 334–350 (2021)

Malaspinas O. and Sagaut P., "Consistent subgrid scale modelling for lattice Boltzmann methods", J. Fluid Mech. 700, 514–542 (2012)

Mercier P., Grondeau M., Guillou S.S., Thiébot J., and Poizot E., "Numerical study of the turbulent eddies generated by the seabed roughness. Case study at a tidal power site", Appl. Ocean Res. 97, 102082 (2020).

Mercier P., Ikhennicheu M., Guillou S.S., Germain G., Poizot E., Grondeau M., Thiébot J., and Druault P., "The merging of Kelvin-Helmholtz vortices into large coherent flow structures in a high Reynolds number flow past a wall-mounted square cylinder", Ocean Engineering 204, 107274 (2020).

Mercier P., Thiébaut M., Guillou S.S., Maisondieu C., Poizot E., Pieterse A., Thiébot J., Filipot J.-F., and Grondeau M., "Turbulence measurements: An assessment of Acoustic Doppler Current Profiler accuracy in rough environment", Ocean Engineering 226, 108819 (2021).

Mercier P., and Guillou S.S, "The impact of the seabed morphology on turbulence generation in a strong tidal stream", Phys. of Fluids 33, 055125 (2021).

Mercier P., Guillou S.S., Thiébot J., and Poizot E., "Turbulence characterisation during ebbing and flooding tides in the Raz Blanchard with large eddy simulation", Proceedings of the 14th European Wave and Tidal Energy Conference 5-9th Sept 2021, Plymouth, UK.

Mercier P. and Guillou S.S., Spatial and temporal variations of the flow characteristics at a tidal stream power site: a high-resolution numerical study, Energy Conversion and Management, 269 (2022) 116123. https://doi.org/10.1016/j.enconman.2022.116123

Mercier P. and Guillou S.S., Simulation des grandes échelles de la turbulence dans un écoulement de marée : effet d'une turbulence synthétique en condition d'entrée. Congrès Français de Mécanique, 29 août - 2 sept. 2022, Nantes.

Nguyen V.T., Guillou S.S., Thiébot J., and Santa Cruz A., "On the use of turbulent models for simulating the flow behind a tidal turbine represented by a porous media", Renewable Energy 97, 625-635 (2016).

Polleto R., Craft T., and Revell A., "A new divergence free synthetic eddy method for the reproduction of inlet flow conditions for LES", Flow Turbul. Combust. 91, 519–539 (2013).

Section 5 - Telemac

Bourgoin A., Guillou S.S., Thiébot J., Ata R (2019) Use of Large-Eddy Simulation for the bed shear stress estimation over a dune. International Journal of Sediment Research, 36(6), pp. 687-695.

Bourgoin A., Guillou S.S., Thiébot J., Ata R. (2020) Turbulence characterization at tidal energy sites using Large Eddy Simulations: Case of the Alderney Race. Philosophical Transactions of the Royal Society A, 378: 20190499.

Djama Dirieh N., Thiébot J., Guillou S., Guillou N. (2022) Blockage Corrections for Tidal Turbines—Application to an Array of Turbines in the Alderney Race. Energies, 15, Article 3475.

Guillou S., Bourgoin A., Thiébot J., Ata R. (2021) On the spatial variability of the flow characteristics at a Tidal energy site: Case of the Raz Blanchard, EWTEC 21.

Thiébot J., Bailly du Bois P., Guillou S. (2015) Numerical modeling of the effect of tidal stream turbines on the hydrodynamics and the sediment transport - Application to the Alderney Race (Raz Blanchard), France. Renewable Energy, 75, pp. 356-365.

Thiébot J., Guillou S.S., Nguyen V.T. (2016) Modelling the effect of large arrays of tidal turbines with depth-averaged Actuator Disks. Ocean Engineering, 126, pp. 265-275.

Thiébot J., Guillou N., Guillou S.S, Good A., Lewis M. (2020) Wake field study of tidal turbines under realistic flow conditions. Renewable Energy. 151, pp. 1196-1208.

Thiébot J., Djama Dirieh N., Guillou S., Guillou N. (2021) The Efficiency of a Fence of Tidal Turbines in the Alderney Race: Comparison between Analytical and Numerical Models. Energies, 14(4), Article 892.

Thiebot J, Guillou N, Coles DS, Guillou S, 2022, On nodal modulations of tidal-stream energy resource in north-western Europe, Applied Ocean Research, 121:103091

Section 6 - DOROTHY

C. Choma Bex, C. Carlier, A. Fur, G. Pinon, G. Germain, et al. (2020a). A stochastic method to account for the ambient turbulence in Lagrangian Vortex computations. *Applied Mathematical Modelling*, Elsevier, 2020, 88, pp.38-54. ⟨10.1016/j.apm.2020.05.025⟩. ⟨hal-03400955⟩

C. Choma Bex, G. Pinon, M. Slama, B. Gaston, G. Germain, et al. (2020b). Lagrangian Vortex computations of turbine wakes: recent improvements using Poletto's Synthetic Eddy Method (SEM) to account for ambient turbulence. *Journal of Physics: Conference Series*, IOP Publishing, 2020, 1618 (6), pp.062028. ⟨10.1088/1742-6596/1618/6/062028⟩. ⟨hal-03776677⟩

C. Choma Bex, M.-A. Dufour, Y. Ben Belkacem, G. Pinon, G. Germain, E. Rivoalen (2022). Tidal and wind turbine simulation with the simulation code DOROTHY. Accepted for presentation at RENEW2022 conference

A. van Garrel, (2003). Development of a wind turbine aerodynamics simulation module. Technical Report ECN-C–03-079, Energy research Centre of the Netherlands.

J. Katz, A. Plotkin, (2001). Low-Speed Aerodynamics (2nd ed.). Cambridge University Press.

G. Pinon, P. Mycek, G. Germain, E. Rivoalen (2012). Numerical simulation of the wake of marine current turbines with a particle method. *Renewable Energy*, Elsevier, 2012, 46, pp.111-126. ⟨10.1016/j.renene.2012.03.037⟩. ⟨hal-03515424⟩

G. Pinon, C. Carlier, A. Fur, B. Gaurier, G. Germain, et al. (2017). Account of ambient turbulence for turbine wakes using a Synthetic-Eddy-Method. *Journal of Physics: Conference Series*, IOP Publishing, 2017, 854, pp.012016. ⟨10.1088/1742-6596/854/1/012016⟩. ⟨hal-03776682⟩

G.T. Scarlett (2019). Unsteady hydrodynamics of tidal turbine blades. PhD thesis, University of Edinburgh, August 2019.

K. Shaler, E. Branlard, A. Platt (2020). Olaf user's guide and theory manual. Technical Report NREL/TP-5000-75959, Golden, CO: National Renewable Energy Laboratory.

M. Slama, C. Choma Bex, G. Pinon, M. Togneri, L. Evans (2021a). Lagrangian Vortex Computations of a Four Tidal Turbine Array: An Example Based on the NEPTHYD Layout in the Alderney Race. *Energies*, MDPI, 2021, 14 (13), pp.3826. ⟨10.3390/en14133826⟩. ⟨hal-03296921⟩

M. Slama, G. Pinon, Y. Ben Belkacem, C. Choma Bex, M. Togneri, et al. (2021b). Fluctuating load perceived by the downstream turbine in a farm. *14th European Wave and Tidal Energy Conference*, Sep 2021, Plymouth, United Kingdom. ⟨hal-03372956⟩

Section 7 – MIKE 21

DHI (2007). MIKE 21 & MIKE 3 flow model FM . Hørsholm, Denmark.

DHI (2012). MIKE SHE User Manual, Volume-1.

Section 8 – DOFAS

P. Ouro, L. Ramirez, & M. Harrold (2019). Analysis of array spacing on tidal stream turbine farm performance using Large-Eddy Simulation. Journal of Fluids and Structures 91, 102732.

P. Ouro & T. Stoesser (2019). Impact of Environmental Turbulence on the Performance and Loadings of a Tidal Stream Turbine. Flow, Turbulence and Combustion 102, 613–639.

P. Ouro & T. Nishino (2021). Performance and wake characteristics of tidal turbines in an infinitely large array. Journal of Fluid Mechanics 925, A30.

P. Ouro, P. Stansby & T. Stallard (2021). Investigation of the wake recovery behind a tidal stream turbine for various submergence levels. 14th EWTEC, Plymouth, United Kingdom.

P. Ouro, H. Mullings & T. Stallard (2022). Establishing confidence in predictions of fatigue loading for floating tidal turbines based on large-eddy simulations and unsteady blade element momentum. Trends in Renewable Energy Offshore. RENEW conference, Lisbon, Portugal.

T. Stallard, T. Feng, & P. K. Stansby (2015). Experimental study of the mean wake of a tidal stream rotor in a shallow turbulent flow. Journal of Fluids and Structures 54, 235–246.

P. Stansby & P. Ouro (2022). Modelling marine turbine arrays in tidal flows. Journal of Hydraulic Research 60, 187–204.

Section 9 – Unsteady BEM

D. Peacock, "Power Performance Assessment of Electricity Producing Tidal Energy Converters Commissioned by IEC," no. Cd, 2011

P. Ouro, H. Mullings, T. Stallard, (2022) Establishing confidence in predictions of fatigue loading for floating tidal turbines based on large-eddy simulations and unsteady blade element momentum, *Trends in Renewable Energies Offshore,* 915-924, DOI: 10.1201/9781003360773-101.

H. Mullings, T. Stallard, (2022) Analysis of tidal turbine blade loading due to blade scale flow, *Journal of Fluids and Structures,* Volume 114, DOI: https://doi.org/10.1016/j.jfluidstructs.2022.103698.

G.S. Payne, T. Stallard, R. Martinez, T. Bruce, (2018). Variation of loads on a three-bladed horizontal axis tidal turbine with frequency and blade position. Journal of Fluids and Structures, 83, 156-170.

G. T. Scarlett, B. Sellar, T. van den Bremer, I. M. Viola, (2019). Unsteady hydrodynamics of a full-scale tidal turbine operating in large wave conditions. Renewable Energy 143, 199–213.

Annex A – Resource Cross-Comparison

Deltares, 2019 Delft3D-FLOW: User Manual. Technical report.

Mullings H, Stallard T. (2021) Assessment of dependency of unsteady onset flow and resultant tidal turbine fatigue loads on measurement position at a tidal site. *Energies*, volume: Special Issue Tidal Turbines. https://doi.org/10.3390/en14175470.

Mullings H, Stallard T. (2022) Impact of spatially varying flow conditions on the prediction of fatigue loads of a tidal turbine. *International Marine Energy Journal.* 5(1) 103-111. DOI: https://doi.org/10.36688/imej.5.103-111.

Sellar BG, Sutherland DR, "Tidal Energy Site Characterisation At the Fall of Warness, EMEC, UK. Energy Technologies Institute Redapt Ma1001 (Md3.8)," December, 2016. [Online]. Available: http://redapt.eng.ed.ac.uk

Thiebot J, Guillou N, Guillou S, Good A, Lewis M, Wake field study of tidal turbines under realistic flow conditions, *Renewable Energy* 151 (2020) 1196–1208. doi:10.1016/j.renene.2019.11.129